

THE TROPHIC ECOLOGY OF PHREATIC KARST AQUIFERS

by

Benjamin T. Hutchins

A dissertation submitted to the Graduate Council of
Texas State University in partial fulfillment
of the requirements for the degree of
Doctor of Philosophy
with a Major in Aquatic Resources
December 2013

Committee Members:

Benjamin F. Schwartz, Chair

Timothy H. Bonner

Annette S. Engel

Stephen E. MacAvoy

Weston H. Nowlin

COPYRIGHT

By

Benjamin T. Hutchins

2013

FAIR USE AND AUTHOR'S PERMISSION STATEMENT

Fair Use

This work is protected by the Copyright Laws of the United States (Public Law 94-533, section 107). Consistent with fair use as defined in the Copyright Laws, brief quotations from this material are allowed with proper acknowledgment. Use of this material for financial gain without the author's express written permission is not allowed.

Duplication Permission

As the copyright holder of this work I, Benjamin T. Hutchins, authorize duplication of this work, in whole or in part, for educational or scholarly purposes only.

DEDICATION

This dissertation is dedicated to my wife, Carrie, who has been my friend and partner on many adventures including the long strange trip of graduate school. Her understanding, perspective, assistance, and encouragement have been essential.

ACKNOWLEDGEMENTS

Numerous individuals representing public and private institutions were fundamental to the success of this research through provision of data, access to sites, field or lab assistance. These include Randy Gibson (U.S. Fish and Wildlife Service) Geary Schindel, Steve Johnson, Gizelle Luevano, and Robert Esquilin, (Edwards Aquifer Authority), Jean Krejca and William Larson (Zara Environmental LLC), David Mahula and Paul Dunster (San Antonio Water Systems), Brian Hunt and Brian Smith (Barton Springs Edwards Aquifer Conservation District), Jon Cradit (Texas Cave Management Association), and Fran Hutchins (Bat Conservation International). Data were also provided by the Texas Speleological Survey. Several individuals from Texas State University also assisted with field work and laboratory analysis including Philip Ramirez, Gabrielle Timmins, Brett Gerard, Benjamin Tobin, Carrie Hutchins, Kenny Behen, Steven Curtis, Chasity Stenson, Mitchell Plath, and Kathleen Brennon. My committee members provided me with invaluable guidance, especially Benjamin Schwartz who put forth an unnatural and unhealthy amount of effort into providing instruction, feedback, support, and friendship for his students. Sources of funding are acknowledged in individual chapters.

TABLE OF CONTENTS

	Page
ACKNOWLEDGEMENTS	v
LIST OF TABLES	ix
LIST OF FIGURES.....	xi
LIST OF ABBREVIATIONS	xiii
ABSTRACT	xv
CHAPTER	
I. ENVIRONMENTAL CONTROLS ON ORGANIC MATTER PRODUCTION AND TRANSPORT ACROSS SURFACE- SUBSURFACE AND GEOCHEMICAL BOUNDARIES IN THE EDWARDS AQUIFER, TEXAS, USA.....	1
Abstract	1
Keywords	2
Introduction.....	2
Materials & Methods	6
Field sampling and geochemical analyses	6
Estimation of mean $\delta^{13}\text{C}_{\text{FPOM}}$ for recharge streams	8
Statistical analysis.....	9
Results.....	11
Discussion	14
Contributions of organic matter from surface recharge	15
Contributions of organic matter from the FWSWI.....	17
Conclusion	21
Acknowledgements.....	22
References.....	23
Appendices.....	34

II. FOOD CHAIN LENGTH IN GROUNDWATER: PATTERNS IN $\delta^{15}\text{N}$ RANGE.....	36
Abstract.....	36
Introduction.....	37
Methods.....	38
Results.....	41
Discussion.....	44
Conclusions.....	49
Acknowledgements.....	49
References.....	50
III. MORPHOLOGIC AND TROPHIC SPECIALIZATION IN A SUBTERRANEAN AMPHIPOD ASSEMBLAGE.....	53
Summary.....	53
Keywords.....	54
Introduction.....	54
Materials & Methods.....	60
Amphipod collection.....	60
Stable isotope data.....	62
Mouthpart morphometry.....	63
Statistical analysis.....	64
Results.....	68
Discussion.....	71
Conclusions.....	76
Acknowledgements.....	77
References.....	78
Appendices.....	97

IV: TROPHIC COMPLEXITY IN A SUBTERRANEAN FOOD WEB WITH CHEMOLITHOAUTOTROPHIC AND PHOTOSYNTHETIC FOOD CHAINS.....	99
Abstract.....	99
Introduction.....	100
Evidence for chemolithoautotrophy in the Edwards Aquifer	103
A biogeochemical gradient between recharge dominated and freshwater – saline water interface dominated groundwater	104
Trophic structure along a photosynthesis – chemolithoautotrophy gradient.....	107
Disparate resources promote niche specialization	109
Discussion.....	111
Is the Edwards Aquifer unique?.....	112
Methods.....	115
Sample collection and analysis	115
Geographic information systems	117
Food web structure.....	118
Statistical analyses	121
Supplement	123
Supplement 1: Defining scraping forager and filter feeding trophic groups for mixing models.....	123
Supplement 2: Comparison of Bayesian mixing models using different estimates of chemolithoautotrophic endmember	123
References.....	125

LIST OF TABLES

Table	Page
1.1. Summary of statistical tests of predictions	33
2.1. Sample size, $\delta^{15}\text{N}$, and mean trophic level estimates for species sampled from an artesian well and Comal Springs, Edwards Aquifer Texas, USA.....	43
2.2. Published species average $\delta^{15}\text{N}$ ranges and covariate data used for linear regressions.....	45
3.1. Mean $\delta^{13}\text{C}$ and $\delta^{15}\text{N}$ values for amphipod species and groupings based on Fishers LSD post-hoc test of ANOVA results	85
3.2. Morphometric variables chosen as predictor variables for statistical analysis, and hypothesized feeding mode interpretations.....	86
3.3. Significant models of isotopic composition as a function of mouthpart morphology.....	87
4.1. Quotes from speleobiological literature that summarize the prevailing paradigm of trophic structure of subterranean communities	132
4.2. Posterior estimates of the contribution of food sources to consumers.....	133
4.3. AIC model selection for hydrological and geochemical controls on animal stable carbon isotope content ($\delta^{13}\text{C}_{\text{spp}}$)	135
4.4. Fisher’s LSD groupings for species from SM well	136
4.5. Comparison of mean posterior estimates of proportional contributions of source items to consumers at Comal Springs (95% equal-tail credible intervals) using different methods of estimating chemolithoautotrophic organic matter (COM) endmembers	137
4.6. Comparison of mean posterior estimates of proportional contributions of source items to consumers at Ezell’s Cave (95% ETICI) using different methods of estimating COM endmember	138

4.7. Comparison of mean posterior estimates of proportional contributions of source items to consumers at SM well (95% ETCI) using different methods of estimating COM endmember.....139

LIST OF FIGURES

Figure	Page
1.1. The Edwards Aquifer, formed in Cretaceous limestone, extends in a 400 km arc that varies from 4 to 56 km wide and 137 to 335 m thick.	28
1.2. Hydrographs for Comal Springs (the largest Edwards Aquifer spring) (dark grey) and Blanco River (a major source of recharge) (light grey), and Palmer Drought Severity Index (PDSI) (black) values for Division 6, Edwards Plateau (as defined by the National Climate Data Center), January 2005 to January, 2013	29
1.3. Boxplots for $\delta^{13}\text{C}$ values for different sampled OM fractions at A. stream sites and B. FWSWI sites.....	30
1.4. Regressions for stream sites (A-D) and FWSWI sites (E-H) of A and D: $\delta^{13}\text{C}_{\text{FPOM}}$ values against FPOM C:N ratios; B and F: $\delta^{13}\text{C}_{\text{FPOM}}$ values against $\delta^{13}\text{C}$ -DIC values; C and G: $\delta^{13}\text{C}$ -FPOM values versus distance along the Edwards Aquifer flowpath; D: $\delta^{13}\text{C}$ -DIC values versus distance; and H: $\delta^{13}\text{C}$ -DIC values versus distance and conductivity (multiple regression surface)	31
1.5. Results of linear mixed effects models for $\delta^{13}\text{C}$ -FPOM values versus time for stream sites (A-D), and FWSWI sites (E-G)	32
2.1. Significant regressions of $\delta^{15}\text{N}$ range versus A) ecosystem size, B) ecosystem age, and C) the presence of vertebrates	48
3.1. Isotope biplot of individual amphipods and fine particulate organic matter (FPOM) from the sampling site	88
3.2. Species-specific $\delta^{15}\text{N}$ – body length and $\delta^{13}\text{C}$ – body length relationships.....	89
3.3. PCA biplot of amphipod positions in morphometric space	90
3.4. A: PCA biplot on PC 2 and PC 3. B: Biplot of result of redundancy analysis (RDA) showing relation between significant principal components, shown in A, and stable isotope values for individuals	91
3.5. SEM images of setae on the distal margin of outer plate of 1 st maxilla (mx1).....	92

3.6. Linear regression of species average isotope values as a function of morphometric or morphometric · isotopic data.....	93
3.7. SEM images of the left molar (mdb)	94
3.8. SEM images of the left incisor and lacinae mobilis (inc & lac)	95
3.9. SEM images of 2 nd maxilla (mx2)	96
4.1. Conductivity and major hydrological divisions of the Edwards Aquifer, Texas, USA.....	140
4.2. Simple and multiple linear regression results of $\delta^{13}\text{C}_{\text{DIC}}$ (A), chromophoric dissolved organic matter biologic index (BIX) (B), and species' mean $\delta^{13}\text{C}$ (C) as a function of log transformed distance to freshwater saline water interface (m) (FWSWI) and sum of molar concentration of the major electron acceptors O ₂ and NO ₃ ⁻ (Acceptors).....	141
4.3. Isotope biplots for stygobionts from A: SM well, B: Comal Springs, and C: Ezell's Cave	142
4.4. Quantile regression of species richness as a function of distance from the freshwater saline water interface (FWSWI)	143

LIST OF ABBREVIATIONS

Abbreviation	Description
AIC	– Akaike Information Criterion
ANCOVA	– Analysis of Covariance
ANOVA	– Analysis of Variance
BIX	– Biological/ Autochthonous Index
COM	– Chemolithoautotrophic Organic Matter
CPOM	– Coarse Particulate Organic Matter
DIC	– Dissolved Inorganic Carbon
DO	– Dissolved Oxygen
DOC	– Dissolved Organic Carbon
DOM	– Dissolved Organic Matter
ENSO	– El Niño Southern Oscillation
ETCI	– Equal-Tail Credible Interval
FCL	– Food Chain Length
FPOM	– Fine Particulate Organic Matter
FWSWI	– Freshwater-Saline Water Interface
GIS	– Geographic Information System
HCL	– Hydrochloric Acid
IRMS	– Isotope Ratio Mass Spectrometer
LSD	– Least Significant Difference

MANOVA – Multivariate Analysis of Variance

MCMC – Markov Chain Monte Carlo

Mdbarea – Planar Area of Mandible

Mdbincw – Mandible incisor width

Mdbridges – Number of Molar Ridges

Mx1sdentnum – Number of Denticles on Maxilla 1

NSS – National Speleological Society

OM – Organic Matter

PC – Principal Component

PCA – Principal Component Analysis

PDSI – Palmer Drought Severity Index

POM – Photosynthetic Organic Matter

RDA – Redundancy Analysis

SCUBA – Self Contained Underwater Breathing Apparatus

SEM – Scanning Electron Microscopy

SM – San Marcos

TDS – Total Dissolved Solids

TOC – Total Organic Carbon

TX – Texas

ABSTRACT

The trophic structure of groundwater communities is profoundly influenced by the availability of resources derived from allochthonous, photosynthetic detritus or autochthonous, chemolithoautotrophic production. The four themes of the research presented here, corresponding to the four chapters of this dissertation were: 1) quantification of temporal and spatial variability in organic matter within a biodiverse phreatic karst aquifer, 2) identification of historical and ecological factors that influence trophic length in groundwater systems on a global scale, 3) identification of mechanisms by which sympatric stygobionts partition food resources, and 4) quantification of how the relative importance of photosynthetic and chemolithoautotrophic organic matter to stygobiont communities change in response to hydrogeochemical conditions. These themes are summarized below. Although many of the results of this research specifically relate to the Edwards Aquifer of Central Texas, many of the implications are relevant to other groundwater systems and food webs in general.

Chapter 1. $\delta^{13}\text{C}$ values for fine particulate OM (FPOM) in streams recharging the Edwards Aquifer decreased during regional drought between fall 2010 and spring 2012 and were positively related to FPOM C:N ratios, possibly due to an increasing contribution of periphyton. Along the freshwater-saline water interface of the Edwards Aquifer (FWSWI), $\delta^{13}\text{C}_{\text{FPOM}}$ values were positively related to $\delta^{13}\text{C}$ values for dissolved inorganic carbon ($\delta^{13}\text{C}_{\text{DIC}}$) and were depleted relative to $\delta^{13}\text{C}_{\text{DIC}}$ values by 28.44‰, similar to fractionation values attributed to chemolithoautotrophic carbon fixation

pathways using DIC as the substrate. $\delta^{13}\text{C}_{\text{FPOM}}$ values also became enriched through time, and $\delta^{13}\text{C}_{\text{DIC}}$ values and $\delta^{13}\text{C}_{\text{FPOM}}$ values at FWSWI sites increased with distance along the southwest-northeast flowpath of the aquifer. Spatial variability in FWSWI $\delta^{13}\text{C}_{\text{DIC}}$ values is likely due to variable sources of acidity driving carbonate dissolution, and the temporal relationship is explained by changes to recharge and aquifer levels that affected transport of chemolithoautotrophic OM across the FWSWI.

Chapter 2: Trophic level and uncertainty in trophic level was estimated for 19 stygobiont species from two geochemically distinct sites in the Edwards Aquifer. Additionally, historical and environmental determinates of food chain length (FCL) were assessed using stable nitrogen isotope data from published studies of global groundwater habitats. Despite uncertainty associated with intraspecific $\delta^{15}\text{N}$ variability and low sample sizes, species averages span 9‰ and strongly suggest the presence of 2° predators. Ecosystem age and, to a lesser extent, ecosystem size and the presence of vertebrates are all positively correlated with FCL. However, incomplete sampling of taxa for isotope analysis obfuscates the strength of these relationships.

Chapter 3: Isotopic and mouthpart morphometric data were used to investigate feeding strategies of seven sympatric subterranean amphipods. Amphipods occupied significantly different regions of isotopic space, suggesting utilization of different food resources and trophic specialization. Trophic position, measured as $\delta^{15}\text{N}$, was significantly negatively associated with planar area of the mandible and number of molar ridges and significantly positively associated with incisor width. These morphologies are

associated with predatory feeding strategies in non-subterranean amphipods. $\delta^{13}\text{C}$ exhibited weaker relationships with morphometrics, but was significantly negatively correlated with the number of denticles on the setae of the distal margin of the 2nd maxilla. Morphologic and isotopic data suggest the presence of specific scraping and filter feeding food chains. Species showed moderate to absent ontogenetic shifts in trophic position, and body size had little to no effect on trophic position.

Chapter 4: I present isotopic and geochemical evidence of a groundwater food chain in which primary consumers show morphologic specializations for scraper/benthic foraging and filter feeding. Specialization is an adaptation to the presence of two disparate food sources: chemolithoautotrophic production by epilithic biofilm and photosynthetic organic matter, the relative prevalence of which varies as a function of hydrological proximity to geographically separated chemolithoautotrophic and photosynthetic organic matter inputs. Horizontal trophic diversity resulting from scraping/ chemolithoautotrophic and filtering/ photosynthetic food chains increases biomass available to support higher trophic levels, including secondary predators. Within the aquifer, species richness decreases with increasing distance from chemolithoautotrophic sources, indicating that chemolithoautotrophy is fundamental for supporting this trophic complexity, especially during periods of decreased photosynthetic production and groundwater recharge during the mid-Holocene altithermal period.

**I. ENVIRONMENTAL CONTROLS ON ORGANIC MATTER PRODUCTION
AND TRANSPORT ACROSS SURFACE-SUBSURFACE AND GEOCHEMICAL
BOUNDARIES IN THE EDWARDS AQUIFER, TEXAS, USA**

Abstract

Karst aquifer phreatic zones are energy limited habitats supported by organic matter (OM) flow across physical and geochemical boundaries. Photosynthetic OM enters the Edwards Aquifer of Central Texas via streams sinking along its northeastern boundary. The southeastern boundary is marked by a rapid transition between oxygenated freshwaters and anoxic saline waters where OM is likely produced by chemolithoautotrophic microbes. Spatial and temporal heterogeneity in OM composition at these boundaries was investigated using isotopic and geochemical analyses. $\delta^{13}\text{C}$ values for stream fine particulate OM (FPOM) (-33.34‰ to -11.47‰) decreased during regional drought between fall 2010 and spring 2012 ($p < 0.001$), and were positively related to FPOM C:N ratios ($r^2 = 0.47$, $p < 0.001$), possibly due to an increasing contribution of periphyton. Along the freshwater-saline water interface (FWSWI), $\delta^{13}\text{C}_{\text{FPOM}}$ values (-7.23‰ to -58.18‰) correlated to $\delta^{13}\text{C}$ values for dissolved inorganic carbon ($\delta^{13}\text{C}_{\text{DIC}}$) (-0.55‰ to -7.91‰) ($r^2 = 0.33$, $p = 0.005$) and were depleted relative to $\delta^{13}\text{C}_{\text{DIC}}$ values by 28.44‰, similar to fractionation values attributed to chemolithoautotrophic carbon fixation pathways using DIC as the substrate. $\delta^{13}\text{C}_{\text{FPOM}}$ values also became enriched through time ($p < 0.001$), and $\delta^{13}\text{C}_{\text{DIC}}$ values ($r^2 = 0.43$, $p < 0.001$) and $\delta^{13}\text{C}_{\text{FPOM}}$ values ($r^2 = 0.35$, $p = 0.004$) at FWSWI sites increased with distance along the southwest-northeast flowpath of the aquifer. Spatial variability in FWSWI

$\delta^{13}\text{C}_{\text{DIC}}$ values is likely due to variable sources of acidity driving carbonate dissolution, and the temporal relationship is explained by changes to recharge and aquifer level that affected transport of chemolithoautotrophic OM across the FWSWI.

Keywords

carbon stable isotopes, spatial and temporal variability, chemolithoautotrophic production, allochthonous input; karst

Introduction

The phreatic zone of karst aquifers can support diverse metazoan communities (stygobionts). In fact, some of the most diverse subterranean assemblages yet documented are recorded from extensive phreatic groundwater systems (Culver & Pipan 2009). However, karst aquifers are considered to be nutrient-poor, and aquifer assemblages are dependent on organic matter (OM) produced photosynthetically and imported into the subterranean realm via recharging water, gravity, animals (Poulson & Lavoie 2000; Poulson 2005), and plant root exudates (Jasinska *et al.* 1996), or produced *in-situ* through chemolithoautotrophy (Sarbu *et al.* 1996; Pohlman 1997). Consequently, in systems dependent on photosynthetic OM, stygobiont diversity should be predominately focused at the surface-subsurface interface. But, the quantity and quality of OM entering karst aquifers via recharges change as a function of the seasonality of C3 and C4 plant communities on the surface, as well as benthic stream periphyton production along spatial and seasonal precipitation gradients (Bird *et al.* 1998; Artman *et al.* 2003; Silva *et al.* 2012). These differences can influence stygobiont distribution, such

that if surface recharge contributions diminish seasonally or over a long period of time due to aquifer evolution, then *in-situ* OM sources become prevalent and stygobionts may be found at redox gradients between oxidizing and reducing waters in chemolithoautotrophic systems. There has been limited research to investigate OM heterogeneity along redox gradients in chemolithoautotrophic aquifer systems, although geochemical gradients move vertically (Humphreys *et al.* 2012), and potentially laterally (Perez 1986). Therefore, to understand how OM controls the distribution and diversity of stygobionts in karst aquifers, as well as establishes groundwater food webs, more research is needed at the groundwater basin scale (Simon *et al.* 2007).

The Edwards Aquifer of Central Texas is one of the most prolific karst aquifers in the world (Lindgren *et al.* 2004) and the sole source of drinking water for nearly two million people (Johnson *et al.* 2009) (Fig. 1.1). The regional climate is sub-tropical humid, with average annual precipitation ranging from 610 mm in the west to 914 mm in the east (Nielson-Gammon 2008). Precipitation primarily occurs in spring, and potentially in the fall coinciding with tree leaf drop-off (Short *et al.* 1984). Recharge (and input of photosynthetic OM) to the aquifer predominantly occurs by streams, fed by karstic groundwater from the adjacent Trinity Aquifer, that cross exposed limestone in the recharge zone (Fig. 1.1). Cross-formational flow from the Trinity Aquifer (Gary *et al.* 2011 and references therein) is also important, but the nature of OM from this source is not known. South and west of the recharge zone, Edwards limestones are confined below non-karstic rocks that prevent input of allochthonous OM. In this confined portion of the aquifer, the southwestern boundary of freshwater is marked by a rapid transition between

oxygenated, low total dissolved solids (TDS) waters and dysoxic to anoxic, high TDS waters that contain variably high levels of reduced compounds, including sulfides and ammonia. Six distinct geochemical facies in the saline waters (Oetting *et al.* 1996) correlate to changes in microbial communities (Gray & Engel 2013) and OM characteristics (Birdwell & Engel 2009). Several lines of evidence suggest that organic matter in the transition zone is dominated by chemolithoautotrophic production (Birdwell & Engel 2009; Gray & Engel 2013). Chemolithoautotrophic production in this part of the aquifer is independent of terrestrial inputs and the habitat is buffered against seasonal geochemical changes (i.e. changes in water temperature, discharge, conductivity, etc.). In the last three decades, widely available and inexpensive methods to analyze stable carbon isotope ratios and carbon (C): nitrogen (N) ratios in OM have contributed to studies of OM origins, OM fluxes, food web structure, and the growth and fitness of consumers (Bukovinsky *et al.* 2012). Because of enzymatic discrimination against the heavier isotope of carbon (^{13}C) and isotopically distinct inorganic carbon sources, different carbon fixation pathways result in OM with distinct carbon isotope compositions ($\delta^{13}\text{C}$) including $\delta^{13}\text{C}_{\text{terrestrial C3 plants}} = -22$ to -32‰ , $\delta^{13}\text{C}_{\text{terrestrial C4 plants}} = -9$ to -16‰ , and $\delta^{13}\text{C}_{\text{chemolithoautotrophic organic matter}} = -35$ to $< -50\text{‰}$ (Sarbu *et al.* 1996; Opsahl & Chanton 2006; Finlay & Kendall 2007; van Dover 2007). In surface aquatic systems, carbon isotopes have been successfully used to quantify the relative contributions of C3 and C4 plants (Stribling & Cornwell 1997), and in subterranean systems, isotopic data have been used to differentiate between photosynthetic and chemolithoautotrophic OM (Sarbu *et al.* 1996).

As part of an ongoing investigation of food web dynamics in the Edwards Aquifer, OM at both the surface-subsurface and freshwater-saline water interface (FWSWI) was isotopically analyzed in a geochemical and environmental framework to quantify spatial and temporal changes and to test the following hypotheses related to OM sources:

- (H1) the C isotope composition of OM ($\delta^{13}\text{C}_{\text{OM}}$) in recharge streams would become progressively less negative along the northeast to southwest precipitation gradient, reflecting a decrease in the relative proportion of C3 plants;
- (H2) FWSWI $\delta^{13}\text{C}_{\text{FPOM}}$ values would be more negative than stream $\delta^{13}\text{C}_{\text{FPOM}}$ values, reflecting a greater contribution of chemolithoautotrophic production, and values would vary across the study area, reflecting regional differences in $\delta^{13}\text{C}_{\text{DIC}}$ values (the substrate for chemolithoautotrophic production);
- (H3) Recharge stream $\delta^{13}\text{C}_{\text{OM}}$ values and C:N ratios would decrease in the summer, reflecting a greater relative contribution of riparian C3 plants and periphyton during the dry season; and
- (H4) FWSWI $\delta^{13}\text{C}_{\text{FPOM}}$ values and FPOM C:N values would remain constant over time, reflecting a decoupling between surface seasonality and chemolithoautotrophic production.

The results from this study provide additional evidence for both photosynthetic and chemolithoautotrophic OM in the Edwards Aquifer. More generally, this research identifies potential drivers of spatial and temporal variability in both sources.

Materials & Methods

Field sampling and geochemical analyses

Seven surface streams crossing the Edwards Aquifer recharge zone and 11 wells along the FWSWI (Fig. 1.1) were sampled between one and six times between 3 November 2010 and 29 March 2012 (streams) and between 16 April 2011 and 2 April 2012 (wells). The sampling period was marked by declining aquifer levels and declining stream and spring flows (Fig. 1.2), corresponding to a period of prolonged regional drought. Palmer Drought Severity Index (PDSI) data for the Edwards Plateau were obtained from the National Oceanic and Atmospheric Administration, through the Climate Prediction Center (www.ncdc.noaa.gov/) to verify regional water imbalance based on precipitation and soil moisture supply (Palmer 1965). PDSI values above zero correspond to wetter than normal conditions, values below zero indicate drier than normal conditions, and values below -4 indicate extreme drought.

In recharge streams, FPOM and coarse particulate organic matter (CPOM) were collected in 8 L of unfiltered water in sterile carboys after lightly disturbing the benthos by walking back and forth approximately 7 m upstream of the collection site. The benthos was disturbed to better represent benthic OM that enters the aquifer during storm events and via downwelling. Periphyton was collected from cobbles using the methods of Saito *et al.* (2007), in which three cobbles each from a riffle, run, and pool were scrubbed in the lab using a nylon brush to remove attached periphyton. At FWSWI wells (Fig. 1.1), two to three well volumes were purged, and physicochemistry was monitored for constituent

stability before collecting 8 L of unfiltered water in sterile carboys. Samples were stored in the dark on ice until filtration in the lab. FPOM, CPOM, and periphyton were filtered onto 0.7 μm , pre-combusted Whatman glass fiber filters for isotopic analysis. Filters were fumigated with HCl for 12 to 24 hrs and dried at $\sim 45^\circ\text{C}$.

Temperature, dissolved oxygen (DO), pH, and electrical conductivity (conductivity) were recorded with an In-Situ Inc. Troll[®] 9500 multi-parameter probe with optical DO sensor (accuracy = $\pm 0.1\text{mg/L}$ at 0 -8mg/L DO and $\pm 0.2\text{ mg/L}$ at $> 8\text{ mg/L}$ DO). Sulfide and ammonia concentrations were measured with a CHEMetrics[®] V-2000 Multi-analyte photometer via the methylene blue and salicylate methods, respectively. If sulfide concentration was above the detection limit (0.2 mg/L), sulfate concentration was also measured in the field colorimetrically using the turbidimetric method. This was done to avoid erroneously high laboratory sulfate concentration measurements (see below) resulting from abiotic sulfide oxidation. Additional water samples for ion chromatography and for $\delta^{18}\text{O}$ and δD determination were collected and filtered through 0.45 μm Fisherbrand nylon syringe filters. In the lab, dissolved ion concentrations were measured using Dionex ICS-1600 ion chromatographs (Bannockburn, IL). Alkalinity as total titratable bases dominated by bicarbonate was measured via end-point titration with 1.6 N sulfuric acid. $\delta^{18}\text{O}$ and δD in liquid water were measured on a Los Gatos Research Liquid Water Isotope Analyzer (Mountain View, CA).

Water samples for analysis of $\delta^{13}\text{C}_{\text{DIC}}$ and $\delta^{13}\text{C}$ of dissolved organic carbon ($\delta^{13}\text{C}_{\text{DOC}}$) were collected and poisoned with 15 mM sodium azide and stored in glass vials with

butyl rubber septa (Doctor et al. 2008). Carbon isotope analysis was conducted at the UC Davis Stable Isotope Facility using an O.I. Analytical Model 1030 TOC Analyzer (OI Analytical, College Station, TX) interfaced to a PDZ Europa 20-20 isotope ratio mass spectrometer (Sercon Ltd., Cheshire, UK).

Estimation of mean $\delta^{13}\text{C}_{\text{FPOM}}$ for recharge streams

The mean carbon isotope composition of FPOM entering the aquifer via recharging streams ($\delta^{13}\hat{\text{C}}_{\text{FPOM}}$) was estimated using Bayesian modeling and isotope values weighted by discharge. This approach allows uncertainty in $\delta^{13}\hat{\text{C}}_{\text{FPOM}}$ to be quantified by treating each FPOM isotope measurement, c_i , as a sample from a separate normal distribution with separate means, μ_i , and a common precision, τ_0 (Eq. 1). Uninformative priors were given for μ_i and τ_0 (Eq. 2-3).

$$c_i \sim N(\mu_i, \tau_0) \quad (1)$$

$$\mu_i \sim N(0, 1e^{-6}) \quad (2)$$

$$\tau_0 \sim \text{gamma}(0.001, 0.001) \quad (3)$$

Each isotopic value was weighted by daily average stream discharge p_i calculated as a proportion of the sum of all daily discharge measurements q_i of all streams throughout the study period (Eq. 4). Discharge values were obtained from the nearest United States Geological Survey gauging stations on the sampled streams.

$$p_i = \frac{q_i}{\sum_{i=1}^{538} q_i} \quad (4)$$

The parameter c_i was estimated for all unsampled days between the first and last sampling events by linear interpolation between c_i values. The posterior probability distribution for $\delta^{13}\hat{C}_{FPOM}$ (Eq. 5) was estimated using a Markov Chain Monte Carlo (MCMC) procedure.

$$\delta^{13}\hat{C}_{FPOM} = \sum_{i=1}^{538} \mu_i * p_i \quad (5)$$

Two MCMC chains were run, each with 500,000 iterations, a thinning rate of 50 and a burn-in of 1000. Plots of parameter estimates as a function of MCMC iteration were assessed for adequate burn in, and convergence was assessed using Gelman and Ruben potential scale reduction factors (Gelman & Ruben 1992). MCMC chains were run in R v2.15 using the rjags package (Plummer 2010).

Statistical analysis

Simple linear regressions were used to test for spatial differences in $\delta^{13}C_{FPOM}$ and $\delta^{13}C_{DIC}$ values in streams and FWSWI sites (H1 & H2). Spatial data for sampling sites were assigned in ArcMap 10.0. A curved polyline extending between the southwest and northeast margins of the aquifer (approximating the general northwest-southwest direction of groundwater flow) was created using the arc tool. The polyline was converted into 806 points spaced 0.38 km apart from one another and sequentially

numbered, beginning with one, at the southwest end. Sampling sites were assigned a whole number location value corresponding to the number of the nearest point. For FWSWI sites, nested linear models were run to assess relationships between $\delta^{13}\text{C}_{\text{DIC}}$ values and location, conductivity, and the interaction between location and conductivity. Conductivity was log transformed to meet the assumption of normality and the relative fit of models was assessed using Akaike Information Criterion (AIC) for finite samples. Conductivity was not used as a covariate for regressions of stream $\delta^{13}\text{C}_{\text{FPOM}}$ values against location. Stream $\delta^{13}\text{C}_{\text{FPOM}}$ values were square-root transformed to meet the assumption of normality.

To quantify differences in OM in streams versus FWSWI sites, analyses of covariance (ANCOVA) were used to test for differences in $\delta^{13}\text{C}_{\text{DOC}}$ and $\delta^{13}\text{C}_{\text{FPOM}}$ values between stream and FWSWI samples, controlling for date as a confounding variable (H2). To elucidate potential influences (e.g., origins and processing) on the $\delta^{13}\text{C}$ of OM in both streams and FWSWI sites, simple linear regressions were used to test for relationships between $\delta^{13}\text{C}_{\text{FPOM}}$ values and $\delta^{13}\text{C}_{\text{DIC}}$ values (H2) and between $\delta^{13}\text{C}_{\text{FPOM}}$ values and FPOM C:N ratios (H3). C:N ratios were log transformed. A matrix of Pearson's product-moment correlation coefficients for isotopic and physicochemical data was visually assessed for additional, potentially significant correlations (H2). Analysis of variance (ANOVA) was used to test for differences in $\delta^{13}\text{C}$ of different fractions of OM in recharge streams (FPOM, CPOM, DOC, and periphyton) (H3), and a two-sided unpaired Student's t-test was used to test for differences in $\delta^{13}\text{C}$ of different fractions of

OM at FWSWI sites (FPOM and DOC) (H4). Stream OM $\delta^{13}\text{C}$ values were raised to the 0.3 power to meet the assumption of normality.

To test for temporal changes in 1) $\delta^{13}\text{C}_{\text{FPOM}}$ values in both streams and FWSWI sites, 2) C:N ratios in recharge streams, and 3) $\delta^{13}\text{C}_{\text{DIC}}$ values in FWSWI sites, linear mixed effect models were employed, grouping data by sampling site (H3 and H4). Four recharge streams and three groundwater sites that were each sampled four or more times were used in the analysis. Additional sites were sampled but excluded because of small sample size. C:N ratios were log transformed and adjusted r^2 values were calculated by treating each site-specific regression as a simple linear regression with a single covariate.

All statistical analyses were conducted in R v2.15 (R Core Team 2012). Mixed effects models were run using the nlme package (Pinheiro *et al.* 2009). False discovery rate due to multiple comparisons was controlled by adjusting α using the method of Benjamini & Hochberg (1995). Sixteen statistical analyses were performed (Table 1.1), and significance was set to $\alpha = 0.03$. For clarity, test statistics are not included in text but are listed in table 1.1.

Results

During the 16 month study, 24 samples were collected from recharge streams and 32 samples were collected from FWSWI sites (Fig. 1.1). Stream flow varied between $0 \text{ m}^3/\text{s}$ and $73.1 \text{ m}^3/\text{s}$ over the course of the entire study period (Fig. 1.2). However, during individual sampling events, streams always had detectible flows (Fig. 1.2). Sampling corresponded to a period of declining stream and spring flows during the summer of 2011

and a period of increasing stream and spring flows in the fall and winter of 2011 and 2012 (Fig. 1.2). PDSI values ranged from wetter than normal conditions prior to July 2010 through declining values indicative of drought conditions throughout 2011 and 2012. The most severe drought condition recorded was in August 2011, which corresponded to lowest discharge for the Blanco River and Comal Springs (Fig. 1.2). The mean of the posterior probability distribution for the estimate of $\delta^{13}\text{C}_{\text{FPOM}}$ in recharging streams weighted by discharge was -21.75‰ (95% equal-tail credible interval = -23.39‰ to -20.13‰), and was similar to the unweighted analytical average value (-24.22‰).

FWSWI sites had 5.1‰ higher $\delta^{13}\text{C}_{\text{DIC}}$ values, 8.76‰ lower $\delta^{13}\text{C}_{\text{FPOM}}$ values, and 2.6 X lower FPOM C:N ratios than streams (Fig. 1.3). The average FPOM C:N ratio was 3.3 (range = 1.85 to 5.17) at FWSWI sites and 8.6 (range = 2.14 to 33.70) at streams.

$\delta^{13}\text{C}_{\text{DOC}}$ values were not significantly different between streams and FWSWI sites (Table 1.1). However, on average, DOC concentrations were 5 X lower at FWSWI sites (1.0 mg/L; range = 0.5 to 3.1 mg/L) than streams (5.0 mg/L; range = 1.2 to 13.6 mg/L), and 75% of FWSWI DOC concentrations were below the minimum concentrations of the analytical facility's calibration standards (1.1 mg/L).

In streams, $\delta^{13}\text{C}$ values for CPOM, FPOM, periphyton, and DOC were not significantly different (Table 1.1; Fig. 1.3), and $\delta^{13}\text{C}_{\text{FPOM}}$ values were not correlated with $\delta^{13}\text{C}_{\text{DIC}}$ values (Fig. 1.4D). A significant relationship between $\delta^{13}\text{C}_{\text{FPOM}}$ values and C:N ratios was observed in streams (Fig. 1.4A), but no correlations were observed between $\delta^{13}\text{C}_{\text{FPOM}}$ and ion concentrations or physicochemistry (Pearson's $r < 0.2$). Stream $\delta^{13}\text{C}_{\text{FPOM}}$ values

increased from the southwest to the northeast (Fig. 1.4C), but $\delta^{13}\text{C}_{\text{DIC}}$ values in streams were not correlated with location (Fig. 1.4B). Visual examination of $\delta^{13}\text{C}_{\text{periphyton}}$ data did not reveal a spatial pattern, but a relationship was not statistically assessed because, unlike allochthonous OM, I had no reason *a priori* to expect the isotopic composition of periphyton to vary spatially.

At FWSWI sites, $\delta^{13}\text{C}_{\text{FPOM}}$ values were significantly more negative than $\delta^{13}\text{C}_{\text{DOC}}$ values by 6.71‰ (Table 1.1), and a significant positive relationship between $\delta^{13}\text{C}_{\text{FPOM}}$ and $\delta^{13}\text{C}_{\text{DIC}}$ values was observed (Table 1.1; Fig. 1.4F), with the average $\delta^{13}\text{C}_{\text{FPOM}}$ value being 28.44‰ lower than the average $\delta^{13}\text{C}_{\text{DIC}}$ value. No relationship between $\delta^{13}\text{C}_{\text{FPOM}}$ values and C:N ratios was observed at FWSWI sites, although sample size was small (Table 1.1; Fig. 1.4E). At FWSWI sites, strong correlations were observed between $\delta^{13}\text{C}_{\text{DIC}}$ values, conductivity and concentrations of several dissolved ions, including sulfide, ammonia, chloride, sulfate, lithium, sodium, potassium, magnesium, and calcium ($r > 0.70$), but not between $\delta^{13}\text{C}_{\text{DIC}}$ values/conductivity and other physicochemistry measurements (pH, temperature, δD , $\delta^{18}\text{O}$, manganese, barium, fluoride, nitrite, and nitrate concentrations) ($r < 0.5$). At FWSWI sites, both $\delta^{13}\text{C}_{\text{DIC}}$ values (at sites with conductivity $< 4000\mu\text{S}/\text{cm}$) and $\delta^{13}\text{C}_{\text{FPOM}}$ values increased from southwest to northeast (Table 1.1; Fig. 1.4G-H). AIC strongly suggested that a linear model incorporating location, log conductivity, and an interaction term was substantially more likely than nested models (AIC weight $\gg 1$); all parameters were significant.

Temporal changes in $\delta^{13}\text{C}_{\text{FPOM}}$ values were observed at both recharge streams and FWSWI sites. Stream $\delta^{13}\text{C}_{\text{FPOM}}$ values increased between 30 September 2010 and 20 March 2012, although the strength of the relationship varied greatly among streams ($r^2 = 0.01$ to 0.98) (Table 1.1; Fig. 1.5). This decrease did not correspond directly with stream discharge or PDSI, as the last two sampling events (late January and late March, 2012) followed precipitation events that resulted in increased flow in all sampled streams (Fig. 1.2). Visual assessment of CPOM and periphyton isotopic compositions did not indicate temporal patterns. FPOM C:N ratios in streams exhibited a weaker, but significant, negative relationship with time (Table 1.1). Unexpectedly, at FWSWI sites, $\delta^{13}\text{C}_{\text{FPOM}}$ values increased between 16 April 2011 and 2 April 2012. Again, the strength of the relationship varied between sites ($r^2 = -0.03$ to 0.96) (Table 1.1; Fig. 1.5). $\delta^{13}\text{C}_{\text{DIC}}$ values at FWSWI sites showed no temporal trend (Table 1.1).

Discussion

The distribution and diversity of karst aquifer metazoan communities, as well as aquifer-wide food web structure, are influenced by OM that originates from, and migrates across, physical and geochemical boundaries. Research on the factors influencing DOM variability in karst aquifer systems has been limited, with previous work suggesting that OM flux into karst groundwater varies temporally based on precipitation and OM composition in soil and epikarst dripwaters (van Beynen *et al.* 2000; Datry *et al.* 2005; Ban *et al.* 2008), and the relative contributions of photosynthetic and chemolithoautotrophic OM are spatially variable (Sarbu *et al.* 1996; Opsahl & Chanton 2006; Birdwell & Engel 2009; Roach *et al.* 2011; Neisch *et al.* 2012). The isotopic

compositions of OM in Edwards Aquifer recharge and aquifer waters, and the spatial and temporal variability in OM sources into the aquifer, have not been previously assessed, even though they support one of the richest stygobiont communities on Earth (Longley 1981). I hypothesized that OM in the Edwards Aquifer would be influenced by 1) the relative proportion of C3 and C4 plant OM in recharging streams that changes in response to an east-west precipitation gradient, 2) FWSWI $\delta^{13}\text{C}_{\text{FPOM}}$ values that reflect regional differences in $\delta^{13}\text{C}_{\text{DIC}}$ values due to chemolithoautotrophic production, 3) the importance of OM from periphyton and riparian C3 plants in recharge streams that increases during the dry season, and 4) the constant composition of OM at the FWSWI over time.

Contributions of organic matter from surface recharge

Two of our hypotheses focus on the contribution of OM from recharge (H1 & H3).

Numerous factors influence the relative importance of allochthonous and autochthonous OM in streams, including stream width and riparian cover (Vannote *et al.* 1980), land cover and the quantity of allochthonous input (Benfield 1997), and nutrient availability (Biggs 1995). The importance of these factors in Edwards Aquifer recharge streams is unknown, but the decrease in $\delta^{13}\text{C}_{\text{FPOM}}$ values and FPOM C:N ratios in recharging streams during the summer of 2011, and the negative relationship between FPOM C:N ratios and $\delta^{13}\text{C}_{\text{FPOM}}$ values (Figs. 4 - 5) may suggest that the observed temporal isotopic shift in FPOM results from a decrease in the relative contribution of allochthonous OM and an increase in the relative contribution of periphyton. This shift could result from decreased allochthonous input (i.e. both C3 and C4 plants), but is not likely to result from

increased in-stream productivity because $\delta^{13}\text{C}_{\text{FPOM}}$ minima values do not occur during spring and summer when periphyton growth is greatest (Finlay & Kendall 2007). Alternatively, the observed temporal pattern is consistent with a decrease in the relative contribution of C4 plants from beyond the riparian zone because of a decline in overland flows and a subsequent increase in allochthonous input from the C3 dominated riparian zone, as has been documented for a river in Cameroon (Bird *et al.* 1998). Decreasing $\delta^{13}\text{C}_{\text{FPOM}}$ values in streams continued through increased flows in winter and spring of 2012, although the pattern was inconsistent among streams (Figs. 2 & 5). In particular, $\delta^{13}\text{C}_{\text{FPOM}}$ values from the Sabinal River changed minimally after an initial decrease after September 2010. A small increase in $\delta^{13}\text{C}_{\text{FPOM}}$ values in the Sabinal and Blanco Rivers corresponded to increased flow in winter and spring of 2012, but this was not observed in Helotes Creek. Spring and stream hydrographs and the PDSI show 2-3 year oscillations with wetter than normal periods corresponding to El Niño periods (Fig. 1.2), and the general trend of declining stream $\delta^{13}\text{C}_{\text{FPOM}}$ values may be linked to these longer ENSO time-scale trends in stream discharge. The relatively small increase in discharge in winter and spring of 2012, and the negative trend in $\delta^{13}\text{C}_{\text{FPOM}}$ values, were embedded within a longer drying trend, as illustrated by the PDSI values from spring of 2011 through December 2012 (Fig. 1.2).

Although the relationship was weak, stream $\delta^{13}\text{C}_{\text{FPOM}}$ values became more enriched from southwest to northeast (Table 1.1, Fig. 1.4), which does not support our hypothesis of increasing contributions of C3 plant material in the northeast. Furthermore, the lack of spatial gradients in $\delta^{13}\text{C}_{\text{periphyton}}$ and $\delta^{13}\text{C}_{\text{DIC}}$ values, and of a significant regression

between $\delta^{13}\text{C}_{\text{FPOM}}$ and $\delta^{13}\text{C}_{\text{DIC}}$ values (Table 1.1, Fig. 1.4), indicates that the observed spatial gradient in $\delta^{13}\text{C}_{\text{FPOM}}$ values is not the result of spatial differences in $\delta^{13}\text{C}_{\text{periphyton}}$ values that would result from regional differences in $\delta^{13}\text{C}_{\text{DIC}}$ values. Rather, the observed gradient may indicate decreasing contributions of periphyton and increased contributions of terrestrial plant OM in the northeast, although our data do not allow for estimated proportions because of the large degree of overlap in $\delta^{13}\text{C}_{\text{CPOM}}$ and $\delta^{13}\text{C}_{\text{periphyton}}$ values.

The estimated discharge-weighted average value for $\delta^{13}\text{C}_{\text{FPOM}}$ entering streams (-21.75‰) was similar to the unweighted average, yet the employed Bayesian method of estimation has several advantages to an unweighted analytical average. Most obviously, an unweighted analytical average can over-emphasize values collected during low recharge periods and under-emphasize values collected during high recharge periods. Secondly, this method incorporates uncertainty associated with individual isotopic measurements, allowing for calculation of 95% equal tail credible intervals. Finally, although not investigated here, the model has potential for incorporation of increased complexity. Specifically, the relationship between the amount of OM entering the aquifer and discharge could be modeled non-linearly (e.g., it may reach an asymptote at some discharge threshold), and the relationship between the amount of OM entering the aquifer and discharge could be modelled to vary among streams.

Contributions of organic matter from the FWSWI

The juxtaposition of reduced electron donors (e.g., H_2S) and electron acceptors (e.g., O_2 , NO_3^-) at the FWSWI, coupled with a plentiful source of inorganic carbon source (DIC as

HCO₃⁻ and CO₂) from carbonate dissolution support chemolithoautotrophic metabolic processes. Pronounced differences in OM dynamics between recharge stream and FWSWI well waters were revealed through isotope analysis. $\delta^{13}\text{C}_{\text{FPOM}}$ values were significantly more negative at FWSWI sites than in recharging streams (Table 1.1, Fig. 1.3), which suggests strong isotopic discrimination against ¹³C during autotrophic C fixation. I hypothesized that chemolithoautotrophic production occurred along the FWSWI, based on identification of putative sulfur-oxidizing microbial groups from the FWSWI (e.g., *Epsilonproteobacteria*, *Thiothrix* spp., *Thiobacillus* spp.) (Engel & Randall 2011; Gray & Engel 2013). The results support our hypothesis, and also corroborate previous findings that microbial, rather than surface (i.e. plant), humic-like, OM is present at the FWSWI (Birdwell & Engel 2009). However, the positive relationship between $\delta^{13}\text{C}_{\text{FPOM}}$ and $\delta^{13}\text{C}_{\text{DIC}}$ at FWSWI sites (Fig. 1.4) illustrates that C isotope data alone are insufficient to quantify the relative proportions of photosynthetic and chemolithoautotrophic OM in a sample. Several factors influence the isotopic composition of chemolithoautotrophic OM, including the isotopic signature of the C substrate, C limitation (Cowie *et al.* 2009), C fixation rate (Laws *et al.* 1995), and the C fixation pathway utilized (Berg *et al.* 2010).

The 6.71‰ difference between $\delta^{13}\text{C}_{\text{FPOM}}$ and $\delta^{13}\text{C}_{\text{DOC}}$ values at FWSWI sites could be the result of several processes. Relative to DOM, CPOM and FPOM are not transported great distances into groundwater systems (Simon *et al.* 2003), so FWSWI DOC may be comprised of a greater proportion of surface derived, photosynthetic OM. Alternatively, DOC may represent more processed or recalcitrant OM. In soils, preferential metabolism

of ^{12}C in OM during decomposition can increase $\delta^{13}\text{C}_{\text{OM}}$ by 1-3‰ (Boström *et al.* 2007). To our knowledge, however, this has not been documented for groundwater. Lastly, the values may suggest additional C assimilation due to methanotrophy (Whiticar 1999). Although analysis of the spatial distribution of CH_4 in the Edwards Aquifer saline zone has not been studied in detail, Zhang *et al.* (1998) report a positive relationship between CH_4 and SO_4^{2-} concentrations in the saline zone, and I cannot rule out regional differences in CH_4 concentration that could influence regional variability in FWSWI $\delta^{13}\text{C}_{\text{OM}}$.

Reasons for the enrichment in FWSWI $\delta^{13}\text{C}_{\text{FPOM}}$ values between April 2011 and March 2012 (Fig. 1.5) are unclear, but heterotrophic processing of OM is insufficient to account for the observed isotopic differences, as much as 18‰. The observed temporal changes could be the result of changing contributions of OM produced in geochemically distinct portions of the aquifer. These changes may be the result of declining aquifer levels and variability in flow along the FWSWI due to drought; however, there are currently no data to support this hypothesis.

The significant positive relationship between $\delta^{13}\text{C}_{\text{DIC}}$ and $\delta^{13}\text{C}_{\text{FPOM}}$ values (Table 1.1, Figs. 4) supports our prediction that regional differences in $\delta^{13}\text{C}_{\text{DIC}}$ values, the substrate for chemolithoautotrophic production, affect $\delta^{13}\text{C}_{\text{FPOM}}$ values. $\delta^{13}\text{C}_{\text{DIC}}$ values at FWSWI sites increased from southwest to northeast for sites with conductivity < 4000 $\mu\text{S}/\text{cm}$ (Fig. 1.4H) and showed no significant temporal variation. This trend mirrors patterns in stable isotopes of helium (Hunt *et al.* 2010), which were interpreted as evidence of increasing

groundwater residence times from the southwest to northeast. Increased residence times, and subsequent increased time for rock-water interaction, can shift $\delta^{13}\text{C}_{\text{DIC}}$ values towards the isotopic composition of the host rock ($\sim -2\text{‰}$ for Edwards carbonates) (Ellis 1985; Gonfiantini & Zuppi 2003).

Variable sources of acidity may also have an important role in the isotopic composition of FWSWI $\delta^{13}\text{C}_{\text{DIC}}$ values. Dissolution of calcite by carbonic acid (derived from CO_2 respired during decomposition of plant matter in soils and/or hyporheic zones) results in DIC with a $\delta^{13}\text{C}$ value intermediate between that of the calcite and carbonic acid (Finlay 2003; Brecker *et al.* 2012). Dissolution of Edwards limestones by carbonic acid derived from respired CO_2 will produce DIC with $\delta^{13}\text{C}$ values $\sim -10\text{‰}$ for calcite-saturated water, as well as alkalinities and Ca^{2+} concentrations similar to those observed in surface streams (appendix 1). However, DIC sourced from dissolution of calcite by an acid other than carbonic acid (e.g., sulfuric acid) will have an isotopic composition closer to that of the host rock, as is observed in FWSWI sites. The strong positive relationship between FWSWI $\delta^{13}\text{C}_{\text{DIC}}$, conductivity (Fig. 1.4H), and sulfide, supports the hypothesis that dissolution in low conductivity freshwaters is driven by carbonic acid, and in high conductivity saline waters (with locally high levels of sulfide ~ 100 mg/L), dissolution is driven by sulfuric acid derived from microbially mediated oxidation of reduced sulfur compounds (Gray & Engel 2013).

Conclusion

Groundwater ecosystems can be supported, at least in part, by allochthonous OM input from the surface, whereby the composition and supply rate is temporally variable and dependent on water balance conditions at the surface. In streams supplying allochthonous OM to the Edwards Aquifer, $\delta^{13}\text{C}_{\text{FPOM}}$ values and FPOM C:N ratios decreased during and after a severe drought in 2011, suggesting a diminished contribution of terrestrial plant material (especially C4 material from beyond the riparian zone) and an increasing contribution of in-stream production. A spatial gradient in stream $\delta^{13}\text{C}_{\text{FPOM}}$ values due to changes in the relative abundance of C3 and C4 plants was not apparent. Weighting $\delta^{13}\text{C}_{\text{FPOM}}$ values for FPOM input into aquifers by recharge provides a more realistic estimate, and quantification of uncertainty around estimates is both important and straightforward using a Bayesian approach. In addition to allochthonous inputs, chemolithoautotrophy along the FWSWI is an important source of autochthonous OM, based on geochemical, microbial, and isotopic evidence. For the Edwards Aquifer, allochthonous and autochthonous OM sources were, on average, isotopically distinct, although the isotopic composition of chemolithoautotrophic OM was spatially variable and dependent on the isotopic composition of DIC. Additional research is needed to understand the degree to which the distinct OM sources are utilized by the diverse microbial and metazoan community in the Edwards Aquifer, as well as to characterize the OM geochemically (e.g., through high-resolution spatial analyses of OM isotopic composition and degree of humification). These analyses would allow for better quantification of the relative proportions of allochthonous and autochthonous OM throughout the aquifer.

Acknowledgements

This research was funded by the National Science Foundation (#0742306; #1110503) the U.S. Geological Survey (#9658-11), and the Jones Endowment for Aqueous Geochemistry at the University of Tennessee. The San Antonio Water System, The Edwards Aquifer Authority, Zara Environmental, and several private landowners provided or facilitated access to sampling sites. Kevin Simon and an anonymous reviewer provided valuable comments during the revision of this manuscript.

References

- Artman, U., J. A. Waringer & M. Schagerl, 2003: Seasonal dynamics of algal biomass and allochthonous input of coarse particulate organic matter in a low-order sandstone stream (Weidlingbach, Lower Austria).- *Limnologia*, 33: 77-91.
- Ban, F., G. Pan, J. Zhu, B. Cai & M. Tan, 2008: Temporal and spatial variations in the discharge and dissolved organic carbon of drip waters in Beijing Shihua Cave, China.- *Hydrological Processes*, 22: 3749-3758.
- Barker, R. A., P. W. Bush & E. T. Baker, Jr., 1994: Geologic History and Hydrogeologic Setting of the Edwards-Trinity Aquifer System, West-Central Texas.- United States Geological Survey, Report number: Water Resources Investigations Report 94-4039.
- Benfield, E. F., 1997: Comparison of litterfall input to streams.- *Journal of the North American Benthological Society*, 16: 104-108.
- Benjamini, Y. & Y. Hochberg, 1995: Controlling the False Discovery Rate: A Practical and Powerful Approach to Multiple Testing.- *Journal of the Royal Statistical Society*, 57: 289-300.
- Berg, I. A., D. Kockelkorn, W.H. Ramos-Vera, R. F. Say, J. Zarzycki, M. Hügler, B. E. Alber & G. Fuchs, 2010: Autotrophic carbon fixation in Archaea.- *Nature Reviews Microbiology*, 8: 447-460.
- Biggs, B. J. F., 1995: The Contribution of Flood Disturbance, Catchment Geology and Land Use to the Habitat Template of Periphyton in Stream Ecosystems.- *Freshwater Biology*, 33: 419-438.
- Bird, M. I., P. Giresse, & S. Ngos, 1998: A seasonal cycle in the carbon-isotope composition of organic carbon in the Sanaga River, Cameroon.- *Limnology and Oceanography*, 43: 143-146.
- Birdwell, J. E. & A. S. Engel, 2009: Variability in Terrestrial and Microbial Contributions to Dissolved Organic Matter Fluorescence in the Edwards Aquifer, Central Texas.- *Journal of Cave and Karst Studies*, 71: 144-156.
- Boström, B., D. Comstedt & A. Ekblad, 2007: Isotope Fractionation and ¹³C Enrichment in Soil Profiles During the Decomposition of Soil Organic Matter.- *Oecologia*, 153: 89-98.
- Breeker, D. O., A. E. Payne, J. Quade, J. L. Banner, C. E. Ball, K. W. Meyer, & B. D. Cowan, 2012: The sources and sinks of CO₂ in caves under mixed woodland and grassland vegetation.- *Geochimica et Cosmochimica Acta*, 96: 230-246.

- Bukovinskey, T., A. M. Verschoor, N. R. Helmsing, T. M. Bezemer, E. S. Bakker, M. Vos, & L. N. de Senerpont Domis, 2012: The Good, the Bad and the Plenty: Interactive Effects of Food Quality and Quantity on the Growth of Different *Daphnia* Species.- PLOS ONE, 7: e42966.
- Cowie, B. R., G. F. Slater, L. Bernier & L. A. Warren, 2009: Carbon Isotope Fractionation in Phospholipid Fatty Acid Biomarkers of Bacteria and Fungi Native to an Acid Mine Drainage Lake.- Organic Geochemistry, 40: 956-962.
- Culver, D. C. & T. Pipan, 2009: *The Biology of Caves and Other Subterranean Habitats*.- The Biology of Habitats, Oxford University Press, pp. 254, Oxford.
- Datry, T., F. Malard & J. Gibert, 2005: Response of invertebrate assemblages to increased groundwater recharge rates in a phreatic aquifer.- Journal of the North American Benthological Society, 24: 461-477.
- Doctor, D. H., C. Kendall, S. D. Sebestyen, J. B. Shanley, N. Ohte & E. W. Boyer, 2008: Carbon Isotope Fractionation of dissolved Inorganic Carbon (DIC) Due to Outgassing of Carbon Dioxide from a Headwater Stream.- Hydrological Processes, 22: 2410-2423.
- Ellis, P. M., 1985: *Diagenesis of the Lower Cretaceous Edwards Group in the Balcones Fault Zone Area, South-Central Texas*.- PhD thesis, University of Texas at Austin, pp. 326.
- Engel, A. S. & K. W. Randall, 2011: Experimental Evidence for Microbially Mediated Carbonate Dissolution from the Saline Water Zone of the Edwards Aquifer, Central Texas.- Geomicrobiology Journal, 28: 313-327.
- Finlay, J. C., 2003: Controls of Streamwater Dissolved Inorganic Carbon Dynamics in a Forested Watershed.- Biogeochemistry, 62: 231-252.
- Finlay, J. C. & C. Kendall, 2007: Stable Isotope Tracing of Temporal and Spatial Variability in Organic Matter Sources to Freshwater Ecosystems.- In: Michener, R. & K. Lajtha (eds.) *Stable Isotopes in Ecology and Environmental Science*, Blackwell Publishing, pp. 283-333, Malden.
- Gary, M. O., R. H. Gary & B. B. Hunt (eds.), 2011: *Interconnection of the Trinity (Glen Rose) and Edwards Aquifers Along the Balcones Fault Zone and Related Topics, Karst Conservation Initiative February 17, 2011 Meeting Proceedings*, pp. 46, Austin.
- Gelman, A. & D. B. Rubin, 1992: Inference from Iterative Simulation Using Multiple Sequences.- Statistical Science, 7: 457-472.

- Gonfiantini, R. & G. M. Zuppi, 2003: Carbon Isotope Exchange Rate of DIC in Karst Groundwater.- *Chemical Geology*, 197: 319-336.
- Gray, C. J. & A. S. Engel, 2012: Microbial Diversity and Impact on Carbonate Geochemistry Across a Changing Geochemical Gradient in a Karst Aquifer.- *The ISME Journal*, 7: 325-337.
- Humphreys, W., S. Tetu, L. Elbourne, M. Gillings, J. Seymour, J. Mitchell & I. Paulsen, 2012: Geochemical and Microbial Diversity of Bundera Sinkhole, an Anchialine System in the Eastern Indian Ocean.- *Natura Croatica*, 21: 59-63.
- Hunt, A. G., R. B. Lambert, L. Fahlquist, 2010: *Sources of Groundwater Based on Helium Analyses in and Near the Freshwater/ Saline-Water Transition Zone of the San Antonio Segment of the Edwards Aquifer, South-Central Texas, 2002-03*.- United States Geological Survey, Report Number: Scientific Investigations Report 2010-5030
- Jasinska, E. J., B. Knott, A. J. McComb, 1996: Root Mats in Ground Water: A Fauna-Rich Cave Habitat.- *Journal of the North American Benthological Society*, 15: 508-519.
- Johnson, S., G. Schindel, J. Hoyt, 2009: *Water Quality Trends Analysis of the San Antonio Segment, Balcones Fault Zone Edwards Aquifer, Texas*.- Edwards Aquifer Authority, Report Number: 09-03.
- Laws, E. A., B. N. Popp, R. R. Bidigare, M. C. Kennicutt & S. A. Macko, 1995: Dependence of Phytoplankton Carbon Isotopic Composition on Growth Rate and $[CO_2]_{aq}$: Theoretical Considerations and Experimental Results.- *Geochimica et Cosmochimica Acta*, 59: 1131-1138.
- Lindgren, R. J., A. R. Dutton, S. D. Hovorka, S. R. H. Worthington & S. Painter, 2004: *Conceptualization and Simulation of the Edwards Aquifer, San Antonio Region, Texas*.- United States Geological Survey, Report Number: Scientific Investigations Report 2004-5277.
- Neisch, J. A., J. W. Pohlman & T. M. Iliffe, 2012: The use of stable and radiocarbon isotopes as a method for delineating sources of organic material in anchialine systems.- *Natura Croatica*, 21: 83-85.
- Nielsen-Gammon, J. W., 2008: The Changing Climate of Texas.- In: Schmandt, J., J. Clarkson & G. R. North (eds.) *The Impact of Global Warming on Texas*, 2nd edition. University of Texas Press, pp. 39-68, Austin.

- Oetting, G. C., J. L. Banner & J. M. Sharp, Jr., 1996: Regional Controls on the Geochemical Evolution of Saline Groundwaters in the Edwards Aquifer, Central Texas.- *Journal of Hydrology*, 181: 251-283.
- Opsahl, S. P. & J. P. Chanton, 2006: Isotopic evidence for methane-based chemosynthesis in the Upper Floridan aquifer food web.- *Oecologia*, 150: 89-96.
- Palmer, W. C., 1965: Meteorologic drought.- U.S. Weather Bureau, Resource Paper 45.
- Perez, R., 1986: *Potential for Updip Movement of Saline water in the Edwards Aquifer, San Antonio, Texas*.- United States Geological Survey, Report Number: Water-Resources Investigations Report 86-4032.
- Pinheiro, J., D. Bates, S. DebRoy & D. Sarkar, 2009: nlme: Linear and Nonlinear Mixed Effects Models. R package version 3,1-96.- R Foundation for Statistical Computing, Vienna.
- Plummer, M., 2010: rjags: Bayesian Graphical Models Using MCMC.- R package version 2.1, 0-10.
- Pohlman, J. W., T. M. Iliffe & L. A. Cifuentes, 1997: A Stable Isotope Study of Organic Cycling and the Ecology of an Anchialine Cave Ecosystem.- *Marine Ecology Progress Series*, 155: 17-27.
- Poulson, T. L., 2005: Food Sources.- In: Culver, D. C. & W. B. White (eds.) *Encyclopedia of Caves*. Elsevier Academic Press, pp. 255-263, Amsterdam.
- Poulson, T. L. & K. H. Lavoie, 2000: The Trophic Basis of Subsurface Ecosystems.- In: Wilkens, H., D. C. Culver & W. F. Humphreys (eds.) *Subterranean Ecosystems*. Ecosystems of the World 30. Elsevier Academic Press, pp. 231-250, Amsterdam.
- R Core Team, 2012: R: A Language and Environment for Statistical Computing.- R Foundation for Statistical Computing, Vienna.
- Roach, K. A., M. Tobler & K. O. Winemiller, 2011: Hydrogen sulfide, bacteria, and fish: a unique, subterranean food chain.- *Ecology*, 92: 2056-2062.
- Saito, L., C. Redd, S. Chandra, L. Atwell, C. H. Fritsen and M. R. Rosen, 2007: Quantifying Food web Interactions with Simultaneous Linear Equations: Stable Isotope Models of the Truckee River, USA.- *Journal of the North American Benthological Society*, 26: 642-662.
- Sarbu, S. M., T. C. Kane & B. K. Kinkle, 1996: A Chemoautotrophically Based Cave Ecosystem.- *Science*, 272: 1953-1955.

- Short, R. A., S. L. Smith, D. W. Guthrie, J. A. Stanford, 1984: Leaf litter processing rates in four Texas streams.- *Journal of Freshwater Ecology*, 2: 469-473.
- Silva, M. S., L. F. de Oliveira Bernardi, R. P. Martins & R. L. Ferreira, 2012: Transport and Consumption of Organic Detritus in a Neotropical Limestone Cave.- *Acta Carsologica*, 41: 139-150.
- Simon, K. S., E. F. Benfield & S. A. Macko, 2003: Food Web Structure and the Role of Epilithic Biofilms in Cave Streams.- *Ecology*, 84: 2395-2406.
- Simon, K. S., T. Pipan & D. C. Culver, 2007: A Conceptual Model of the Flow and Distribution of Organic Carbon in Caves.- *Journal of Cave and Karst Studies*, 69: 279-284.
- Stribling, J. M. & J. C. Cornwell, 1997: Identification of Important Primary Producers in a Chesapeake Bay Tidal Creek System Using Stable Isotopes of Carbon and Sulfur.- *Estuaries*, 20: 77-85.
- van Beynen, P. v., D. Ford & H. Schwarcz, 2000: Seasonal variability in organic substances in surface and cave waters at Marengo Cave, Indiana.- *Hydrological Processes*, 14: 1177-1197.
- van Dover, C. L., 2007: Stable isotope studies in marine chemoautotrophically based ecosystems: an update.- In: Michener, R. & K. Lajtha (eds.) *Stable Isotopes in Ecology and Environmental Science*, Blackwell Publishing, pp. 202-237, Malden.
- Vannote, R. L., G. W. Minshall, K. W. Cummins, J. R. Sedell & C. E. Cushing, 1980: The River Continuum Concept.- *Canadian Journal of Fisheries and Aquatic Science*, 37: 130-137.
- Whiticar, M. J., 1999: Carbon and Hydrogen Isotope Systematics of Bacterial Formation and Oxidation of Methane.- *Chemical Geology*, 161: 291-314.
- Zhang, C., E. L. Grossman & J. W. Ammerman, 1998: Factors Influencing Methane Distribution in Texas Ground Water.- *Ground Water*, 36: 58-66.

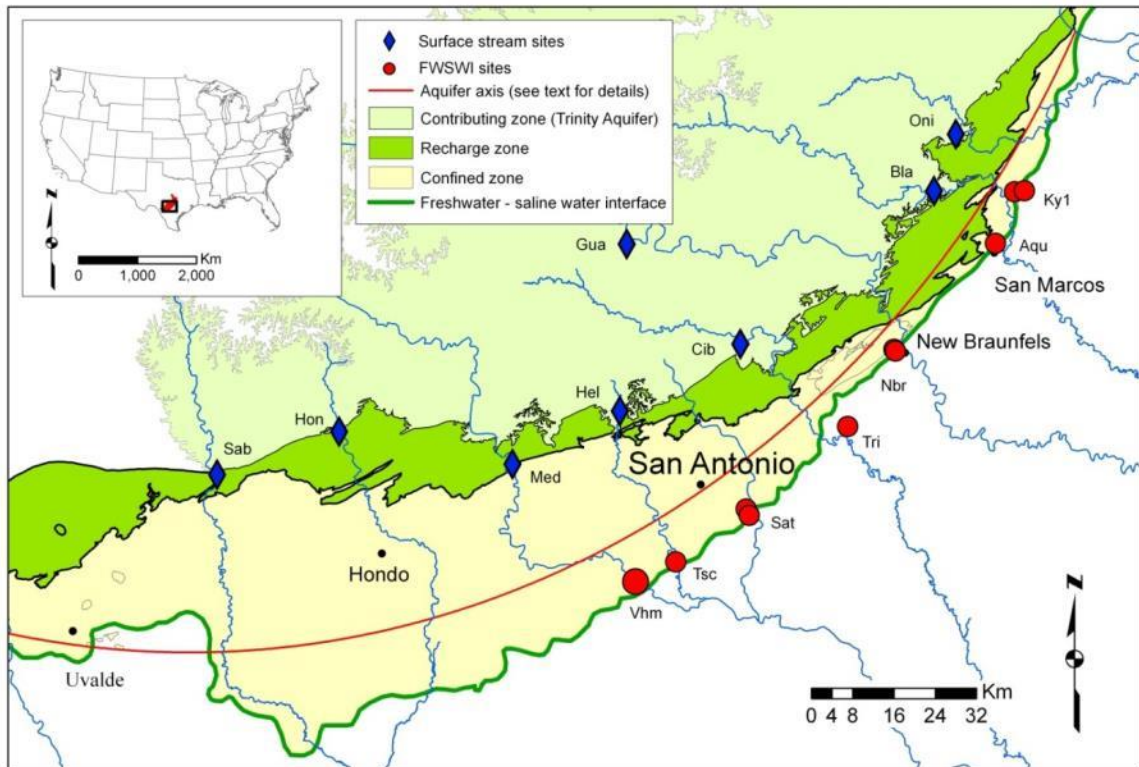


Figure 1.1: The Edwards Aquifer, formed in Cretaceous limestone, extends in a 400 km arc that varies from 4 to 56 km wide and 137 to 335 m thick. Uplift of the Edwards Plateau during the late Cretaceous and downwarping of the Gulf of Mexico during the early Cenozoic led to exposure of Edwards formation limestones at the northern and western boundary of the aquifer (recharge zones) along west-east and southwest-northeast trending en echelon faults associated with the confined zone (Barker *et al.* 1994). Recharge stream sampling sites occur in or northwest of the recharge zone. Freshwater-saline water interface sampling sites occur along the freshwater-saline water interface. SAB = Sabinal Rv.; Hon = Hondo Cr.; Med = Medina Rv.; Hel = Helotes Cr.; Gua = Guadalupe Rv.; Bla = Blanco Rv.; Oni = Onion Cr.; Vhm = Verstuyft Home Farm well; Tsc = Tschirhart well; Sat = San Antonio transect wells 1 & 2; Tri = Tri-County 2 well; Nbr = Paradise Alley Shallow; Girl Scout Shallow; and Girl Scout Deep wells; Aqu = Aquarena well; Kyl = Kyle transect wells 1 & 2.

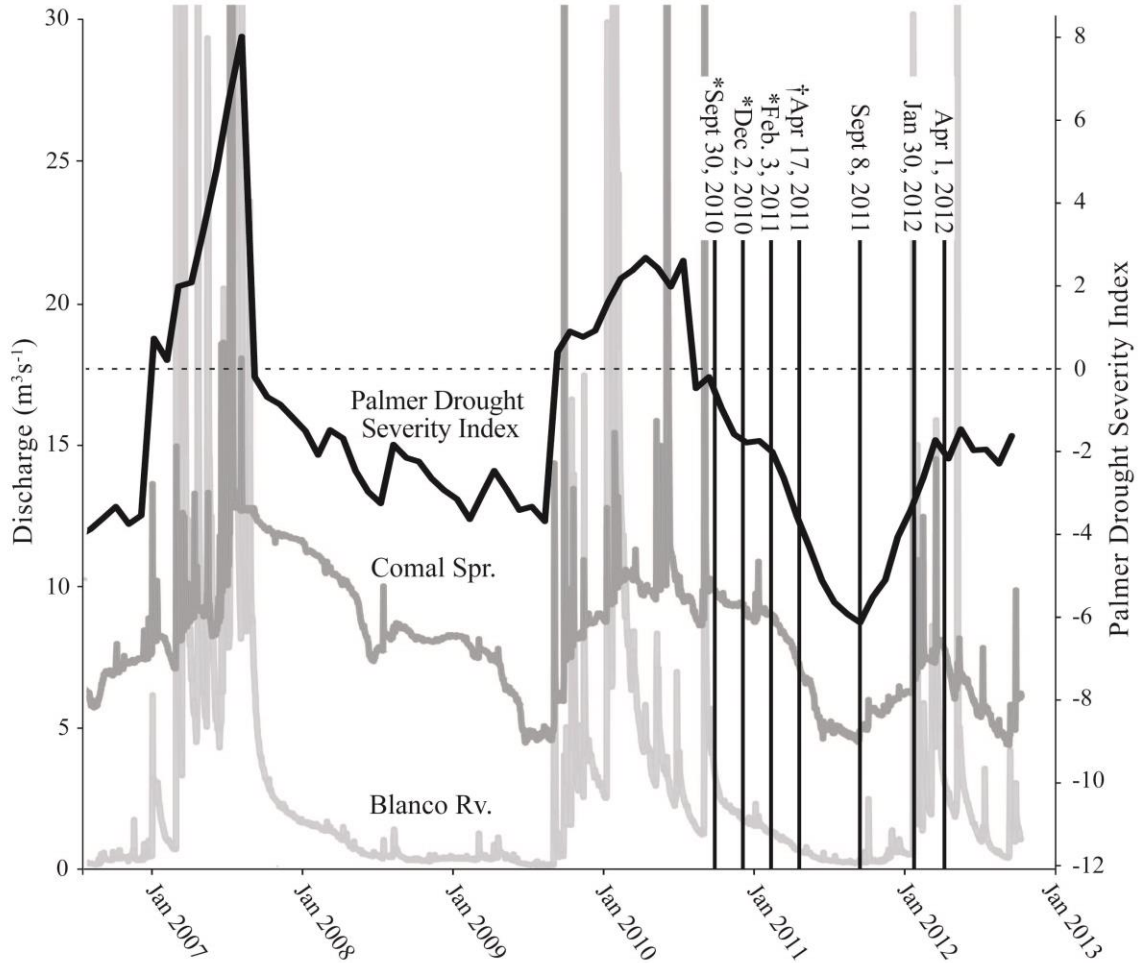


Figure 1.2: Hydrographs for Comal Springs (the largest Edwards Aquifer spring) (dark grey) and Blanco River (a major source of recharge) (light grey), and Palmer Drought Severity Index (PDSI) (black) values for Division 6, Edwards Plateau (as defined by the National Climate Data Center), January 2005 to January, 2013. Sampling events are shown by black vertical bars. * indicates stream sampling only. † indicates FWSWI site sampling only. Dashed horizontal line is PDSI = 0, representing normal conditions.

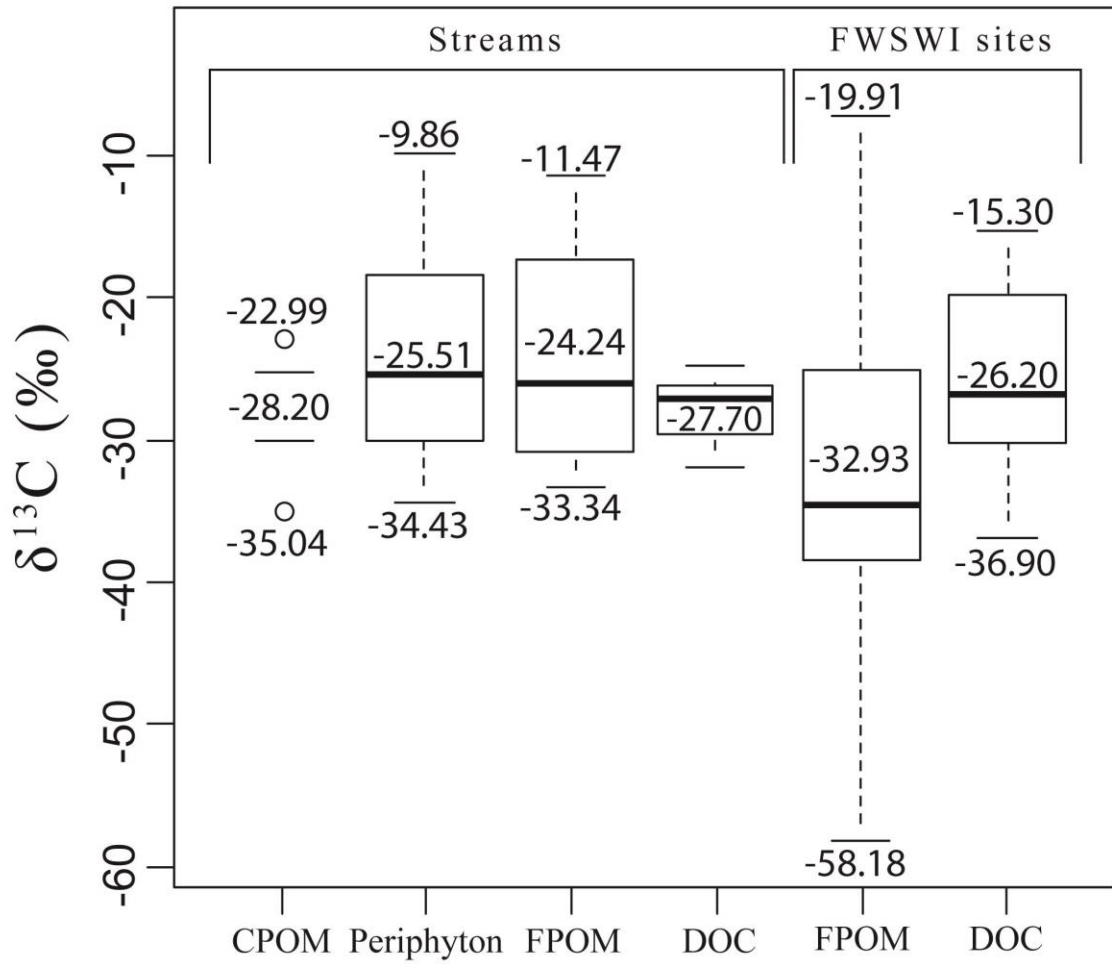


Figure 1.3: Boxplots for $\delta^{13}\text{C}$ values for different sampled OM fractions at stream sites and FWSWI sites.

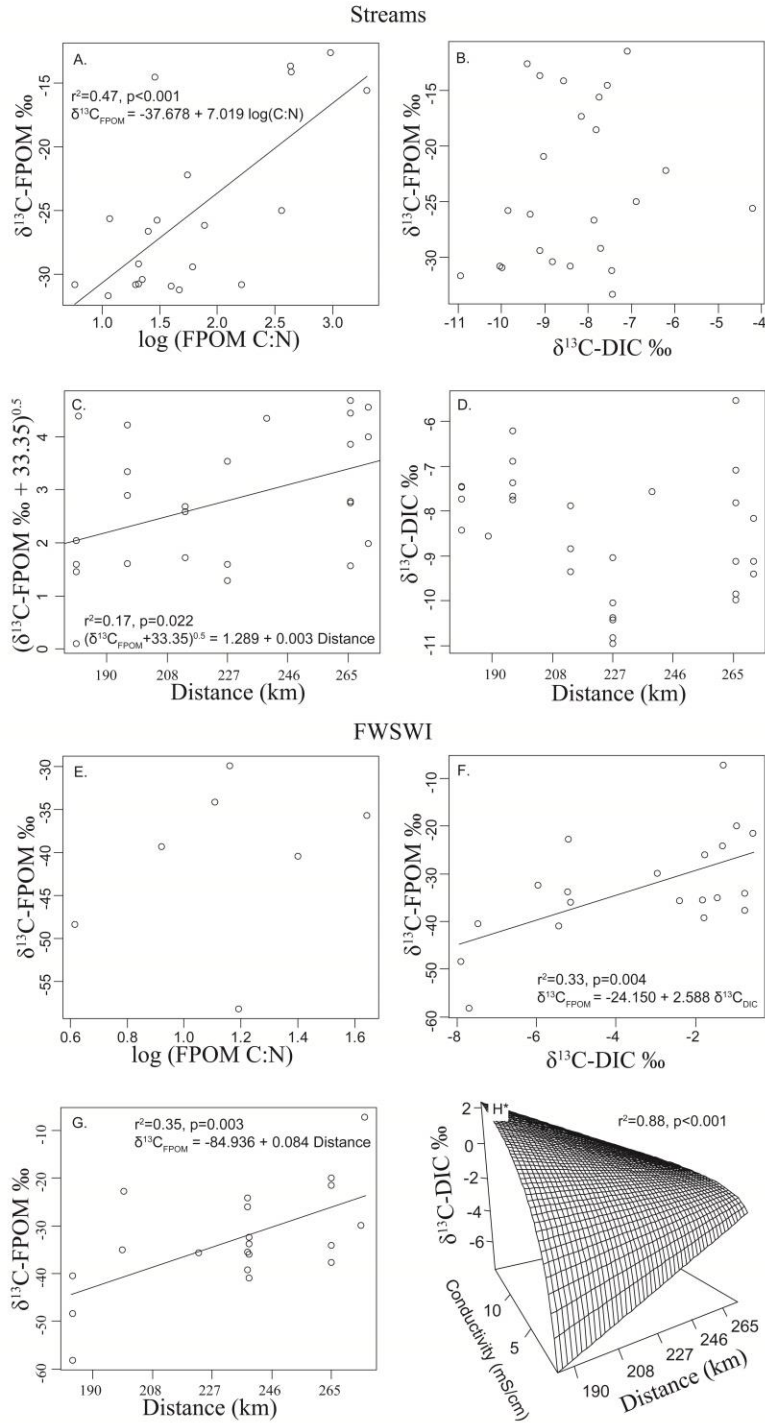


Figure 1.4: Regressions for stream sites (A-D) and FWSWI sites (E-H) of A and D: $\delta^{13}\text{C}_{\text{FPOM}}$ values against FPOM C:N ratios; B and F: $\delta^{13}\text{C}_{\text{FPOM}}$ values against $\delta^{13}\text{C}\text{-DIC}$ values; C and G: $\delta^{13}\text{C}\text{-FPOM}$ values versus distance along the Edwards Aquifer flowpath; D: $\delta^{13}\text{C}\text{-DIC}$ values versus distance; and H: $\delta^{13}\text{C}\text{-DIC}$ values versus distance and conductivity (multiple regression surface). All isotope values are reported in per mil (‰). Trendlines are shown for significant regressions. * $\delta^{13}\text{C}\text{-DIC} = -66.165 + 0.082$ distance + $7.808 \log(\text{conductivity}) - 0.010$ distance $\log(\text{conductivity})$

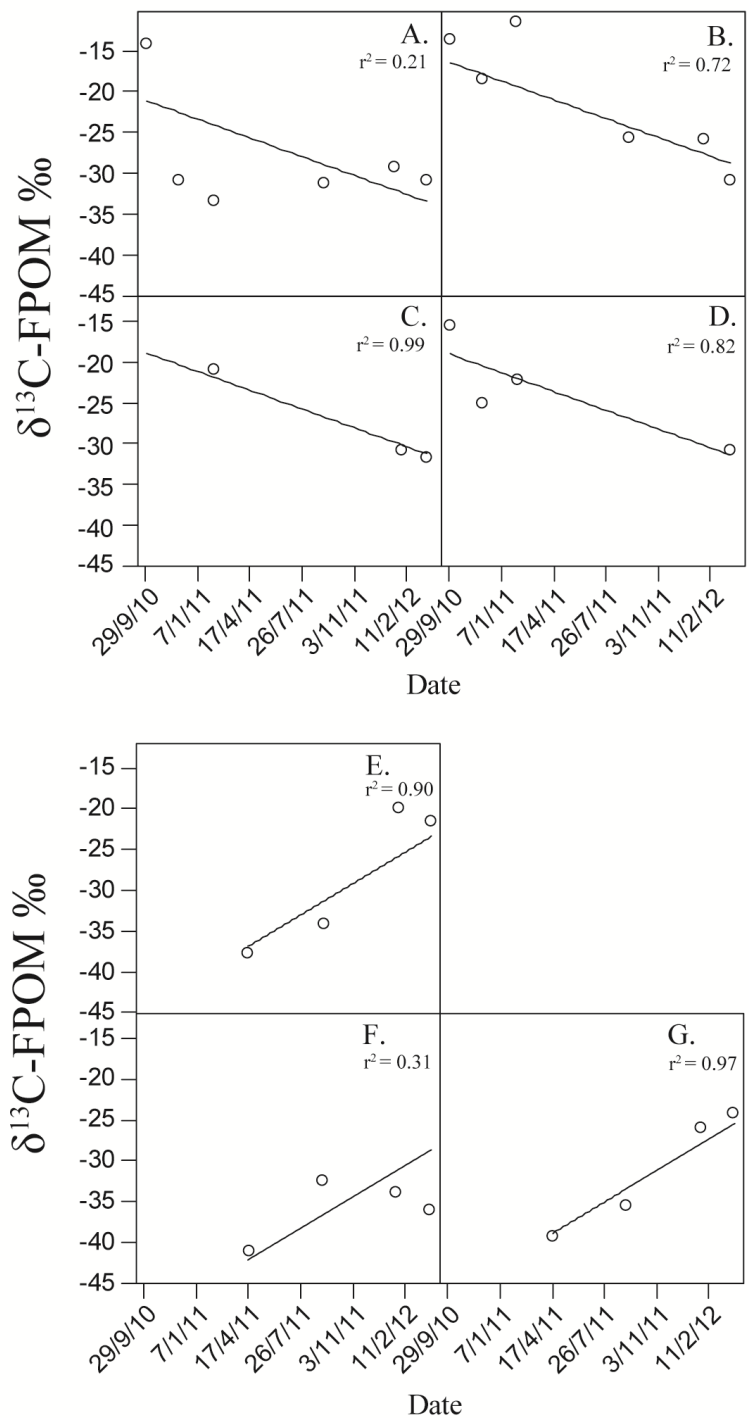


Figure 1.5: Results of linear mixed effects models for $\delta^{13}\text{C-FPOM}$ values versus time for stream sites (A-D), and FWSWI sites (E-G). A. Sabinal Rv.; B. Hondo Cr.; C. Helotes Cr.; D. Blanco Rv.; E. Aquarena parking lot well; F. Girl scout deep well; G. Paradise alley well. All isotope values are reported in per mil (‰). Note that mixed effect models assess relationships between $\delta^{13}\text{C-FPOM}$ and date using site as a grouping variable. Site-specific regressions may not be significant.

Table 1.1: Summary of statistical tests of predictions. 1: See text for hypotheses. * denotes statistically significant results.

Hypotheses ¹	Null predictions	Statistical analysis	F or t	N	df	p	r ²
1	Stream $\delta^{13}\text{C}$ -DIC is not related to location	simple linear regression	1.74	30	1 & 28	0.198	0.03
1	Stream $\delta^{13}\text{C}$ -FPOM is not related to location	simple linear regression	5.96	26	1 & 24	0.022*	0.17
1 & 3	Stream $\delta^{13}\text{C}$ -FPOM and $\delta^{13}\text{C}$ -DIC are not related	simple linear regression	0.62	24	1 & 22	0.439	-0.02
1 & 2	Stream and FWSWI $\delta^{13}\text{C}$ -DOC does not differ	ANCOVA	0.73	38	1	0.399	NA
1 & 2	Stream and FWSWI $\delta^{13}\text{C}$ -FPOM does not differ	ANCOVA	10.16	46	1	0.003*	NA
2	FWSWI $\delta^{13}\text{C}$ -DIC is not related to location	simple linear regression	20.17	26	1&24	<0.001*	0.43
2	FWSWI $\delta^{13}\text{C}$ -FPOM is not related to location	simple linear regression	11.19	20	1 & 18	0.004*	0.35
2	FWSWI $\delta^{13}\text{C}$ -FPOM and $\delta^{13}\text{C}$ -DIC are not related	simple linear regression	10.42	20	1 & 18	0.005*	0.33
2	FWSWI $\delta^{13}\text{C}$ -FPOM and FPOM C:N are not related	simple linear regression	0.41	7	1 & 5	0.552	-0.11
3	Stream $\delta^{13}\text{C}$ -OM fractions do not differ	ANOVA	2.66	89	3 & 85	0.053	NA
3	Stream $\delta^{13}\text{C}$ -FPOM does not change with time	linear mixed effect model	4.02	19	14	<0.001*	0.01 to 0.98
3	Stream FPOM C:N does not change with time	linear mixed effect model	2.72	17	12	0.019*	0.14 to 0.75
3	Stream $\delta^{13}\text{C}$ -FPOM and FPOM C:N are not related	simple linear regression	18.70	21	1 & 19	<0.001*	0.47
4	FWSWI $\delta^{13}\text{C}$ -FPOM and $\delta^{13}\text{C}$ -DOC do not differ	t test	2.44	44	28,577	0.021*	NA
4	FWSWI $\delta^{13}\text{C}$ FPOM does not change with time	linear mixed effect model	4.48	12	8	0.002*	-0.03 to 0.96
4	FWSWI $\delta^{13}\text{C}$ -DIC does not change with time	linear mixed effect model	0.16	18	13	0.874	NA

Appendices

Appendix 1: Physicochemical data average values (min/max) for recharge stream and FWSWI sites.

	Recharge Streams						
	Sab	Hon	Med	Hel	Gua	Bla	Oni
DO (mg/L)	8.29 (5.50/10.65)	8.98 (8.22/9.59)	8.00 (6.58/9.26)	8.41 (6.71/10.90)	9.14 (na)	9.76 (7.87/12.45)	9.19 (7.25/10.97)
pH	7.81 (7.05/8.37)	7.86 (7.46/8.11)	7.51 (7.13/8.05)	7.68 (6.95/8.14)	7.52 (na)	8.16 (7.40/9.44)	7.33 (7.23/7.54)
Cond (µS/cm)	405 (234/548)	312 (297/320)	411 (348/484)	538 (434/693)	349 (na)	432 (358/504)	445 (350/557)
T (C°)	16.42 (10.02/26.21)	10.69 (7.88/15.99)	18.20 (13.24/24.46)	16.69 (13.12/22.35)	8.17 (na)	14.74 (3.68/21.16)	13.26 (6.45/21.81)
δ¹³C_{DIC} (‰)	-7.92 (-8.56/-7.44)	-6.55 (-6.89/-6.21)	-8.67 (-9.34/-7.87)	-10.25 (-10.95/-9.03)	-7.55 (na)	-8.00 (-9.98/-4.20)	-8.88 (-9.40/-8.15)
δ¹³C_{DOC} (‰)	-30.0 (-32.0/-26.4)	-25.7 (na)	nm (nm)	-27.9 (-28.6/-27.2)	nm (nm)	-28.1 (-30.1/-26.4)	nm (nm)
δD (‰)	-16.59 (-20.76/-11.63)	-16.23 (-22.40/-11.83)	-16.34 (-24.38/-10.39)	-22.04 (-35.43/-11.71)	-20.11 (na)	-20.66 (-31.25/-12.54)	-26.63 (-33.98/-21.68)
δ¹⁸O(‰)	-2.86 (-3.41/-1.79)	-2.26 (-2.87/-1.60)	-2.13 (-3.73/-0.53)	-3.03 (-5.95/0.20)	-2.81 (na)	-2.97 (-5.32/-1.38)	-3.73 (-5.47/-1.79)
Sulfide (ppm S)	0.05 (0.04/0.06)	0.05 (na)	nm (nm)	0.05 (0.05/0.07)	nm (nm)	0.08 (0.05/0.16)	nm (nm)
FI (ppm)	0.16 (0.15/0.20)	0.20 (0.19/0.23)	0.18 (0.17/0.19)	0.11 (0.09/0.12)	0.24 (na)	0.21 (0.16/0.30)	0.20 (0.19/0.22)
Cl⁻ (ppm)	15.38 (6.09/20.54)	14.44 (12.40/15.87)	12.97 (11.90/13.62)	46.80 (15.07/76.14)	26.70 (na)	14.93 (13.78/15.45)	24.92 (21.07/27.66)
NO₂⁻ (ppm)	0.00 (0.00/0.00)	0.00 (0.00/0.00)	0.00 (0.00/0.00)	0.00 (0.00/0.00)	0.00 (na)	0.00 (0.00/0.00)	0.00 (0.00/0.00)
Br⁻ (ppm)	0.00 (0.00/0.00)	0.00 (0.00/0.00)	0.00 (0.00/0.00)	0.00 (0.00/0.00)	0.00 (na)	0.00 (0.00/0.00)	0.00 (0.00/0.00)
NO₃⁻ (ppm)	0.89 (0.00/3.12)	0.76 (0.43/1.27)	1.52 (1.14/2.12)	2.10 (0.00/8.04)	2.67 (na)	2.72 (0.00/8.58)	0.44 (0.00/1.17)
PO₄³⁻ (ppm)	0.00 (0.00/0.00)	0.00 (0.00/0.00)	0.00 (0.00/0.00)	0.00 (0.00/0.00)	0.00 (na)	0.00 (0.00/0.00)	0.00 (0.00/0.00)
SO₄²⁻ (ppm)	51.53 (29.21/107.6)	65.24 (52.95/76.78)	57.58 (53.80/60.20)	63.08 (21.87/115.9)	29.61 (na)	37.20 (26.07/56.65)	49.65 (40.34/55.73)
Alkalinity (ppm)	233.29 (152.79/295.72)	88.71 (na)	nm (nm)	194.68 (192.22/197.15)	256.29 (na)	156.07 (88.72/202.08)	nm (nm)
Li⁺ (ppm)	0.00 (0.00/0.01)	0.00 (0.00/0.01)	0.00 (0.00/0.00)	0.00 (0.00/0.01)	0.00 (na)	0.00 (0.00/0.01)	0.00 (0.00/0.00)
Na⁺ (ppm)	8.79 (5.51/10.77)	10.55 (9.97/11.56)	7.77 (7.37/8.15)	19.17 (8.16/26.14)	15.03 (na)	7.48 (5.51/8.74)	10.08 (9.17/11.33)
NH₄⁺ (ppm)	0.01 (0.00/0.09)	0.00 (0.00/0.00)	0.00 (0.00/0.00)	0.00 (0.00/0.00)	0.00 (na)	0.00 (0.00/0.03)	0.00 (0.00/0.00)
Ka⁺ (ppm)	1.29 (0.77/2.89)	1.45 (1.04/2.20)	1.46 (1.36/1.52)	1.42 (0.72/2.10)	1.54 (na)	1.34 (1.06/1.47)	1.11 (0.86/1.36)
Mg²⁺ (ppm)	12.00 (5.56/18.32)	8.77 (7.57/10.00)	12.01 (11.38/13.10)	15.40 (10.05/19.63)	27.53 (na)	16.92 (13.01/22.65)	15.95 (12.26/18.73)
Mn²⁺ (ppm)	0.00 (0.00/0.00)	0.00 (0.00/0.00)	0.00 (0.00/0.00)	0.00 (0.00/0.00)	0.00 (na)	0.00 (0.00/0.00)	0.00 (0.00/0.00)
Ca²⁺ (ppm)	62.28 (37.27/79.76)	55.77 (46.38/60.60)	60.58 (54.22/63.83)	63.41 (50.99/81.83)	61.47 (na)	51.87 (35.21/69.78)	73.08 (69.24/76.76)
Sr²⁺ (ppm)	0.58 (0.00/2.04)	0.25 (0.00/0.75)	0.00 (0.00/0.00)	0.33 (0.00/0.99)	0.00 (na)	0.67 (0.00/2.26)	0.00 (0.00/0.00)
Ba²⁺ (ppm)	0.07 (0.00/0.36)	0.00 (0.00/0.00)	0.00 (0.00/0.00)	0.01 (0.00/0.07)	0.00 (na)	0.09 (0.00/0.31)	0.00 (0.00/0.00)

Appendix 1 (cont.)

FWSWI Sites											
	Vhm	Tsc	Sat1	Sat2	Tri	Par	Gss	Gsd	Aqu	KylI	Kyl2
DO (mg/L)	2.62 (1.86/3.39)	1.06 (0.04/2.90)	0.00 (na)	0.00 (na)	0.00 (na)	0.21 (0.00/1.05)	0.00 (na)	0.05 (0.00/0.27)	0.06 (0.00/0.25)	0.06 (trace)	0.06 (trace)
pH	7.42 (na)	7.31 (7.24/7.38)	7.27 (na)	6.77 (na)	6.78 (na)	7.38 (6.90/8.10)	6.30 (na)	7.45 (7.26/7.83)	6.42 (6.23/6.51)	7.33 (7.08/7.59)	6.95 (6.92/6.98)
Cond (µS/cm)	769 (723/816)	549 (533/572)	991 (na)	3890 (na)	676 (na)	1796 (1250/2800)	504 (na)	534 (506/561)	14653 (14400/14806)	991 (937/1045)	6141 (6050/6233)
T (C°)	31.25 (30.10/32.41)	26.02 (24.9/27.52)	28.76 (na)	27.80 (na)	26.10 (na)	26.00 (25.62/26.20)	26.00 (na)	25.55 (24.89/26.23)	24.59 (24.14/25.00)	24.91 (24.85/24.98)	24.95 (24.91/25.00)
δ¹³C_{DIC} (‰)	-5.95 (-6.41/-5.50)	-7.45 (-7.91/-7.00)	-5.20 (na)	-1.46 (na)	-2.40 (na)	-1.65 (-1.82/-1.32)	-5.87 (na)	-5.38 (-5.97/-5.14)	-0.90 (-1.48/-0.55)	-3.02 (-3.08/-2.96)	-1.01 (-1.31/-0.72)
δ¹³C_{DOC} (‰)	nm (nm)	-24.6 (-31.2/-18.0)	-34.0 (na)	-30.4 (na)	-27.8 (na)	-25.1 (-30.0/-19.0)	-26.4 (na)	-27.1 (-33.1/-19.7)	-26.0 (-36.9/-19.4)	-27.6 (-36.4/-18.8)	-24.7 (-34.2/-15.3)
δD(‰)	-28.01 (-30.51/-25.52)	-25.40 (-27.25/-21.80)	nm (nm)	nm (nm)	-29.26 (na)	-25.85 (-27.72/-23.83)	-22.56 (na)	-23.05 (-27.72/-10.98)	-23.58 (-28.77/-5.77)	-22.19 (-24.71/-19.67)	-25.39 (-25.90/-24.88)
δ¹⁸O(‰)	-5.57 (-6.36/-4.78)	-4.12 (-4.79/-2.92)	nm (nm)	nm (nm)	-5.14 (na)	-4.51 (-5.07/-4.15)	-5.11 (na)	-3.40 (-5.03/1.25)	-3.28 (-5.33/3.58)	-3.70 (-4.16/-3.24)	-3.99 (-4.67/-3.32)
Sulfide (ppm S)	0.63 (na)	0.04 (0.02/0.07)	0.20 (na)	1.77 (na)	0.62 (na)	4.08 (2.39/6.00)	0.00 (na)	0.16 (0.09/0.31)	100.62 (79.75/114.66)	0.201 (0.16/0.24)	9.25 (8.00/10.50)
FI (ppm)	0.60 (0.50/0.71)	0.34 (0.33/0.36)	1.23 (na)	2.82 (na)	2.82 (na)	3.24 (3.01/3.46)	1.59 (na)	2.16 (1.63/2.47)	3.20 (2.91/3.34)	3.13 (3.06/3.21)	3.50 (3.26/3.76)
Cl⁻ (ppm)	55.02 (45.97/64.07)	32.08 (31.48/33.50)	106.32 (na)	826.36 (na)	2237.06 (na)	346.04 (280.00/378.04)	19.04 (na)	28.89 (26.02/34.74)	6241.76 (6080.67/6520.46)	12.23 (11.47/12.99)	2211.62 (2091.57/2331.68)
NO₂⁻ (ppm)	0.00 (0.00/0.00)	0.00 (0.00/0.00)	0.00 (na)	0.00 (na)	0.00 (na)	0.00 (0.00/0.00)	0.00 (na)	0.00 (0.00/0.00)	0.00 (0.00/0.00)	0.00 (0.00/0.00)	0.00 (0.00/0.00)
Br⁻ (ppm)	0.25 (0.24/0.26)	0.09 (0.00/0.21)	0.40 (na)	3.71 (na)	6.64 (na)	0.85 (0.00/1.22)	0.00 (na)	0.02 (0.00/0.12)	21.80 (21.24/22.42)	0.00 (0.00/0.00)	0.00 (11.42/12.72)
NO₃⁻ (ppm)	0.00 (0.00/0.00)	3.03 (0.00/5.44)	0.07 (na)	0.00 (na)	0.00 (na)	0.05 (0.00/0.21)	0.20 (na)	0.00 (0.00/0.00)	3.98 (0.00/8.31)	0.00 (0.00/0.00)	0.00 (0.00/0.00)
PO₄³⁻ (ppm)	0.00 (0.00/0.00)	0.00 (0.00/0.00)	0.00 (na)	4.73 (na)	5.77 (na)	0.00 (0.00/0.00)	0.00 (na)	0.00 (0.00/0.00)	0.00 (0.00/0.00)	0.00 (0.00/0.00)	0.00 (0.00/0.00)
SO₄²⁻ (ppm)	106.69 (82.06/131.33)	40.18 (39.68/41.37)	221.38 (na)	1571.44 (na)	1776.86 (na)	437.13 (290.65/731.05)	51.44 (na)	50.74 (47.34/56.60)	3607.36 (3431.43/3741.62)	516.85 (410.27/623.43)	938.75 (894.19/983.31)
Alkalinity (ppm)	197.15 (16.44/23.86)	197.15 (142.93/251.36)	231.65 (na)	241.51 (na)	290.79 (na)	257.53 (241.51/266.15)	nm (nm)	227.95 (187.29/266.15)	400.50 (345.01/443.59)	246.44 (na)	241.51 (na)
Li⁺ (ppm)	0.02 (0.00/0.04)	0.01 (0.00/0.02)	0.10 (na)	0.65 (na)	0.83 (na)	0.14 (0.12/0.14)	0.00 (na)	0.01 (0.00/0.02)	2.58 (2.41/2.74)	0.02 (0.00/0.04)	0.81 (0.69/0.93)
Na⁺ (ppm)	20.14 (16.44/23.86)	13.08 (12.69/13.63)	45.53 (na)	326.18 (na)	859.68 (na)	150.03 (132.63/186.46)	11.42 (na)	13.92 (10.70/15.31)	2084.27 (1951.07/2322.48)	9.06 (8.29/9.83)	881.58 (879.05/884.13)
NH₄⁺ (ppm)	0.03 (0.00/0.06)	0.00 (0.00/0.00)	0.44 (na)	2.92 (na)	6.34 (na)	0.78 (0.00/1.22)	0.00 (na)	0.00 (0.00/0.04)	17.84 (15.40/19.5)	0.20 (0.00/0.41)	4.88 (3.48/6.28)
Ka⁺ (ppm)	1.65 (1.22/2.09)	1.30 (1.11/1.45)	4.18 (na)	21.41 (na)	45.34 (na)	10.09 (9.64/10.37)	0.94 (na)	1.55 (1.17/1.78)	94.80 (87.46/101.83)	3.48 (2.80/4.16)	26.11 (25.75/26.49)
Mg²⁺ (ppm)	23.97 (23.65/24.28)	17.99 (16.72/18.73)	32.95 (na)	148.24 (na)	224.36 (na)	65.70 (58.77/81.25)	27.82 (na)	31.08 (25.68/39.83)	484.13 (446.69/521.58)	68.52 (58.46/78.57)	163.60 (161.85/165.36)
Mn²⁺ (ppm)	0.00 (0.00/0.00)	0.00 (0.00/0.00)	0.00 (na)	0.00 (na)	0.00 (na)	0.00 (0.00/0.00)	0.00 (na)	0.00 (0.00/0.00)	0.00 (0.00/0.00)	0.00 (0.00/0.00)	0.00 (0.00/0.00)
Ca²⁺ (ppm)	73.84 (62.55/85.13)	61.67 (54.15/75.99)	52.31 (na)	405.87 (na)	382.26 (na)	98.34 (94.83/103.79)	92.31 (na)	49.24 (29.99/60.25)	934.57 (855.13/1018.89)	95.05 (60.28/129.83)	259.32 (257.94/260.70)
Si²⁺ (ppm)	3.61 (0.00/7.22)	1.92 (0.00/3.02)	3.47 (na)	16.70 (na)	19.83 (na)	37.06 (35.12/38.50)	0.00 (na)	6.49 (0.00/20.40)	39.92 (30.07/52.30)	14.11 (0.98/27.30)	30.97 (na)
Ba²⁺ (ppm)	0.03 (0.00/0.07)	0.30 (0.00/0.46)	0.01 (na)	0.26 (na)	0.00 (na)	0.00 (0.00/0.00)	0.00 (na)	0.13 (0.00/0.56)	0.00 (0.00/0.00)	0.00 (0.00/0.00)	0.00 (0.00/0.00)

II. FOOD CHAIN LENGTH IN GROUNDWATER: PATTERNS IN $\delta^{15}\text{N}$ RANGE

Abstract

There is a large body of empirical and theoretical literature on historical and environmental determinates of food chain length (FCL), but these determinates have not been assessed in groundwater habitats. Stable isotope analysis of nitrogen in animal tissues provides an inexpensive measure of FCL. Trophic level and uncertainty in trophic level was estimated for 19 stygobiont species from two geochemically distinct sites in the Edwards Aquifer of South-Central Texas, USA. Isotopic data revealed large uncertainty associated with intraspecific $\delta^{15}\text{N}$ variability and low sample sizes, but species averages span 9‰ and strongly suggest the presence of 2° predators; unusual for groundwater food webs that are typically assumed to contain few obligate predators. A literature review revealed 10 additional isotope studies of groundwater food webs (excluding hyporheic habitats). Simple linear regressions and Akaike Information Criterion suggested that ecosystem age ($r^2 = 0.66$, $F = 18.26$, $p < 0.01$), and to a lesser extent, ecosystem size ($r^2 = 0.52$, $F = 10.75$, $p = 0.01$) and the presence of vertebrates ($F = 9.98$, $p = 0.01$) are all positively correlated with FCL. However, incomplete sampling of taxa for isotope analysis obfuscates the strength of these relationships. Groundwater habitats are ideal systems to study the relative importance of factors influencing food chain length using a stable isotope approach, but future studies should include larger sample sizes, more complete sampling of taxa, and body mass measurements.

Introduction

Little attention has been given to the historical and current environmental conditions controlling food chain length (FCL) in subterranean habitats. Although research on subterranean food web structure supports the paradigm of truncated food webs (Gibert & Deharveng, 2002), there is both empirical and theoretical literature on historical and environmental controls of FCL in non-subterranean habitats (Post, 2002a; Takimoto & Post, 2012), and the factors influencing variation in FCL in subterranean systems are ripe for investigation. Because they have been summarized elsewhere (Post, 2002a), potential determinates of FCL will only be introduced here. At least 5 major controls on FCL have been discussed at length in the literature, including productivity (Kaunzinger & Morin, 1998), ecosystem size (Schoener, 1989; Post *et al.*, 2000; Post, 2007), ecosystem age (Kitching, 2001), predator-prey mass ratios (Hastings & Conrad, 1979), and disturbance (Pimm & Lawton, 1977).

Groundwater habitats are ideal for studying the relative importance of historical and environmental factors influencing FCL because of relatively simple food chains (Gibert & Deharveng, 2002) and because of the global distribution of groundwater communities often comprised of similar species (e.g., crustaceans) inhabiting aquifers with a broad range of historical and environmental characteristics. Stable isotope ratio analysis of nitrogen (N) in animal tissues is commonly used as a measure of FCL (Takimoto & Post, 2012), although isotope data alone should be interpreted with caution (Post, 2002b). Further, because groundwater food webs are relatively simple, erroneous trophic level estimates due to differences in the proportional contributions of multiple resources to primary consumers (Hoeinghaus & Zeug, 2008) are minimized. I present N isotopic data

from subterranean aquatic species (stylobionts) from the Edwards Aquifer of South-Central Texas, USA. Based on habitat stability, age, size, and predator-prey mass ratios, it was predicted that the Edwards should have a long FCL relative to other groundwater communities. Secondly, I synthesize the isotopic literature on stylobiont food webs, excluding hyporheic and soil groundwater systems, with the aim of assessing the relative importance of potential factors influencing stylobiont FCL.

Methods

The Edwards Aquifer of south-central Texas is exposed to epigenic dissolution along a narrow escarpment and recharge zone on the northern and western margin of the aquifer (Barker *et al.*, 1994). South and east of the escarpment, Edwards limestones are confined below non-karstic carbonates and clays. Farther south and east, oxygenated, low total dissolved solids (TDS) water rapidly changes to anoxic, sulfide-rich, high TDS waters at a transition zone called the freshwater-saline water interface (FWSWI) (Oetting *et al.*, 1996, includes map).

Two sites (an artesian well and Comal Springs) were chosen for repeated sampling of stylobionts because of their hydrological and geochemical distinctiveness, ease of access, and faunal diversity (Longley, 1981; Gibson *et al.*, 2008). The artesian well is in the confined portion of the aquifer approximately 0.5 km from the FWSWI. Comal Springs is a series of springs at the base of the escarpment between the unconfined and confined portions of the aquifer. Discharge at the springs averages $9 \text{ m}^3 \text{ s}^{-1}$. At both sites, animals were collected (USFWS permit# SPR-0390-045) multiple times between June, 2010 and March, 2012, using 250 μm or 500 μm nets left in place between 4 and 24 hrs. Animals

were identified to the lowest possible level (usually species) and kept in filtered spring water for ~5 hrs to allow digestive tracts to clear. Animals were dried at 40°C for 24-48 hrs. One milligram of dry mass was used for isotope analysis, and multiple individuals were pooled to attain adequate mass for small species. Snails were removed from their shells prior to analysis. N and C isotope analyses were conducted at the UC Davis Stable Isotope Facility.

For each animal, trophic level was estimated using a Bayesian extension of Post's equation where trophic level of animal $j = 2 + (\delta^{15}N_j - \delta^{15}N_{base})/\Delta\delta^{15}N$, where $\delta^{15}N_j$ and $\delta^{15}N_{base}$ are the stable N isotope ratios for species j and primary consumers, respectively, and $\Delta\delta^{15}N$ is the per trophic level enrichment in N isotope composition (Post, 2002b).

Trophic level 1 is defined as primary producers. A Bayesian approach allows uncertainty in the estimate to be quantified by treating all three variables as normal distributions with associated means and precisions estimated using sample data ($\delta^{15}N_j$ and $\delta^{15}N_{base}$) and published values ($\Delta\delta^{15}N$). Published values for $\Delta\delta^{15}N_i$ were obtained from McCutchan *et al.*, (2003) and Caut *et al.* (2009) for guanicotelic and ammonotelic freshwater and terrestrial invertebrates (Vanderklift & Ponsard, 2003). Uninformative priors are given for population level means (normal distribution with $\mu = 0$, $\tau = 1e-6$) and precisions (gamma distribution with $\alpha = 0.001$, $\beta = 0.001$). To estimate possible effects of infrequent feeding or nutritional stress, trophic level estimates were also calculated by setting $\Delta\delta^{15}N_{starvation} = \Delta\delta^{15}N + 1.34\text{‰}$ based on the observed 1.34‰ increase in $\Delta\delta^{15}N$ due to starvation in a lycosid spider observed by Oelbermann & Scheu (2002). The posterior probability distribution for the trophic level of species j was estimated using a Markov Chain Monte Carlo (MCMC) procedure. Two MCMC chains were run, each with

500,000 iterations, a thinning rate of 50, and a burn-in of 1000. Plots of parameter estimates as a function of MCMC iteration were assessed for adequate burn in, and MCMC convergence was assessed using Gelman and Rubin potential scale reduction factors (Gelman & Rubin, 1992). Analyses were run in R v2.15 and JAGS v3.2.0.

To identify stable isotope studies of groundwater food webs, Google Scholar (<http://scholar.google.com>) was searched using the words isotope, troglobite, and stygobite simultaneously, and the words isotope, troglobiont, and stygobiont simultaneously. Results were cross-referenced for additional studies. In several instances, isotope data were available only as a figure, in which case values were estimated by overlaying the figure on a grid with grid size = 0.1‰ in Adobe Illustrator CS. FCL was defined as maximum average species $\delta^{15}\text{N}$ – minimum average species $\delta^{15}\text{N}$. In instances in which more than one site was sampled, the site with the largest FCL was used for analysis, or if two distinct food webs were indicated, both were used. Individual measurements were used in one instance, when a single species was analyzed. Simple linear regressions were run to assess correlations among $\delta^{15}\text{N}$ range and covariates. Covariates included species richness, ecosystem size, ecosystem age, the presence of vertebrate stygobionts, and ecosystem stability. Ecosystem size was modeled as an ordinal variable with four size classes corresponding to systems with a two dimensional extent of less than 10 km², tens of km², hundreds of km², and >1000 km². Ecosystem age was estimated as the approximate age of initial karstification, which represents the earliest date in which colonization of a site can begin, whether by epigean or groundwater species. In several instances in which a precise age of karstification was unknown, the beginning of the appropriate epoch was used (e.g., 23.8 million years

before present for Miocene). Ecosystem age was square root transformed to meet the assumption of normality. Presence or absence of vertebrate stygobionts was used as a qualitative measure of predator-prey mass ratios. Ecosystem stability was modeled as an ordinal variable with four classes defined using the following equation: stability = 1 + 1 if food web is partially or wholly dependent on chemolithoautotrophic production + 1 if site was not exposed to late Cenozoic glaciations or marine embayments + 1 if karst is partially confined. To assess whether $\delta^{15}\text{N}$ ranges were an artifact of incomplete sampling, $\delta^{15}\text{N}$ range was also regressed against the proportion of total stygobionts recorded from the site that were included in the isotope analysis (coverage). Multiple regressions were run to assess the interaction between covariates and coverage, but interactions among covariates was not assessed. Significance was adjusted for multiple comparisons using the false discovery rate method of Narum (2006). Akaike information criterion for finite samples size (AICc) was used to evaluate model fit. Analyses were run in R v2.15.

Results

From Comal Springs and the artesian well, 163 individuals from ten different species and 213 individuals from 14 different species were collected, respectively (Table 2.1). The asellid isopods *Lirceolus* spp. and the hadziid amphipod *Mexiweckelia hardeni* from Comal Springs and the snails *Phreatodrobia* spp. and the hadziid amphipod *Texiweckelia texensis* from the artesian well were assigned to trophic level two for trophic level estimates. One species, the crangonyctid amphipod *Stygobromus russelli*, represented by two individuals at the artesian well, had lower $\delta^{15}\text{N}$ values than *Phreatodrobia* spp. or *T.*

texensis but was not assigned to trophic level one because of 1) small sample size, 2) a large body size (11.75mm), making predation by smaller species unlikely, and 3) higher $\delta^{15}\text{N}$ values from individuals collected at Comal Springs. The exclusion of *S. russelli* leads to more conservative (i.e., lower) trophic level estimates for other species. Inspection of $\delta^{13}\text{C}$ and $\delta^{15}\text{N}$ biplots for both sites (data not shown) showed no indication of more than one food chain or evidence that species were feeding on different basal resources. Trophic level estimates were based on 65 estimates of $\Delta\delta^{15}\text{N}$ between -3.2‰ and 8.6‰. The mean of the posterior probability ($E(\Delta\delta^{15}\text{N})$) in guanicotelic and ammonotelic terrestrial and freshwater invertebrates = 2.81‰ with 95% equal-tail credible intervals (95% ETCI) = 2.31-3.31‰. Assuming additional 1.34‰ enrichment due to infrequent feeding, $E(\Delta\delta^{15}\text{N}_{\text{starvation}}) = 4.15‰$ (95% ETCI=3.65 – 4.65‰). Stygobionts in the Edwards Aquifer occupied approximately four consumer trophic levels, assuming trophic enrichment similar to values reported in the literature or three consumer trophic levels assuming higher $\Delta\delta^{15}\text{N}$ due to infrequent feeding (Table 2.1). Depending on sample size and variability among individuals, 95% ETCIs for trophic level estimates typically spanned two trophic levels.

The literature search revealed ten previous stable isotope studies from subterranean aquatic environments (excluding hyporheic systems), and five of these studies analyzed stygobionts from more than one site. Three studies were excluded from analysis. Neisch *et al.* (2012) analyzed two anchialine sites in the Yucatan, Mexico, but one site had been previously investigated (Pohlman *et al.*, 1997), taxonomic resolution was poor, and whether reported values were for individuals or species means was not specified.

Table 2.1: Sample size, $\delta^{15}\text{N}$ (‰), and mean trophic level estimates for species sampled from an artesian well and Comal Springs, Edwards Aquifer Texas, USA, arranged by $\delta^{15}\text{N}$ values. Estimates are based on published $\Delta\delta^{15}\text{N}$ and $\Delta\delta^{15}\text{N} + 1.34\text{‰}$, for infrequent feeding. ETCI = equal tail credible intervals. * indicates that multiple individuals were aggregated for samples.

Species	N	$\delta^{15}\text{N}$ (\pm SD)	Trophic level (95% ETCI) E($\Delta\delta^{15}\text{N}$) = 2.81‰	Trophic level (95% ETCI) E($\Delta\delta^{15}\text{N}$) = 4.15‰
Artesian Well				
<i>Eurycea rathbuni</i> (Caudata)	2	12.28 (\pm 0.95)	4.66 (1.58 - 7.86)	3.8 (1.72 - 5.93)
<i>Stygobromus flagellates</i> (Amphipoda)	23	10.82 (\pm 3.46)	4.14 (3.3 - 5.12)	3.45 (2.89 - 4.05)
<i>Allotexiweckelia hirsute</i> (Amphipoda)	1	10.47	3.72	3.16
<i>Texiweckeliopsis insolita</i> (Amphipoda)	8*	9.61 (\pm 0.91)	3.71 (3.01 - 4.52)	3.16 (2.69 - 3.65)
<i>Lirceolus spp.</i> (Isopoda)	4*	9.08 (\pm 0.91)	3.52 (2.71 - 4.44)	3.03 (2.48 - 3.61)
<i>Cirolanides texensis</i> (Isopoda)	20	8.85 (\pm 1.13)	3.44 (2.78 - 4.19)	2.97 (2.53 - 3.45)
<i>Palaemonetes antrorum</i> (Decapoda)	22	8.23 (\pm 1.33)	3.22 (2.56 - 3.96)	2.83 (2.38 - 3.3)
<i>Moorbdella sp.</i> (Hirudinea)	3	7.77 (\pm 1.38)	3.05 (1.71 - 4.47)	2.71 (1.81 - 3.65)
<i>Haedioporus texanus</i> (Coleoptera)	9*	7.49 (\pm 0.43)	2.95 (2.32 - 3.65)	2.65 (2.22 - 3.09)
<i>Holsingerius samacos</i> (Amphipoda)	4*	6.75 (\pm 3.61)	2.69 (0.44 - 4.88)	2.47 (1.03 - 3.93)
<i>Phreatodrobia spp.</i> (Gastropoda)	1*	5.67	2.31	2.21
<i>Texiweckelia texensis</i> (Amphipoda)	4*	5.62 (\pm 1.79)	2.29 (1.11 - 3.51)	2.2 (1.4 - 3.01)
<i>Stygobromus russelli</i> (Amphipoda)	2	2.74 (\pm 0.01)	1.27 (-1.45 - 1.94)	1.5 (1.03 - 1.96)
Comal Springs				
<i>Cirolanides texensis</i> (Isopoda)	2	12.99 (\pm 0.56)	5.10 (3.33 - 7.08)	4.10 (2.91 - 5.40)
<i>Sphalloplana sp.</i> (Tricladida)	1	12.46	4.91	3.97
<i>Artesia subterranea</i> (Amphipoda)	1	10.68	4.28	3.55
<i>Stygobromus pecki</i> (Amphipoda)	26	9.92 (\pm 0.79)	4.01 (3.61 - 4.54)	3.36 (3.13 - 3.64)
<i>Haedioporus texanus</i> (Coleoptera)	1*	6.66	2.85	2.58
<i>Stygobromus russelli</i> (Amphipoda)	3	6.56 (\pm 1.37)	2.82 (1.58 - 4.09)	2.55 (1.72 - 3.40)
<i>Comaldessus stygius</i> (Coleoptera)	1*	6.45	2.78	2.53
<i>Stygoparnus comalensis</i> (Coleoptera)	2*	5.52 (\pm 2.95)	2.44 (-6.5 - 11.68)	2.30 (-3.73 - 8.50)
<i>Mexiweckelia hardeni</i> (Amphipoda)	3*	4.75 (\pm 0.89)	2.17 (1.36 - 3.00)	2.12 (1.56 - 2.67)
<i>Lirceolus spp.</i> (Isopoda)	6*	4.02 (\pm 0.97)	1.91 (1.46 - 2.37)	1.94 (1.64 - 2.25)

Paoletti *et al.* (2011) investigated one fully aquatic isopod *Monolistra lavalensis*, but $\delta^{15}\text{N}$ range could not be calculated because individual values were not reported. Finally, Roach *et al.*, (2011) analyzed insects and a poeceliid fish in a cave in Tobasco, Mexico, but no species were stygobionts. The remaining seven studies sampled freshwater and saline phreatic and vadose karst groundwater habitats with a broad range of faunal characteristics. These include 1) Peștera Movile and a nearby sulfidic well in Constanța, Romania (Sarbu *et al.*, 1996), 2) the Frasassi Cave System in Marche, Italy (Sarbu *et al.*, 2000), 3) Cave Springs Cave Arkansas, USA (Graening *et al.*, 2003), 4) the upper

Floridan aquifer in Georgia, USA (Opsahl & Chanton, 2006), 5) Organ Cave in West Virginia, USA (Simon *et al.*, 2003), 6) Bundera Sinkhole in North Western Australia (Humphreys, 1999), and 7) the Mayan Blue cenote in Quintana Roo, Mexico (Pohlman *et al.*, 1997). Table 2.2 summarizes characteristics of these systems and results of the isotope studies.

Eleven regressions were run, and significance was set at $p \leq 0.017$. Statistical analysis revealed significant positive relationships between $\delta^{15}\text{N}$ range and ecosystem age ($r^2 = 0.66$, $F = 18.26$, $df = 1 \ \& \ 8$, $p < 0.01$), ecosystem size ($r^2 = 0.52$, $F = 10.75$, $df = 1 \ \& \ 8$, $p = 0.01$), and the presence of vertebrates (r^2 not estimated, $F = 9.98$, $df = 1 \ \& \ 8$, $p = 0.01$) but not with stability, species richness, or sample coverage (Fig. 2.2). Significant interactions between coverage and age ($r^2 = 0.80$, $F = 36.78$, $df = 1 \ \& \ 8$, $p < 0.001$) and between coverage and vertebrates ($r^2 = 0.69$, $F = 10.82$, $df = 2 \ \& \ 7$, $p = 0.007$) were detected. AICc suggested that the ecosystem age * coverage model was the best fit, being 5.3 times more likely than the next best model (ecosystem age). The remaining models were highly unlikely to be the best fit models (AICc $\Delta > 8$).

Discussion

Analytical solutions for trophic level using fixed values for $\Delta\delta^{15}\text{N}$ and trophic base ignore uncertainty in both parameters and provide little information on confidence in trophic level estimates (Post, 2002b). Trophic level estimate 95% ETCIs from Edwards Aquifer fauna typically span approximately one trophic level on either side of the mean. This has important implications for interpretation of food web structure. For example, *Lirceolus* spp. has a slightly higher mean trophic level than the larger cirolanid isopod

Cirolanides texensis. However, the 95% ETCIs for these estimates overlap, and given the observed data, it is not unlikely that *C. texensis* occupies a higher trophic level than *Lirceolus* spp.

Table 2.2: Published species average $\delta^{15}\text{N}$ ranges (minimum to maximum values) and covariate data used for linear regressions. Proportion of species is the proportion of total species recorded from the site that were analyzed for stable isotope composition. See text for isotope study references. * indicates $\delta^{15}\text{N}$ range for a single species. Covariate references available on request.

System	$\delta^{15}\text{N}$ range	Age (mya)	Stability	Species richness	Ecosystem size	Vertebrate stygobionts	Proportion of species
Comal Springs	9.0 (4.0 - 13.0)	23.8	4	16	4	1	0.63
artesian well	8.4(5.62 - 14.06)	23.8	4	22	4	1	0.64
Peștera Movile	3.7(-4.75 - -1.05)	5.2	4	20	2	0	0.15
sulfidic well, Romania	4.5(0.2 - 4.7)	5.2	4	20	2	0	0.15
Frasassi Grotto del Fiume	1.6 (-5.5 - -3.9)*	0.2	2	3	1	0	0.33
Cave Springs Cave	6.6 (10.7 - 17.3)	5.0	1	4	2	1	0.50
Radium Springs	6.3 (11.8 - 18.1)	3.4	3	4	4	0	0.75
Organ Cave	3.8 (12.2 - 16)	5	1	8	2	0	0.38
Bundera sinkhole (deep)	7.5 (4.8 - 12.3)	23.8	2	8	3	1	0.38
Mayan Blue Cenote	4.9 (8.4 - 13.3)	14	2	19	4	1	0.42

The high $\delta^{15}\text{N}$ values observed in some species strongly suggest that their diet is dominated by other predators. This is especially true of the artesiid amphipod *Artesia subterranea*, from the artesian well, and is likely true of several other species, although small sample size precludes a confident estimate of trophic level (e.g., the plethodontid salamander *Eurycea rathbuni* and the flatworm *Sphalloplana* sp.). Despite the surprisingly high trophic level estimate for *A. subterranea*, a 3° predator seems unlikely in a groundwater habitat, even though they occur in other habitats (Vander Zanden & Fetzer, 2007). Two possibilities could lead to erroneous trophic level estimates. $\Delta\delta^{15}\text{N}$ for these stygobionts may be higher than average values reported for ammonotelic and guanicotelic organisms from freshwater and terrestrial environments. Several studies have discussed potential sources of variability in $\Delta\delta^{15}\text{N}$ (Scrimgeour *et al.*, 1995;

McCutchan *et al.*, 2003; Vanderklift & Ponsard, 2003; Caut *et al.*, 2009). There is no *a priori* evidence for nutritional stress or some other mechanism that would lead to higher $\Delta\delta^{15}\text{N}$ in stygobionts, but if the estimated $\Delta\delta^{15}\text{N}$ due to infrequent feeding ($E(\Delta\delta^{15}\text{N}_{\text{starvation}}) = 4.15\text{‰}$) more closely approximates actual enrichment in the Edwards Aquifer, then the highest trophic level is approximately four. This still suggests the presence of 2° predators: a departure from typical groundwater food webs. However, the mechanism by which these “apex” predators selectively feed on 1° predators is unknown. These data also suggest that animal tissue (either through predation or scavenging) is an important dietary component for several small or presumably detritivorous species, such as *Lirceolus* spp. and the atyid shrimp, *Palaemonetes antrorum*.

Incorrect assignment of trophic level two species would also produce erroneous trophic level estimates. Average $\delta^{15}\text{N}$ of fine particulate organic matter in the Edwards Aquifer is 2.28‰, but it is spatially and temporally variable with measured values bracketing values of trophic level two species (data not shown). If species such as *P. antrorum*, *C. texensis*, and *Lirceolus* spp. are primary consumers, then species such as *A. subterranea* and *E. rathbuni* would feed approximately at trophic level four or three depending on $\Delta\delta^{15}\text{N}$. This does not explain the lower $\delta^{15}\text{N}$ values observed in several other species and would require that those other species are not consumed by other members of this food web.

On a global scale, analysis of $\delta^{15}\text{N}$ ranges revealed important differences among sites, but incomplete sampling of species for isotopic measurements (coverage) significantly interacted with other covariates, resulting in uncertainty in the strength of interactions between $\delta^{15}\text{N}$ range and covariates. Nevertheless, ecosystem age appeared to be the most

important factor influencing FCL in the stygobiont dominated communities assessed, despite the effect of incomplete coverage. Relatively young habitats may not have had the time necessary for colonization by the species required to fill specific trophic niches and create complex food chains. This may explain the low $\delta^{15}\text{N}$ range observed in the productive Frasassi Caves and Radium Springs in the upper Floridan aquifer, but it contrasts with findings from lakes, in which older systems had shorter food chains (Doi *et al.*, 2012). As seen in other systems (Sabo *et al.*, 2010), FCL is also correlated with habitat size. This may be, in part, through interaction with other important mechanisms, such as mitigating the negative effects of disturbance (Sabo *et al.*, 2010) or affecting nutrient availability (Post, 2002). Severely nutrient limited systems likely do not have adequate resources to maintain viable populations of higher trophic level species, regardless of age or size. FCL in temperate cave systems dependent on allochthonous input, including Organ Cave and Cave Springs Cave, may ultimately be limited by resource availability. Data were not available to assess productivity in this study, but in surface habitats, support for a productivity – FCL relation has been weak (Post *et al.*, 2000; Sabo *et al.*, 2010, but see Takimoto & Post, 2012). No relation between species richness and FCL was observed, but the relation between species richness and diversity is neither direct nor monotonic (Cardinale *et al.*, 2009). In old and productive systems, long food chains are still unlikely when size differences between primary consumers and predators are small. This may be the case for Movable Cave, where the largest predators (the hemipteran *Nepa anophthalma* and the leech *Haemopsis caeca*) are small relative to large decapod crustaceans or vertebrate predators present in other groundwater habitats. However, the presence of vertebrates is a poor measure of predator-prey mass ratios, and

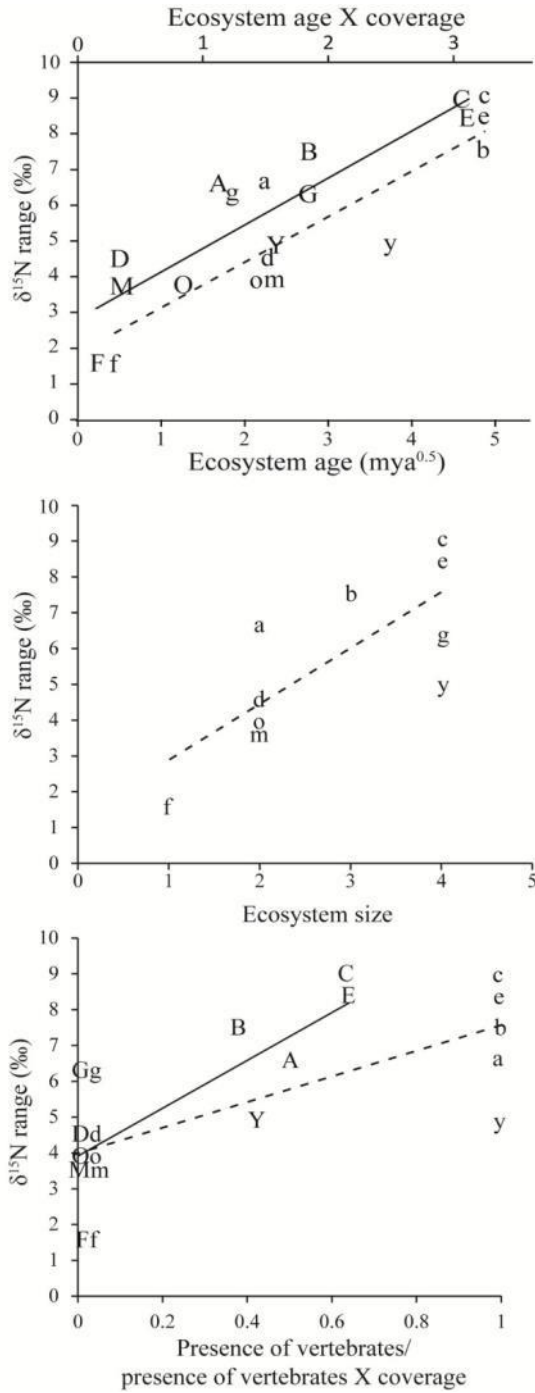


Figure 2.1: Significant regressions of $\delta^{15}\text{N}$ range versus A) ecosystem size, B) ecosystem age, and C) the presence of vertebrates. Solid regression lines, capital letters, and top X axis (pane A only) are for interaction effects models and dashed lines and lower case letters, and bottom X axis (pane A only) are for direct effects (no interaction with coverage).

its effect was also dependent on coverage, so additional data is necessary to better understand the importance of this variable. In old, large, and productive systems with taxa exhibiting a diverse range of body sizes, FCL may be determined by the long-term stability of the system. FCL in the Edwards Aquifer ecosystem appears to be longer than FCL in the Mayan Blue Hole and Bundera Sinkhole ecosystems, and this may be due to the semi-confined nature of the Edwards Aquifer and its distance from Pleistocene shorelines. The latter systems are both anchialine, having connections to the surface and the ocean. The “openness” of anchialine habitats makes them susceptible to disturbance associated with variability in temperature, precipitation, and allochthonous input and to fluctuating sea levels during the Pleistocene.

Conclusions

Determination of $\delta^{15}\text{N}$ range in stygobiont tissues is a simple and inexpensive method for quantifying FCL. $\delta^{15}\text{N}$ values for stygobionts from the Edwards Aquifer suggest the longest FCL yet reported from a groundwater system. These data strongly suggest the presence of secondary predators, which is unusual for subterranean systems. Quantifying the relative importance of historical and environmental factors influencing groundwater FCL is limited by the small number of food web studies, incomplete sampling of taxa, and potential covariance among predictor variables. Nevertheless, available data suggest that ecosystem age and, to a lesser extent, ecosystem size and predator-prey interactions influence FCL in groundwater habitats. Because of their relatively low diversity and limited number of potential food resources relative to epigeal habitats, groundwater ecosystems are ideally suited to large scale analyses of historical and environmental influences on FCL.

Acknowledgements

This study was partially funded by U.S. Geological Survey, The Crustacean Society, and the National Science Foundation. Dr. Weston H. Nowlin and Dr. Daniel W. Fong provided valuable comments.

References

- Barker R, Bush P, Baker Jr. E, 1994. Geologic history and hydrogeologic setting of the Edwards-Trinity aquifer system, West-central Texas. U.S. Geological Survey Water-resources investigations report 94-4039.
- Cardinale B, Bennett D, Nelson C, Gross K, 2009. Does productivity drive diversity or vice versa? A test of the multivariate productivity-diversity hypothesis in streams. *Ecology*, 90, 1227-1241.
- Caut S, Angulo E, Courchamp F, 2009. Variation in discrimination factors ($\Delta^{15}\text{N}$ and $\Delta^{13}\text{C}$): the effect of diet isotopic values and applications for diet reconstruction. *Journal of Applied Ecology*, 46, 443-453.
- Doi H, Vander Zanden M, Hillbrand H, 2012. Shorter food chain length in ancient lakes: evidence from a global synthesis. *PLoS One*, 7, e37856.
- Gelman A, Rubin D, 1992. Inference from iterative simulation using multiple sequences. *Statistical Science*, 7, 457-472.
- Gibert J, Deharveng L, 2002. Subterranean ecosystems: a truncated functional biodiversity. *BioScience*, 52, 473-481.
- Gibson J, Harden S, Fries J, 2008. Survey and distribution of invertebrates from selected springs of the Edwards Aquifer in Comal and Hays Counties, Texas. *The Southwest Naturalist*, 53, 74-84.
- Graening G, Brown A, 2003. Ecosystem dynamics and pollution effects in an Ozark cave stream. *Journal of the American Water Resources Association*, 39, 1497-1507.
- Hastings H, Conrad M, 1979. Length and evolutionary stability of food chains. *Nature*, 282, 838-839.
- Hoeninghaus D, Zeug S, 2008. Can stable isotope ratios provide for community-wide measures of trophic structure? Comment. *Ecology*, 89, 2353-2357.
- Humphreys W, 1999. Physico-chemical profile and energy fixation in Bundera Sinkhole, an anchialine remipede habitat in north-western Australia. *Journal of the Royal Society of Western Australia*, 82, 89-98.
- Kaunzinger C, Morin P, 1998. Productivity controls food-chain properties in microbial communities. *Letters to Nature*, 395, 495-497.

- Kitching R, 2001. Food webs in phytotelmata: “bottom-up” and “top-down” explanations for community structure. *Annual Review of Entomology* 46: 729-760.
- Longley G, 1981. The Edwards Aquifer: Earth’s most diverse groundwater ecosystem? *International Journal of Speleology*, 11, 123-128.
- McCutchan J, Lewis W, Kendall C, McGrath C, 2003. Variation in trophic shift for stable isotope ratios of carbon, N, and sulfur. *Oikos*, 102, 378-390.
- Narum S, 2006. Beyond Bonferroni: less conservative analyses for conservation genetics. *Conservation Genetics* 7: 793-787.
- Neisch J, Pohlman J, Iliffe T, 2012. The use of stable and radiocarbon isotopes as a method for delineating sources of organic material in anchialine systems. *Natura Croatica*, 21, 83-85.
- Oelbermann K, Scheu S, 2002. Stable isotope enrichment ($\delta^{15}\text{N}$ and $\delta^{13}\text{C}$) in a generalist predator (*Pardosa lugubris*, Araneae: Lycosidae): effects of prey quality. *Oecologia*, 130, 337-344.
- Oetting G, Banner J, Sharp Jr. J, 1996. Regional controls on the geochemical evolution of saline groundwaters in the Edwards aquifer, Central Texas. *Journal of Hydrology*, 181, 251-283.
- Opsahl S, Chanton J, 2006. Isotopic evidence for methane-based chemosynthesis in the Upper Floridan aquifer food web. *Oecologia*, 150, 89-96.
- Paoletti M, Beggio M, Dreon A, Pamio A, Gomiero T, Brilli M, Dorigo L, Concheri G, Squartini A, Engel A, 2011. A new food web based on microbes in calcitic caves: the *Cansiliella* (Beetles) case in Northern Italy. *International Journal of Speleology*, 40, 45-52.
- Pimm S, Lawton J, 1977. The number of trophic levels in ecological communities. *Nature*, 268, 329-331.
- Pohlman J, Iliffe T, Cifuentes L, 1997. A stable isotope study of organic cycling and the ecology of an anchialine cave ecosystem. *Marine Ecology Progress Series* 155, 17-27.
- Post D, Pace M, Hairston Jr. N, 2000. Ecosystem size determines food-chain length in lakes. *Letters to Nature*, 405, 1047-1049.
- Post D, 2002a. The long and short of food-chain length. *TRENDS in Ecology & Evolution*, 17, 269-277.

- Post D, 2002b. Using stable isotopes to estimate trophic level: models, methods, and assumptions. *Ecology*, 83, 703-718.
- Post D, 2007. Testing the productive-space hypothesis: rational and power. *Oecologia*, 153, 973-984.
- Roach K, Tobler M, Winemiller K, 2011. Hydrogen sulfide, bacteria, and fish: a unique, subterranean food chain. *Ecology*, 92, 2056-2062.
- Sabo J, Finlay J, Kennedy T, Post D, 2010. The role of discharge variation in scaling of drainage area and food chain length in rivers. *Science*, 330: 965-967.
- Sarbu S, Kane T, Kinkle B, 1996. A chemoautotrophically based cave ecosystem. *Science*, 272, 1953-1955.
- Sarbu S, Galdenzi S, Menichetti M, Gentile G, 2000. Geology and biology of the Frasassi Caves in Central Italy: an ecological multidisciplinary study of a hypogenic underground karst system. In: H Wilkins, DC Culver, and WF Humphreys (Eds.). *Subterranean ecosystems*. Elsevier Academic Press, Amsterdam, pp. 359-378.
- Schoener T, 1989. Food webs from the small to the large: the Robert H. MacArthur Award lecture. *Ecology*, 70, 1559-1589.
- Scrimgeour C, Gordon S, Handley L, Woodford J, 1995. Trophic levels and anomalous $\delta^{15}\text{N}$ of insects on raspberry (*Rubus idaeus* L.). *Isotopes in Environmental and Health Studies*, 31, 107-115.
- Simon K, Benfield E, Macko S, 2003. Food web structure and the role of epilithic biofilms in cave streams. *Ecology*, 84, 2395-2406.
- Takimoto G, Post D, 2012. Environmental determinants of food-chain length: a meta-analysis. *Ecological Research*, DOI 10.1007/s11284-012-0943-7.
- Vanderklift M, Ponsard S, 2003. Sources of variation in consumer-diet $\delta^{15}\text{N}$ enrichment: a meta-analysis. *Oecologia*, 136, 169-182.
- Vander Zanden M, Fetzer W, 2007. Global patterns of aquatic food chain length. *Oikos*, 116: 1378-1388.

III. MORPHOLOGIC AND TROPHIC SPECIALIZATION IN A SUBTERRANEAN AMPHIPOD ASSEMBLAGE

Summary

1. Sympatric species are expected to exhibit specialization that reduces interspecific competition for predictable food resources and generalized feeding strategies to exploit variable resources in oligotrophic and unpredictable environments.
2. The trophic structure of a diverse subterranean amphipod assemblage was investigated using an integrative approach combining isotope and mouthpart morphometric data to investigate feeding strategies in what is usually considered an oligotrophic environment with patchy resources.
3. Seven amphipod species occupy different regions of isotopic space, suggesting utilization of different food resources and trophic specialization. Trophic position, measured as $\delta^{15}\text{N}$, was significantly negatively associated with planar area of the mandible and number of molar ridges and significantly positively associated with incisor width. Reduced molars and robust incisors are associated with predatory feeding strategies in non-subterranean amphipods. $\delta^{13}\text{C}$ exhibited weaker relationships with morphometrics but was significantly negatively correlated with the number of denticles on the setae of the distal margin of the 2nd maxilla. Carbon isotope – mouthpart morphology relationships indicate distinct scraping and filter feeding morphologies in primary consumers.

4. One species, *Stygobromus russelli*, had generalized mouthparts, but based on unusual isotope values, apparently had unique and unidentified feeding methods and food source, illustrating the obfuscating effect of phylogeny on form-function relationships.
5. Species showed moderate to absent ontogenetic shifts in trophic position, and body size had little to no effect on trophic position although relationships varied among species.
6. Sympatric subterranean species can exhibit specialized feeding strategies, suggesting that competition among species is driving niche partitioning. This contradicts the widespread assumption that patchy and limiting resources in groundwater habitats select for trophic generalists.

Keywords

Interspecific competition; generalist; specialist; niche partitioning; mouthpart morphometry; stable isotope; stygobiont; Edwards Aquifer, Central Texas, USA

Introduction

Understanding the mechanisms that promote coexistence of potential competitors in natural communities has been a long-standing goal of ecological research (Hutchinson 1961; MacArthur & MacArthur 1961; Pianka 1974; Schoener 1974; Tilman 1982; Abrams 1995). Not surprisingly, a central and ongoing component of this research area has focused on how multiple, potentially competing species utilize resources (e.g., food, nutrients), via the evolution of foraging strategies and niche partitioning (Sims *et al.* 2008; Svanbäck & Schluter 2012; Correa & Winemiller 2013). Species-specific

responses to resource availability depend on the temporal and spatial distribution of food resources, which affects competition intensity (Pianka 1974; Robinson & Wilson 1998). Optimal foraging theory, competition theory, and empirical evidence suggest that in ecosystems with spatially and temporally dependable food resources, species exhibit adaptations that enhance foraging efficiency and preference for a single resource or subset of available resources (resource specialization) (Levinton 1972; Stephens & Krebs 1986; Correa & Winemiller 2013). As populations approach carrying capacity, interspecific competition increases. Under these conditions, species may forage on non-overlapping resources (niche partitioning) as a mechanism to reduce interspecific competition (MacArthur & Pianka 1966; Wilson 2010). Niche partitioning may occur through trophic shifts (i.e. feeding on sub-optimal resources) or niche contraction (i.e. feeding on a subset of optimal resources) (Correa & Winemiller 2013). However, during resource pulses (i.e. infrequent, short duration, large magnitude resource inputs, *sensu* Nowlin *et al.* 2008), in which demand does not exceed supply, multiple consumers may utilize an abundant and high quality resource to maximize feeding efficiency, temporally exhibiting nearly complete niche overlap (Robinson & Wilson 1998; Correa & Winemiller 2013).

In extreme and oligotrophic habitats, the importance of interspecific competition as a driver of specialization has been suggested (Fišer *et al.* 2012), in accordance with classical models of competition theory (Pianka 1974). However, under these conditions resources may also be patchy in time and space (Gibert & Deharveng 2002), and a species' ability to acquire resources is more severely limited by some aspect of the

environment (i.e. environmental heterogeneity or intraspecific competition) rather than interspecific competition (Levinton 1972; Chesson 2000). Under these conditions, trophic generalism is expected as an adaptation to maximize acquisition of varied and unpredictable resources (Levinton 1972).

Subterranean habitats have the potential to serve as unique evolutionary laboratories to study trophic strategies of consumers. In general, subterranean habitats exhibit simplified trophic base devoid of *in-situ* photosynthesizers, relatively stable conditions (Tobin, Hutchins & Schwartz 2013), and often ancient but species poor communities (Jeannel 1943; Culver & Pipan 2012). In addition, subterranean habitats can also serve as highly isolated and replicated natural laboratories containing communities comprised of similar species (Vergnon *et al.* 2013). Relative to surface habitats, subterranean communities are species poor (Gibert & Deharveng 2002), making analysis of a larger proportion of the community feasible. Resource supply rate (*sensu* Gross & Cardinale 2007) in subterranean systems varies from extremely high, as in guano communities supported by large bat colonies (Iskali 2011), to essentially zero, as in caves overlain by non-porous rock types that exclude import of water and nutrients (Barr & Kuehne 1971).

“As a rule” (Gibert & Deharveng 2002), food resources in subterranean habitats are unevenly distributed in space and time, resulting in communities characterized by relatively short food webs comprised of generalist consumers. This paradigm, although well supported in subterranean ecosystems dependent on allochthonous photosynthetic organic matter imported from the surface (i.e. cave streams) (reviewed in Culver & Pipan

2009), is not generalizable to all subsurface systems. Most studies of subterranean ecosystems occur in humanly accessible caves in which resource supply is restricted to surface connections that are relatively rare and heterogeneously distributed (Curl 1966). Aquatic habitats in most caves are dominated by cave streams and drips with very little particulate organic matter (Simon, Benfield & Macko 2003) and low levels of dissolved organic matter (Simon, Pipan & Culver 2007), and chemolithoautotrophy, a potentially predictable and abundant supply of organic matter, is relatively uncommon in these systems (Simon *et al.* 2007).

In contrast to relatively open cave stream systems, phreatic karst aquifers can be large and exhibit a high degree of connectivity (e.g. Barker, Bush & Baker 1994; Smart *et al.* 2006) that can potentially support larger populations. Many of these systems occur at substantial depth (> 100m) and can be confined below non-porous rock layers that buffer the system from environmental variability and disturbance. Furthermore, evidence suggests that chemolithoautotrophic organic matter can be an important, if not dominant, resource in some of these aquifers (Sarbu, Kane & Kinkle 1996; Pohlman, Iliffe & Cifuentes 1997; Humphreys 1999; Opsahl & Chanton 2006). However, because of their inaccessibility relative to humanly accessible caves, ecosystem studies have been less frequent in deep phreatic systems. In such habitats, competition and optimal foraging theories predict the development of complex food webs (Post 2002) and specialized feeding modes that reduce interspecific competition through niche partitioning (Levinton 1972; Pianka 1974; Correa & Winemiller 2013).

The Edwards Aquifer of Central Texas, USA, provides a unique opportunity to investigate trophic complexity and niche partitioning among stygobionts (i.e. obligate subterranean aquatic species). The aquifer has been the site of biological investigations for over a century (Stejneger 1896), and is recognized as a global hotspot of stygobiont biodiversity (Culver & Sket 2000). Of particular interest is the amphipod fauna that is comprised of 18 described species belonging to four families (Holsinger 1967; Holsinger & Longley 1980; Gibson, Harden & Fries 2008) and several undescribed species, including a fifth family (Gibson *et al.* 2008). In particular, one flowing artesian well on the Texas State University campus in San Marcos, hosts an amphipod fauna composed of 10 species, making it one of the most diverse subterranean amphipod communities known (Holsinger & Longley 1980). Furthermore, putative chemolithoautotrophic microbial communities (Engel & Randall 2011; Gray & Engel 2013) and organic matter with carbon isotope ratios depleted in C¹² relative to C¹³ (Hutchins, Schwartz & Engel in press) are present along a steep redox gradient between oxygenated, low total dissolved solids (TDS) waters and dysoxic to anoxic, high TDS, high hydrogen sulfide bearing waters. This suggests that *in-situ* chemolithoautotrophic primary production is a potentially important organic matter contribution to the groundwater food web.

Based on field and laboratory observations, primarily of marine amphipods (but see Mayer *et al.* 2009; Mekhanikova 2010), relationships between mouthpart morphology and feeding mode have been identified for numerous amphipods (Coleman 1983; Saint-Marie 1984). These form and function relationships can serve as testable hypotheses about groundwater amphipod feeding modes. Specifically, reduced setation and grinding

surface of the molar is consistently observed in predators (Haro-Garay 2003; Arndt, Berge & Brandt 2005; Guerra-Garcia & Tierno de Figueroa 2009), increased setation is consistently observed in filter feeders (Cole & Watkins 1997; Mayer *et al.* 2009), and increased grinding surface of the molar and dentate and comb-like spines and setae are consistently observed in scrapers (Arndt *et al.* 2005; Mayer *et al.* 2009). For groundwater species, inaccessibility and difficulty reproducing subterranean conditions in the laboratory (i.e. pressure, confined conditions, and chemolithoautotrophic production) make corroboration of hypothesized feeding modes by direct observation difficult. Additionally, gut content analysis has limited potential for distinguishing between different feeding modes if food items are similar in appearance, and only provides a ‘snapshot’ that may not represent a consumer’s range of potential food items, especially if food items are patchily distributed in time and space (Araújo *et al.* 2007).

Stable isotope analysis, however, can provide indirect evidence of a species’ trophic niche, niche overlap, and (at least qualitatively) specialization versus generalized feeding (Layman *et al.* 2007), as well as more specific information about trophic ecology (i.e. trophic level estimates, or identification or percent contributions of potential food items) (Layman *et al.* 2012). In previous studies of fishes, morphometric and stable isotope data have been combined to provide insights into the trophic ecology and diet specialization of several species of fishes (Matthews *et al.* 2010; Lujan, German & Winemiller 2011; Svanbäck & Schluter 2012). But, to our knowledge, this has not been applied to invertebrates. In this study, I have assessed relationships between feeding modes inferred through mouthpart morphology and diet inferred through stable isotope composition of

seven sympatric amphipod species collected from a single site in the Edwards Aquifer. Hypotheses about general feeding strategies, based on the specific form-function relationships listed above, were evaluated based on trends in $\delta^{13}\text{C}$ and $\delta^{15}\text{N}$ values among species. I predicted that adaptations to predation (e.g., reduced molars and setation and increased size and dentition in incisors and the lacinae mobilis) would be associated with enriched $\delta^{15}\text{N}$ values, and that among primary consumers, adaptations to filter feeding and scraping (e.g., increased setation and dentition of spines and setae, respectively) would be associated with differences in $\delta^{13}\text{C}$ values. Although this integrated approach is valuable for providing insight into the feeding modes of an unusually diverse amphipod assemblage that is difficult to observe *in-situ*, more generally, it serves as a powerful method for exploring whether the potential functional role of specific morphologies is realized as trophic niche partitioning among species.

Materials & Methods

Amphipod collection

For stable isotope analysis, 75 amphipods belonging to seven species were collected, 30 of which were also used for morphometric analysis. Species belonged to the families Crangonyctidae (*Stygobromus flagellatus* Benedict and *Stygobromus russelli* Holsinger), Bogidiellidae (*Artesia subterranea* Holsinger & Longley), and Hadziidae (*Allotexiweckelia hirsuta* Holsinger & Longley, *Texiweckeliopsis insolita* Holsinger & Longley, *Texiweckelia texensis* Holsinger & Longley, and *Holsingerius samacos* Holsinger & Longley) within the suborder Gammaridea. Tethyan distributions, based on landmasses surrounding the ancient Tethys Sea, and extant marine and brackish water

relatives provide strong evidence for a marine origin of Hadziid and Bogidiellid species (Holsinger & Longley, 1980; Lowry & Fenwick 1983). Age of subterranean colonization by these species may have occurred via stranding following regression of marine embayments of the study area in the late Cretaceous or Eocene (Holsinger & Longley, 1980) although a later colonization via active dispersal through hyporheic sediments is also possible (Holsinger & Longley, 1980). Whether speciation proceeded colonization of the subterranean habitat is possible, but unstudied (Holsinger & Longley, 1980). Continental distributions in freshwaters of North America and Asia (Holsinger, 1987) suggest that the Crangonyctidae are of Laurasian freshwater origin (Holsinger & Longley 1980). Hypotheses about the timing of colonization of subterranean habitats by *Stygobromus* species range from Eocene to Pliocene (Holsinger, 1966; Barr & Holsinger, 1985), and speciation via vicariant events is thought to have followed colonization (Bar & Holsinger, 1985).

The two *Stygobromus* species are the largest bodied, and most robust amphipods present at the site, followed by *A. hirsuta* and *A. subterranea*. The remaining three Hadziid amphipods are medium sized or small bodied (*T. insolita*), fragile species with elongated appendages. Holsinger & Longley (1980) speculated that the two *Stygobromus* species are detritivores, *T. insolita* and *H. samacos* are filter-feeders, and *A. subterranea* feeds on “soft, pulpy substances.” Two additional Bogidiellids and a species belonging to a fourth family (Sebidae) also occur at the well, but were excluded from analysis because inadequate numbers of individuals were collected (zero to one) or small body size prevented isotopic analysis of individuals.

Biological collection from the flowing artesian well has been conducted since the late 19th century (Stejneger 1896). The well is completed in the confined portion of the San Antonio pool of the Edwards Aquifer and intersects a karst conduit at 59.5m below ground (Holsinger & Longley 1980). Between May 2010 and July 2013, the water outflow of the well was periodically sampled using either a 100µm or 250µm mesh net. The net was checked every 24 hrs, and only living animals were used for analyses. Live amphipods were identified to species under a Nikon SMZ1500 dissecting microscope using Holsinger & Longley (1980) and Holsinger (1967) for the genus *Stygobromus*. Body length of all sampled individuals was measured using a Nikon Digital Sight DS-5M-L1 digital microscope camera system.

Stable isotope data

Between 4 and 29 individuals per species were analyzed for stable carbon and nitrogen isotope composition (Fig. 3.1). C and N are extensively used as complimentary elements in isotope analyses of food webs. Trophic fractionation of C is small, allowing the contribution of food sources with distinct carbon isotope compositions (C3 and C4 plants, for example) to be traced through food webs (Peterson & Fry 1987). N exhibits predictable trophic fractionation, although the magnitude of fractionation depends on food sources and the physiology of consumers (McCutchan *et al.* 2003; Vanderklift & Ponsard 2003). Comparison of C and N isotope values allows for quantification of the relative contribution of food sources and the relative trophic position of individuals within a food web (Peterson & Fry 1987). The number of individuals analyzed depended

on rarity and adequate body mass. Larger individuals were preferentially analyzed to ensure adequate mass and correct identification. Replicate samples were included for approximately 10% of individuals. Animals were kept alive in filtered spring water for approximately 3 hours to clear digestive tracts. Animals were then dried at 50°C for 48 hours. Between 0.4 µg and 1.2 µg were analyzed for $\delta^{13}\text{C}$ and $\delta^{15}\text{N}$ at the University of California Davis Stable Isotope Facility using a PDZ Europa ANCA-GSL elemental analyzer interfaced to a PDZ Europa 20-20 isotope ratio mass spectrometer (Sercon Ltd., Cheshire, UK). Standard deviations for internal lab standards are reported at 0.2‰ and 0.3‰ for C and N, respectively. To identify potential basal food resources, fine particulate organic matter (FPOM) was collected from surface streams that recharge the aquifer to represent photosynthetic organic matter and from wells along the FWSWI to represent potential chemolithoautotrophic organic matter. FPOM was filtered onto 0.7µm, precombusted, glass fiber filters and analyzed for $\delta^{13}\text{C}$ and $\delta^{15}\text{N}$ using the same methods as animal tissues. For carbon analysis, filters were incubated in a fuming HCL chamber for approximately 24 hours to remove inorganic C (carbonates) prior to isotope analysis. For additional FPOM methods, see Hutchins, Schwartz & Engel (in press).

Mouthpart morphometry

Between two and five individuals per each of seven species were analyzed for mouthpart morphometry (Appendix 1). As with stable isotope analysis, the number of individuals analyzed depended on rarity and size. Maxillipeds, 1st and 2nd maxillae (maxilla and maxillulae), and the left mandible were dissected from the animal under a Nikon SMZ1500 dissecting scope. Amphipod mandibles are asymmetric, and the left mandible

was chosen for analysis to take measurements of the *lacinae mobilis*, which is absent on the right mandible of the Hadziid amphipods. The paragnaths and labrum were not analyzed because few form-function relationships for these mouthparts exist in the literature. Although the gnathopods serve an important function in feeding (Arndt, Berge & Brandt 2005), these were not analyzed because I felt that they provided little additional information. For an overview of amphipod mouthpart morphology and the position of mouthparts in relation to one another, see Mayer *et al.* (2009). Mouthparts were dehydrated using an alcohol dehydration series, critical point dried using CO₂, and sputter coated using a gold-palladium mixture for two minutes at 20 mAmps. Mouthparts were then mounted and imaged using a Helios NanoLab 400-FEI scanning electron microscope (Nanolab Technologies). Images were analyzed using ImageJ software (Schneider, Rasband & Eliceiri 2012). Based on available literature, a suite of 24 morphologic characteristics were chosen for measurement (Appendix 1). Characteristics were either untransformed count data (e.g. number of setae on apical margin of outer inner plate of 2nd maxilla) or continuous data (e.g. planar area of molar surface) standardized by body length.

Statistical analysis

To assess potential ontogenetic shifts in trophic ecology within amphipod species, species-specific $\delta^{15}\text{N}$ – body length and $\delta^{13}\text{C}$ - body length relationships were assessed using simple linear regression. A global regression of $\delta^{13}\text{C}$ and $\delta^{15}\text{N}$ as functions of body length was also performed, combining all individuals from all species. For regressions, alpha was set to minimize both Type I and Type II errors using the method of Mudge *et*

al. (2012) and an *a priori* defined significant effect of $R^2 = 0.3$. A mixed-effect model, grouping by species, was not performed because of 1) variable sample sizes among species, 2) analytical problems relating to over fitting of linear mixed-effect models with species specific slopes and intercepts, and 3) large individuals were preferentially chosen for isotope analysis to ensure adequate body mass (see above).

To assess whether amphipod species occupy the same position in trophic space (as defined by the combination of $\delta^{13}\text{C}$ and $\delta^{15}\text{N}$ values for each species), multivariate analysis of variance (MANOVA) was performed to assess global differences in C and N isotope values among species. Afterwards, post-hoc tests (Fisher's LSD) of two separate analyses of variance (ANOVAS) on $\delta^{13}\text{C}$ and $\delta^{15}\text{N}$ values were used to define putative trophic groups (i.e. groups of species with $\delta^{13}\text{C}$ and $\delta^{15}\text{N}$ values suggesting utilization of at least partially non-overlapping food sources). Species were assumed to represent different trophic groups if they had significantly different mean $\delta^{13}\text{C}$ or mean $\delta^{15}\text{N}$ values (Table 3.1).

To assess potential relationships between mouthpart morphology (and inferred feeding modes) and isotopic composition, morphometric data were used as predictors of isotope values in both linear regressions and redundancy analysis (RDA). Small sample sizes precluded analysis of intraspecific morphology – isotope relationships. For linear regressions, a subset of potential explanatory morphologic variables were chosen for statistical analysis. A matrix of Pearson's correlation coefficients was used to identify a single variable that was correlated with the highest number of other variables at $R >$

0.799. This variable was retained and covariables were removed. This process was repeated until no variables covaried with one another at $R > 0.799$. From these variables, an additional four variables were excluded that did not have clear feeding interpretations (e.g. length of maxilliped palp, mandible incisor length, mandible lacinae mobilis length, maximum length of mandible lacinae mobilis teeth).

Linear regressions of the five variables against either $\delta^{13}\text{C}$ or $\delta^{15}\text{N}$ single isotope value were also used to assess feeding mode. Mean species values were used for both predictor and response variables. The isotope used as a response variable depended on the hypothesized functional significance (Table 3.2). For each morphology- isotope relationship, four competing linear models were evaluated using Akaiki Information Criterion (AIC).

Response isotope ~ predictor isotope (Model 1)

Response isotope ~ predictor morphometric (Model 2)

Response isotope ~ predictor isotope + predictor morphometric (Model 3)

Response isotope ~ predictor isotope * predictor morphometric (Model 4)

For each of the five comparisons, alpha was set to minimize both Type I and Type II errors using the method of Mudge *et al.* (2012) using an *a priori* defined significant effect of $R^2 = 0.3$. As in RDA, analyses with $\delta^{15}\text{N}$ as the response isotope were performed with and without *Stygobromus russelli*, which was an apparent outlier in those regressions. To assess whether apparent morphology – isotope relationships were an artifact of body size

– isotope relationships, linear regressions were also used to assess relationships between the body length of individual amphipods and both species mean $\delta^{13}\text{C}$ and species mean $\delta^{15}\text{N}$. Significance was assessed using the method described above.

RDA was performed to assess linear combinations of morphologic variables that explained linear combinations in $\delta^{13}\text{C}$ and $\delta^{15}\text{N}$ values for individuals. Morphologic variables were reduced to principal components derived from a principal components analysis (PCA) that creates eigenvectors that explain variation in combinations of morphologic variables. Three principal components that explained more than 5% of inertia (i.e. variation) in morphologic characters were selected for RDA. Missing morphologic data (i.e. broken mouthparts) were estimated using body size relationships (if apparent) or species-specific averages. No individuals and no variables had greater than 10% missingness. After testing for global significance of the RDA, forward selection was used to identify and remove non-significant variables using the criterion of Blanchet, Legendre & Borcard (2008). Significance of remaining variables and the significance of RDA axes were quantified using permutation tests ($n = 9000$) (Borcard, Gillet & Legendre 2011).

All statistical analyses were performed in R v3.0.1 (R Core Team, 2013) using the packages *agricolae* (de Mendiburu) (Fishers LSD), *vegan* (Oksanen *et al.* 2013), and *packfor* (Dray *et al.* 2013) (PCA, RDA, and forward selection).

Results

Strong covariation was observed among several mouthpart morphological characteristics (Appendix 2). In particular the number of setae on the distal margin and medial margins of inner and outer plates of the 1st and 2nd maxilla and maxillipeds often covaried. The length of plates of the 1st and 2nd maxilla and maxillipeds also frequently covaried. Few mandible morphometrics, however, were found to covary with one another or with characteristics on other mouthparts. After covariates were excluded, eight variables remained, none of which were strongly correlated with one another. Of these, five had hypothesized relationships to particular feeding modes (Table 3.2)

When data from all species were combined, body length was not a significant predictor of $\delta^{13}\text{C}$ values ($R^2 = -0.001$; $p = 0.687$, $F = 0.02_{1,63}$; optimal $\alpha = 0.02$) although a significant relationship between body length and $\delta^{15}\text{N}$ values was observed, albeit below the *a priori* defined significant effect of $R^2 = 0.3$ ($R^2 = 0.157$; $p = 0.001$ $F = 12.83_{1,63}$; optimal $\alpha = 0.02$). Removal of *Stygobromus russelli* did not increase the magnitude of the effect to $R^2 > 0.3$. *Artesia subterranea* exhibited a modest, but significant decrease in $\delta^{13}\text{C}$ values with increasing body size ($F = 6.49_{1,6}$, $p = 0.044$, $R^2 = 0.440$, optimal $\alpha = 0.27$) (Fig. 3.2). *Allotexiweckelia hirsuta* ($F = 2.94_{1,2}$, $p = 0.229$, $R^2 = 0.393$, optimal $\alpha = 0.39$) and *Texiweckeliopsis insolita* ($F = 7.31_{1,6}$, $p = 0.035$, $R^2 = 0.474$, optimal $\alpha = 0.27$) exhibited a positive relationship between $\delta^{15}\text{N}$ values and body length (Fig. 3.2).

$\delta^{13}\text{C}$ and $\delta^{15}\text{N}$ values across the seven amphipod species displayed large ranges, indicating 1) multiple potential food sources include autochthonous organic matter

produced via chemolithoautotrophy and allochthonous organic matter produced on the surface via photosynthesis (Engel & Randall 2001; Gray & Engel 2013; Hutchins, Schwartz & Engel in press) and 2) the presence of multiple trophic levels, including primary and secondary predators (Hutchins & Schwartz 2013) (Fig. 3.1). MANOVA indicated that amphipod species occupy significantly different positions in isotope bi-plot space (Pillai's trace = 1.215, $F_{6, 58} = 14.964$, $p < 0.001$). Post hoc comparisons revealed that, with the exception of *S. flagellatus* and *A. hirsuta*, all species were significantly different from one another for at least one isotope ($p < 0.05$) (Fig. 3.1, Table 3.1). On average, three species: *A. subterranea*, *S. flagellatus*, and *A. hirsuta* had higher $\delta^{15}\text{N}$ values relative to the other amphipods, and one species, *T. insolita* had lower $\delta^{13}\text{C}$ values relative to other amphipods (although some individuals from other species had equally low $\delta^{13}\text{C}$ values). One species, *S. russelli* had low $\delta^{15}\text{N}$ values relative to other species. Relative to suspended FPOM from the sampling site ($\delta^{13}\text{C} = -28.55 \pm 1.03\text{‰}$, $\delta^{15}\text{N} = 1.47\text{‰}$), most individuals had similar or more negative $\delta^{13}\text{C}$ values and higher $\delta^{15}\text{N}$ values, suggesting that suspended FPOM from the site contributed, in part, to the observed food web.

Principal components analysis revealed strong separation of species in morphologic space, with the exception of the two, closely related species *S. flagellatus* and *S. russelli* (Fig. 3.3). The first three principal components explained 86% of variation in morphology, and described a gradient between species with longer, more setose maxillae to species with reduced setae and a more robust incisor and lacinae mobilis (PC 1, inertia explained = 54%), a gradient between species with elongated, dentate lacinae mobilis (*H.*

samacos) and numerous, dentate distal setae (*T. texensis*) (PC 2, inertia explained = 21%), and a gradient in molar development (PC 3, inertia explained = 11%). Using forward selection, principal components 2 and 3 were identified as significant predictors of $\delta^{13}\text{C}$ and $\delta^{15}\text{N}$ values (PC2: $F = 3.35_{1,2.69}$, $p = 0.047$; PC3: $F = 7.79_{1,6.24}$, $p = 0.005$) (Fig. 3.4), although together they explained a small proportion of variance in isotope values (29%). Only the first RDA axis was significant (RDA 1: $F = 10.95_{1,8.77}$, $p = 0.0005$; RDA 2: $F = 0.19_{1,0.15}$, $p = 0.83$) and explained 29% of variance in isotope values. RDA axis 2 explained less than 1% of variance. Both principal components and isotope vectors were orthogonal to one another in RDA, with PC 2 associated with $\delta^{13}\text{C}$ and PC 3 associated with $\delta^{15}\text{N}$ values.

Linear models: Of the evaluated models incorporating the average number of denticles on setae on the distal margin of the outer plate of the 1st maxilla (*mx1sdentnum*) (Fig. 3.5) as a predictor of $\delta^{13}\text{C}$ values, AIC suggested that the interaction between $\delta^{15}\text{N}$ values and *mx1sdentnum* (Table 3.3, Fig. 3.6) was most likely the best predictor of $\delta^{13}\text{C}$ values (AIC weight = 0.58) although the model incorporating only $\delta^{15}\text{N}$ values as a predictor of $\delta^{13}\text{C}$ values also had substantial support (AIC weight = 0.22, $\Delta = 1.94$). This relationship was primarily due to one species, *T. insolita*, which was a statistical outlier for the *mx1sdentnum*. None of the models incorporating the length of the outer plate of the 2nd maxilla (*mx2op*) as a predictor of $\delta^{13}\text{C}$ values were supported by AIC when compared with a null model using $\delta^{15}\text{N}$ values as the only predictor. Models incorporating the number of molar ridges on the left mandible (*mdbridges*) (Fig. 3.7) were poor predictors of $\delta^{15}\text{N}$ values when *S. russelli* was included. When *S. russelli* was excluded, AIC

provided substantial support that of the evaluated models, mdbridges alone (Table 3.3, Fig. 3.6) was most likely the best predictor of $\delta^{15}\text{N}$ values (AIC weight = 0.74), whereas alternative models had substantially less support ($\Delta_{\text{AIC}} > 2.00$). Similar to mdbridges, models incorporating the planar molar area of the left mandible (mdbarea) (Fig. 3.7) were poor predictors of $\delta^{15}\text{N}$ values when *S. russelli* was included. When *S. russelli* was excluded, AIC suggested that mdbarea alone (Table 3.3, Fig. 3.6) was the most likely predictor of $\delta^{15}\text{N}$ values out of the evaluated models (AIC weight = 0.54), although the model incorporating the interaction between $\delta^{13}\text{C}$ values and mdbarea also had substantial support (AIC weight = 0.29, $\Delta = 0.48$). Similar to mdbridges and mdbarea, models incorporating the width of the incisor of the left mandible (incw) (Fig. 3.8) were poor predictors of $\delta^{15}\text{N}$ when *S. russelli* was included. When *S. russelli* was excluded, AIC suggested that the interaction between incisor width (mdbincw) and $\delta^{13}\text{C}$ values (Table 3.3, Fig. 3.6) was the most likely predictor of $\delta^{15}\text{N}$ values out of the evaluated models (AIC weight = 0.50) although the model incorporating mdbincw alone also had substantial support (AIC weight = 0.38, $\Delta_{\text{AIC}} = 0.56$).

Discussion

Ecological mechanisms that allow for the coexistence of species have received considerable attention (Hutchinson 1961; MacArthur & MacArthur 1961; Pianka 1974; Schoener 1974; Tilman 1982; Abrams 1995). Recent advances in our understanding of the role of biodiversity in ecosystem function and ecosystem services (Cardinale 2011; Carroll, Cardinale & Nisbet 2011) make such studies increasingly important. In the Edwards Aquifer, a diverse and ancient subterranean amphipod assemblage appears to

employ specialized feeding modes, as elucidated by a combination of isotopic and morphometric data. These observations suggest that 1) niche partitioning and feeding specialization are important to the maintenance of biodiversity in phreatic groundwater habitats, and 2) subterranean systems can possess greater trophic diversity than is often assumed (Fig. 3.1, Table 3.1).

As has been observed in marine species (Coleman 1990; Harow-Garay 2003), large, strong incisors (Fig. 3.8) are associated with an increasingly predatory (or necrophagous) feeding strategy in the Edwards Aquifer amphipods studied here. This relationship is evidenced by the positive relationship between $\delta^{15}\text{N}$ values and incisor width (Fig. 3.6, Table 3.3). Similarly, predatory feeding is also associated with reduction of the molar (Saint-Marie 1984; Guerra-Garcia & Tierno de Figueroa 2009) (Fig. 3.7), as evidenced by the negative relationships between $\delta^{15}\text{N}$ values, molar area, and number of molar ridges (Figs. 4-5; Table 3.3). Presumably, strong tearing incisors (i.e. the incisors of the three predacious species, *S. flagellatus*, *A. subterranea*, and *A. hirsuta*, had strongly dentate incisors rather than smooth, cutting edged incisors) are important for biting off pieces of animal tissue that are probably ingested whole rather than being extensively masticated, as evidenced by the reduced size and dentition of molars when compared with lower trophic level species. Lower trophic level species (as indicated by $\delta^{15}\text{N}$ values), such as *T. texensis*, exhibited proportionally larger and more strongly dentate mandibles, suggesting an adaptation to mastication (Fig. 3.4, Fig. 3.6). This has been observed in other basal consumer amphipods (Mayer *et al.* 2009) and could be adaptive

in the Edwards Aquifer for processing benthic sediments or biofilms containing carbonate mineral particles (Roberts *et al.* 2004).

As species grow, they are able to prey on larger food items, potentially reducing intraspecific competition. But although significant body size – $\delta^{15}\text{N}$ relationships have been observed in epigeal ecosystems (Jennings *et al.* 2001), the relationship observed in Edwards Aquifer amphipods was weak and significant for only two species. The lack of a strong body size – trophic level relationship may be due to a lack of correlation between prey body size and trophic position (Layman *et al.* 2005) or obfuscating effects of intraspecific, ontogenetic shifts in food items. Size relationships should be interpreted with caution because, to ensure adequate mass for isotope analysis, samples were biased towards the largest individuals collected and likely do not provide a complete picture of the entire demographic. Although N isotope data do quantify the relative trophic position of the amphipods studied, they do not necessarily imply that the investigated amphipods represent predator-prey systems. In addition to the three additional amphipod taxa that were not investigated, at least 17 species also occur at the study site, all of which could be potential prey items through direct predation (e.g. small species such as copepods, ostracods, and bathynellids, etc.) or necrophagy (e.g. large species, such as salamanders, shrimp, isopods).

Strongly dentate setae on the distal margins of amphipod mouthparts have been associated with scraping algae and biofilms by marine and freshwater amphipods (Arndt *et al.* 2005, Mayer *et al.* 2009). I interpret the positive relationship between $\delta^{13}\text{C}$ values

and the average number of denticles (Fig. 3.4, Fig. 3.6, Table 3.3) on the setae of the distal margin of the 1st maxilla given this form-function relationship. *T. insolita*, exhibited the greatest number of setal denticles on the 1st maxilla (Fig. 3.4-3.5) and $\delta^{13}\text{C}$ values that were more negative than suspended particulate organic matter at the sampling site (Fig. 3.1). Given these data, it seems likely that this species is scraping biofilms from rock surfaces within the aquifer that have more negative $\delta^{13}\text{C}$ signatures (probably due to chemolithoautotrophy) than fine particulate organic matter (FPOM) in the water column that is likely, in part, of photosynthetic (surface) origin. Other species, with mouthparts less specialized for scraping biofilms, are presumably utilizing a greater proportion of entrained FPOM through filter feeding. This hypothesis is supported by $\delta^{13}\text{C}$ values for several species (particularly *T. texensis* and *H. samacos*) that suggest FPOM as a major dietary component (Fig. 3.1). However, I predicted a positive relationship between the length of the outer plate of the 2nd maxilla (which was positively correlated with setation of several mouthparts) and $\delta^{13}\text{C}$ as an additional, statistical indicator of niche partitioning (specifically filter feeding and scraping). This relationship was not observed although several species had morphologies and isotopic signatures that are consistent with filter feeding (Fig. 3.9). *H. samacos* in particular has elongated plates of the 1st and 2nd maxilla that are heavily setose (Fig. 3.9). However, the three additional Hadziids (*A. hirsuta*, *T. insolita*, and *T. texensis*) were also more setose than amphipods of other families (although not to the extent of *H. samacos*) illustrating that phylogeny can potentially obfuscate form-function relationships (Perry & Pianka 1997).

One species, *S. russelli*, has unusually depleted $\delta^{15}\text{N}$ values (Fig. 3.1) despite having “generalized Crangonyctid” (Holsinger & Longley 1980) mouthparts similar to those of *S. flagellatus* (Figs. 5, 7-9). Because of its large size relative to sympatric amphipods (average body length = 6.65 mm for individuals investigated in this study) it is unlikely that *S. russelli* is a food source for other species such as *H. samacos*, *T. texensis*, and Hydrobiid snails (Hutchins & Schwartz 2013) that have higher body tissue $\delta^{15}\text{N}$ values but similar or smaller body sizes. Isotopic data suggest that this species may feed on a 3rd organic matter source (distinct from FPOM utilized by *H. samacos* and *T. texensis* and biofilms utilized by *T. insolita*, although what this source is and how *S. russelli* feeds is unclear.

Limited apparent relationships between morphology and isotope data could result from several confounding factors. As already discussed for Hadziids, morphologic data are limited by phylogenetic history (Perry & Pianka 1997). Furthermore, amphipods are known to employ diverse, highly specialized feeding behaviors, including exoparasitism (Schell, Rowntree & Pfeiffer 2000; Mekhanikova 2010), endoparasitism (Laval 1978; Mekhanikova 2010), predation (Coleman 1990), egg predation (Mekhanikova 2010), scraping ice algae (Arndt *et al.* 2005), and necrophagy (Saint-Marie 1984). The presence of idiosyncratic, species-specific morphologies associated with highly specialized feeding behaviors might not be apparent as general morphologic gradients across multiple species. Finally, apparent trophic specialists may preferentially function as trophic generalists, and morphologic specializations may be adaptations to feed on non-preferred or sub-optimal food resources to avoid interspecific competition when preferred

resources are limiting (Robinson & Wilson 1998). In this circumstance, feeding modes inferred from morphologic characteristics may not be reflected in average resource use, inferred from isotope data. RDA provided relatively little information on combinations of morphometrics that explained both $\delta^{15}\text{N}$ and $\delta^{13}\text{C}$ values. Rather, isotopes were largely associated with independent morphologic variables. This suggests that the separate components of trophic position described by $\delta^{15}\text{N}$ and $\delta^{13}\text{C}$ values (i.e. trophic position, and basal food source, respectively) are influenced by largely separate mouthpart morphologies (i.e. molars and incisors versus setae structure, respectively).

Conclusions

Isotopic data suggest that sympatric amphipods in the Edwards Aquifer of Central Texas utilize partially non-overlapping food resources. Higher trophic level consumers exhibit wider incisors and reduced molars, traits that have been associated with predation in other amphipod species. Lower trophic level consumers appear to employ both scraping, with scrapers exhibiting adaptive mouthpart setation and large triturative molars, and filter-feeding behaviors, with some species exhibiting extensive setation, although statistically significant morphometric evidence for filter-feeding was unobserved, possibly due to obfuscating effects of phylogeny. An integrated approach incorporating both morphologic and isotopic data allowed us to test predictions about trophic generalism and specialization in a community that would otherwise be difficult to observe.

Trophic specialization suggested by isotope data and specialized feeding modes suggested by morphologic variation provide strong support that competition among the

investigated amphipods drives niche partitioning. The occurrence of niche partitioning suggests that food resources in this system are not as patchy as is often assumed in subterranean habitats, and that species are not employing generalist feeding strategies to cope with unpredictable food resources. The observed partitioning of food resources by primary consumers (e.g. horizontal trophic diversity, *sensu* Duffy *et al.* 2007) is likely an important factor in the maintenance of high biological diversity in the Edwards Aquifer because it promotes coexistence of potential competitors and increasing resource exploitation (Finke & Snyder 2008), which in turn, increases resources supporting higher trophic levels.

Acknowledgements

Funding for this research was provide by the National Science Foundation (NSS award #s 1210270, 0742306), The Crustacean Society, and Geological Society of America. Dr. John Andersland provided SEM and image processing training. SEM analysis was made possible through much assistance from staff at the Texas State University College of Science and Engineering SEM laboratory.

References

- Abrams, P.A. (1995) Monotonic or unimodal diversity-productivity gradients: what does competition theory predict? *Ecology*, **76**, 2019-2027.
- Araújo, M. S., Bolnick, D. I., Machado, G., Giaretta, A. A., & dos Reis, S. F. (2007) Using $\delta^{13}\text{C}$ stable isotopes to quantify individual-level diet variation. *Oecologia* **152**: 643-654.
- Arndt, C. E., Berge, J., & Brandt, A. (2005) Mouthpart-atlas of arctic sympagic amphipods- trophic niche separation based on mouthpart morphology and feeding ecology. *Journal of Crustacean Biology*, **25**, 401–412.
- Barr, T. C. Jr., & Holsinger, J. R. (1985) Speciation in cave faunas. *Annual Review of Ecology and Systematics*, **16**, 313-337.
- Chesson, P. (2000) Mechanisms of maintenance of species diversity. *Annual Review of Ecology and Systematics*, **31**, 343-366.
- Barker, R.A., Bush, P.W., & Baker Jr., E.T. (1994) *Geologic history and hydrogeologic setting of the Edwards-Trinity Aquifer System, West-Central Texas*. U.S. Geological Survey Water-Resources Investigations Report 94-4039, Austin.
- Barr Jr., T. C., & Kuehne, R. A. (1971) Ecological studies in the Mammoth Cave System of Kentucky: II. The ecosystem. *Annales de Speleologie*, **26**, 47–96.
- Blanchet, F. G., Legendre, P., & Borcard, D. (2008) Forward selection of explanatory variables. *Ecology*, **89**, 2623-2632.
- Borcard, D., Gillet, F., & Legendre, P. (2011) *Numerical Ecology with R*. Springer, New York.
- Cardinale, B. J. (2011) Biodiversity improves water quality through niche partitioning. *Nature*, **472**, 86–89.
- Carroll, I.T., Cardinale, B. J., & Nisbet, R. M. (2011) Niche and fitness differences relate the maintenance of diversity to ecosystem function. *Ecology*, **92**, 1157-1165.
- Cole, G. A. & Watkins, R. L. (1977) *Hyaella montezuma*, A new species (Crustacea: Amphipoda) from Montezuma Well, Arizona. *Hydrobiologia*, **52**, 175-184.
- Coleman, C. O. (1990) *Bathypanoploea schellenbergi* Holman & Watling, 1983, An Antarctic amphipod (Crustacea) feeding on Holothuroidea. *Ophelia*, **31**, 197-205.

- Correa, S. B., & Winemiller, K. (2013) Niche partitioning among frugivorous fishes in response to fluctuating resources in the Amazonian floodplain forest. *Ecology*, in press.
- Culver, D. C., & Pipan, T. (2009) *The Biology of Caves and Other Subterranean Habitats*. Oxford University Press, Oxford.
- Culver, D. C., & Sket, B. (2000) Hotspots of Subterranean Biodiversity in Caves and Wells. *Journal of Cave and Karst Studies*, **62**, 11–17.
- Curl, R. L. (1966) Caves as a Measure of Karst. *The Journal of Geology*, **74**, 798–830.
- de Mendiburu, F. 2013. agricolae: Statistical Procedures for Agricultural Research v1.4. <http://tarwi.lamolina.edu.pe/~fmendiburu>.
- Dray, S., Bivand, R., Legendre, P., Oksanen, J., Blanchet, F. G., Solymos, P., Thioulouse, J., Simpson, G., & Jombart, T. (2013). packfor: Forward selection with permutation (Canoco p.46) v. 0.8. <http://R-Forge.R-project.org>.
- Duffy, J. E., Cardinale, B. J., France, K. E., McIntyre, P. B., Thébault, E., & Loreau, M. (2007) The functional role of biodiversity in ecosystems: incorporating trophic diversity. *Ecology Letters*, **10**, 522-538.
- Engel, A. S. & Randall, K. W. (2011) Experimental evidence for microbially mediated carbonate dissolution from the saline water zone of the Edwards Aquifer, Central Texas. *Geomicrobiology Journal*, **28**, 313-327.
- Finke, D. L., & Snyder, W. E. (2008) Niche partitioning increases resource exploitation by diverse communities. *Science*, **321**, 1488-1490.
- Gibert, J., & Deharveng, L. (2002). Subterranean ecosystems: a truncated functional biodiversity. *BioScience*, **52**, 473–481.
- Gibson, J. R., Harden, S. J., & Fries, J. N. (2008). Survey and Distribution of Invertebrates from Selected Springs of the Edwards Aquifer in Comal and Hays Counties, Texas. *The Southwestern Naturalist*, **53**, 74–84.
- Gray, C. J., & Engel, A. S. (2013) Microbial diversity and impact on carbonate geochemistry across a changing geochemical gradient in a karst aquifer. *The ISME Journal*, **7**, 325-337.
- Gross, K., & Cardinale, B. J. (2007) Does species richness drive community production or vice versa? Reconciling historical and contemporary paradigms in competitive communities. *American Naturalist*, **170**, 207-220.

- Guerra-García, J. M., & Tierno de Figueroa, J. M. (2009). What do caprellids (Crustacea : Amphipoda) feed on ? *Marine Biology*, **156**, 1881–1890.
- Haro-Garay, M. J. (2003) Diet and functional morphology of the mandible of two planktonic amphipods from the Strait of Georgia, British Columbia, *Parathemisto pacific* (Stebbing, 1888) and *Cyphocaris challengerii* (Stebbing, 1888). *Crustaceana*, **76**, 1291–1312.
- Holsinger, J. R. (1966) Subterranean amphipods of the genus *Stygonectes* (Gammaridae) from Texas. *American Midland Naturalist*, **76**, 100-124.
- Holsinger, J. R. (1967) Systematics, speciation, and distribution of the subterranean amphipod genus *Stygonectes* (Gammaridae). *United States National Museum Bulletin*, **259**.
- Holsinger, J. R. & Longley, G. (1980) The subterranean amphipod crustacean fauna of an artesian well in Texas. *Smithsonian Contributions to Zoology*, **308**.
- Holsinger, J. R. (1987) Redescription of the Stygobiont Amphipod Crustacean *Stygobromus pusillus* (Crangonyctidae) from the Soviet Union, with Comments on Taxonomic and Zoogeographic Relationships. *Journal of Crustacean Biology*, **7**, 249-257.
- Humphreys, W. F. (1999) Physico-chemical profile and energy fixation in Bundera Sinkhole, an anchialine remiped habitat in north-western Australia. *Journal of the Royal Society of Western Australia*, **82**, 89-98.
- Hutchins, B. T., & Schwartz, B. F. (2013) Food chain length in groundwater: patterns in $\delta^{15}\text{N}$ range. *Proceedings of the 2013 International Congress of Speleology*, **16-1**, 403-408.
- Hutchins, B. T., Schwartz, B. F., & Engel, A. E. (in press) Environmental controls on organic matter production and transport across surface-subsurface and geochemical boundaries in the Edwards Aquifer, Texas, USA. *Acta Carsologica*.
- Hutchinson, G. E. (1961) The paradox of the plankton. *The American Naturalist*, **95**, 137-145.
- Iskali, G. (2011) Macrinvertebrate diversity and food web dynamics in a guano subsidized cave ecosystem: Bracken Bat Cave. MS thesis, Texas State University.
- Jeannel, R. (1943) *Les fossils vivants des caverns*. Gallimard, Paris.
- Jennings, S., Pinnegar, J. K., Polunin, N. V., & Boon, T. W. (2001) Weak cross-species relationships between body size and trophic level belie powerful size-based trophic structuring in fish communities. *Journal of Animal Ecology*, **70**, 934-944.

- Laval, P. (1978) The barrel of the pelagic amphipod *Phronima sedentaria* (Forsk.)(Crustacea: hyperiidea). *Journal of Experimental Marine Biology and Ecology*, **33**, 187-211.
- Layman, C. A., Arrington, D. A., Montaña, C. G., & Post, D. M. (2007) Can Stable Isotope Ratios Provide for Community-Wide Measures of Trophic Structure? *Ecology*, **88**, 42–48.
- Layman, C. A., Winemiller, K. O., Arrington, D. A., & Jepsen, D. B. (2005) Body size and trophic position in a diverse tropical food web. *Ecology*, **86**, 2530-2535.
- Layman, C. A., Araujo, M. S., Boucek, R., Hammerschlag-Peyer, C. M., Harrison, E., Jud, Z. R., Matich, P., Rosenblatt, A. E., Vaudo, J. J., Yeager, L. A., Post, D. M., & Bearhop, S. (2012) Applying stable isotopes to examine food web structure: an overview of analytical tools. *Biological reviews of the Cambridge Philosophical Society*, **87**, 545–62.
- Levine J. M. & HilleRisLambers J. (2009) The importance of niches for the maintenance of species diversity. *Nature*, **461**, 254-257.
- Levinton, J. (1972) Stability and trophic structure in deposit-feeding and suspension-feeding communities. *The American Naturalist*, **106**, 472-486.
- Lowry, J. K. & Fenwick, G. D. (1983) The shallow-water gammaridean Amphipoda of the subantarctic islands of New Zealand and Australia: Melitidae, Hadziidae. *Journal of the Royal Society of New Zealand*, **13**, 201-260.
- Lujan, N. K., German, D. P., & Winemiller, W. O. (2011) Do wood-grazing fishes partition their niche?: morphological and isotopic evidence for trophic segregation in Neotropical Loricariidae. *Functional Ecology*, **25**, 1327-1338.
- MacArthur, R. H., & MacArthur, J.W. (1961) On bird species diversity. *Ecology*, **42**, 594-598.
- MacArthur, R. H., & Pianka, E.R. (1966) On optimal use of a patchy environment. *The American Naturalist*, **100**, 603-609.
- Matthews, B., Marchinko, K. B., Bolnick, D. I., & Mazumder, A. (2010). Specialization of trophic position and habitat use by sticklebacks in an adaptive radiation. *Ecology*, **91**, 1025–1034.
- Mayer G., Maier, G., Maas, A., & Walozek, D. (2009). Mouthpart morphology of *Gammarus roeselii* compared to a successful invader, *Dikerogammarus villosus* (Amphipoda). *Journal of Crustacean Biology*, **29**, 161–174.

- McCutchan Jr., J. H., Lewis Jr., W. H., Kendall, C., & McGrath, C. C. (2003). Variation in trophic shift for stable isotope ratios of carbon, nitrogen, and sulfur. *Oikos*, **102**, 378-390.
- Mekhanikova, I. V. (2010). Morphology of mandible and lateralia in six endemic amphipods (Amphipoda, Gammaridea) from Lake Baikal, in relation to feeding. *Crustaceana*, **83**, 865–887.
- Mudge, J. F., Baker, L. F., Edge, C. B., & Houlahan, J. E. (2012). Setting an optimal α that minimizes errors in null hypothesis significance tests. *PloS one*, **7**, e32734.
- Oksanen, J., Blanchet, F. G., Kindt, R., Legendre, P., Minchin, P. R., O'Hara, R. B. Simpson, G. L., Solymos, P., Henry, M., Stevens, H., & Wagner, H. (2013) Vegan: Community ecology package v 2.8. <http://vegan.r-forge.r-project.org/>
- Opsahl, S. P., & Chanton, J. P. (2006). Isotopic evidence for methane-based chemosynthesis in the Upper Floridan aquifer food web. *Oecologia*, **150**, 89–96.
- Perry, G. & Pianka, E. R. (1997) Animal foraging: past, present and future. *Trends in Ecology and Evolution*, **12**, 360-364.
- Peterson, B. J., & Fry, B. (1987) Stable isotopes in ecosystem studies. *Annual Review of Ecology and Systematics*, **18**, 293-320.
- Pianka, E. R. (1974) Niche overlap and diffuse competition. *Proceedings of the National Academy of Sciences*, **71**, 2141-2145.
- Pohlman, J. W., Iliffe, T. M., & Cifuentes, L. A. (1997). A stable isotope study of organic cycling and the ecology of an anchialine cave ecosystem. *Marine Ecology Progress Series*, **155**, 17–27.
- Post, D. M. (2002). The long and short of food-chain length. *Trends in Ecology & Evolution*, **17**, 269–277.
- Poulson, T. L., & Lavoie, K. H. (2000) The trophic basis of subsurface ecosystems. *Ecosystems of the World 30: Subterranean Ecosystems* (eds H. Wilkens, D. C. Culver, & W. F. Humphreys), pp. 231-250. Elsevier, Amsterdam.
- R Core Team. (2013) R: A Language and Environment for Statistical Computing. R Foundation for Statistical Computing, Vienna. <http://www.R-project.org>
- Robinson, B. W., & Wilson, D. S. (1998) Optimal foraging, specialization, and a solution to Liem's Paradox. *The American Naturalist*, **151**, 223-235.

- Roberts, J. A., Bennett, P. C., González, L. A., Macpherson, G. L., & Milliken, K. L. (2004) Microbial precipitation of dolomite in methanogenic groundwater. *Geology*, **32**, 277-280.
- Saint-Marie, B. (1984) Morphological adaptations for carrion feeding in four species of littoral or circalittoral lysianassid amphipods. *Canadian Journal of Zoology*, **62**, 1668-1674.
- Sarbu, S. M., Kane, T. C., & Kinkle, B. (1996). A Chemoautotrophically Based Cave Ecosystem. *Science*, **272**, 1953–1955.
- Schell, D. M., Rowntree, V. J. & Pfeiffer, C. J. (2000) Stable-isotope and electron-microscopic evidence that cyamids (Crustacea: Amphipoda) feed on whale skin. *Canadian Journal of Zoology*, **78**, 721-727.
- Schneider, C. A., Rasband, W. S., & Eliceiri, K. W. (2012) NIH Image to ImageJ: 25 years of image analysis. *Nature Methods*, **9**, 671-675.
- Schoener, T. W. (1974) Resource partitioning in ecological communities. *Science*, **185**, 27-39.
- Schoener, T.W. (1989) The ecological niche. *Ecological Concepts* (ed J.M. Cherrett), pp.79-113. Blackwell, Oxford.
- Simon, K. S., Benfield, E. F., & Macko, S. A. (2003). Food Web Structure and the Role of Epilithic Biofilms in Cave Streams. *Ecology*, **84**, 2395–2406.
- Simon, K. S., Pipan, T., & Culver, D. C. (2007). A Conceptual Model of the Flow and Distribution of Organic Carbon in Caves. *Journal of Cave and Karst Studies*, **69**, 279–284.
- Sims, D. W., Southall, E. J., Humphries, N. E., Hays, G. C., Bradshaw, C. J. A., Pitchford, J. W., James, A., Ahmed, M. Z., Brierley, A. S., Hindell, M. A., Morritt, D., Musyl, M. K., Righton, D., Shepard, E. L. C., Wearmouth, V. J., Wilson, R. P., Witt, M. J., & Metcalfe, J. D. (2008) Scaling laws of marine predator search behaviour. *Nature*, **451**, 1098-1102.
- Smart, P. L., Beddows, P. A., Doerr, S., & Whitaker, F. F. (2006) Cave Development on the Caribbean coast of the Yucatan Peninsula , Quintana Roo , Mexico. *Geological Society of America Special Paper*, **404**, 105–128.
- Stejneger, L. (1896). Description of a new genus and species of blind tailed batrachian from the subterranean waters of Texas. *Proceedings of the United States National Museum*, **18**, 619–621.

- Stephens, D. W. & Krebs, J. R. (1986) *Foraging theory*. Princeton University Press, Princeton.
- Svanbäck, R., & Schluter, D. (2012) Niche specialization influences adaptive phenotypic plasticity in the threespine stickleback. *The American Naturalist*, **180**, 50-59.
- Tilman, D. (1982) *Resource Competition and Community Structure*. Princeton University Press, Princeton.
- Tobin, B. W., Hutchins, B. T., & Schwartz, B. F. (2013) Spatial and temporal changes in invertebrate assemblage structure from the entrance to deep-cave zone of a temperate marble cave. *International Journal of Speleology*, **42**, 203-214.
- Vanderklift, M. A., & Ponsard, S. 2003. Sources of variation in consumer-diet $\delta^{15}\text{N}$ enrichment: a meta-analysis. *Oecologia*, **136**, 169-182.
- Vergnon, R., Leijts, R., van Nes, E. H., & Scheffer, M. (2013). Repeated Parallel Evolution Reveals Limiting Similarity in Subterranean Diving Beetles. *The American Naturalist*, **182**, 67-75.
- Wilson, R. P. (2010) Resource partitioning and niche hyper-volume overlap in free-living Pygoscelid penguins. *Functional Ecology*, **24**: 646-657.

Table 3.1: Mean $\delta^{13}\text{C}$ and $\delta^{15}\text{N}$ values for amphipod species and groupings based on Fishers LSD post-hoc test of ANOVA results. Letters represent unique groups. Species with more than one letter belong to more than one group.

Species	$\delta^{15}\text{N}$ group	$\delta^{13}\text{C}$ group	Mean $\delta^{15}\text{N}$ (‰)	Mean $\delta^{13}\text{C}$ (‰)
Artesia subterranea	a	c	14.07	-37.13
Stygobromus flagellatus	b	b,c	11.65	-35.82
Allotexiweckelia hirsuta	b,c	c	10.42	-37.96
Texiweckeliopsis insolita	c	d	9.64	-42.03
Holsingerius samacos	d	a,b	7.87	-33.47
Texiweckelia texensis	e	a,b	5.70	-31.77
Stygobromus russelli	f	a,b	1.61	-31.34

Table 3.2: Morphometric variables chosen as predictor variables for statistical analysis, and hypothesized feeding mode interpretations. mx1sdentnum = average number of denticles on setae of distal medial of outer plate of 1st maxilla; mdbridges = number of molar ridges on left mandible; mx2op = length of outer plate of 2nd maxilla; mdbarea = planar area of molar of left mandible; mdbincw = width of incisor of left mandible.

Morphometric	Hypothesized interpretation
mx1sdentnum	variable among primary consumers: low in filterers and high in scrapers
mdbridges	variable among trophic levels: lower in predators
mx2op	variable among primary consumers: larger in filter feeders (associated with number of medial endite setae)
mdbarea	variable among trophic levels: lower in predators
mdbincw	variable among trophic levels: higher in predators/ necrophages

Table 3.3: Significant models of isotopic composition as a function of mouthpart morphology. Mx1sdentnum = number of setae on distal margin of outer plate of 1st maxilla; mdbridges = number of ridges of molar of left mandible; mdbarea = planar area of molar of left mandible; mdbincw= left mandible incisor width.

Model	R2	F	DF	p	optimal α
$\delta^{13}\text{C} = -32.99 - 0.03 \cdot \text{mx1sdentnum} \cdot \delta^{15}\text{N}$	0.48	6.57	1,5	0.051	0.29
$\delta^{15}\text{N} = 14.73 - 0.42 \cdot \text{mdbridges}$	0.73	14.28	1,4	0.019	0.31
$\delta^{15}\text{N} = 13.24 - 6.74 \cdot \text{mdbarea}$	0.74	15.31	1,4	0.017	0.31
$\delta^{15}\text{N} = 6.73 - 10.12 \cdot \text{mdbincw}$	0.42	4.63	1,4	0.098	0.31

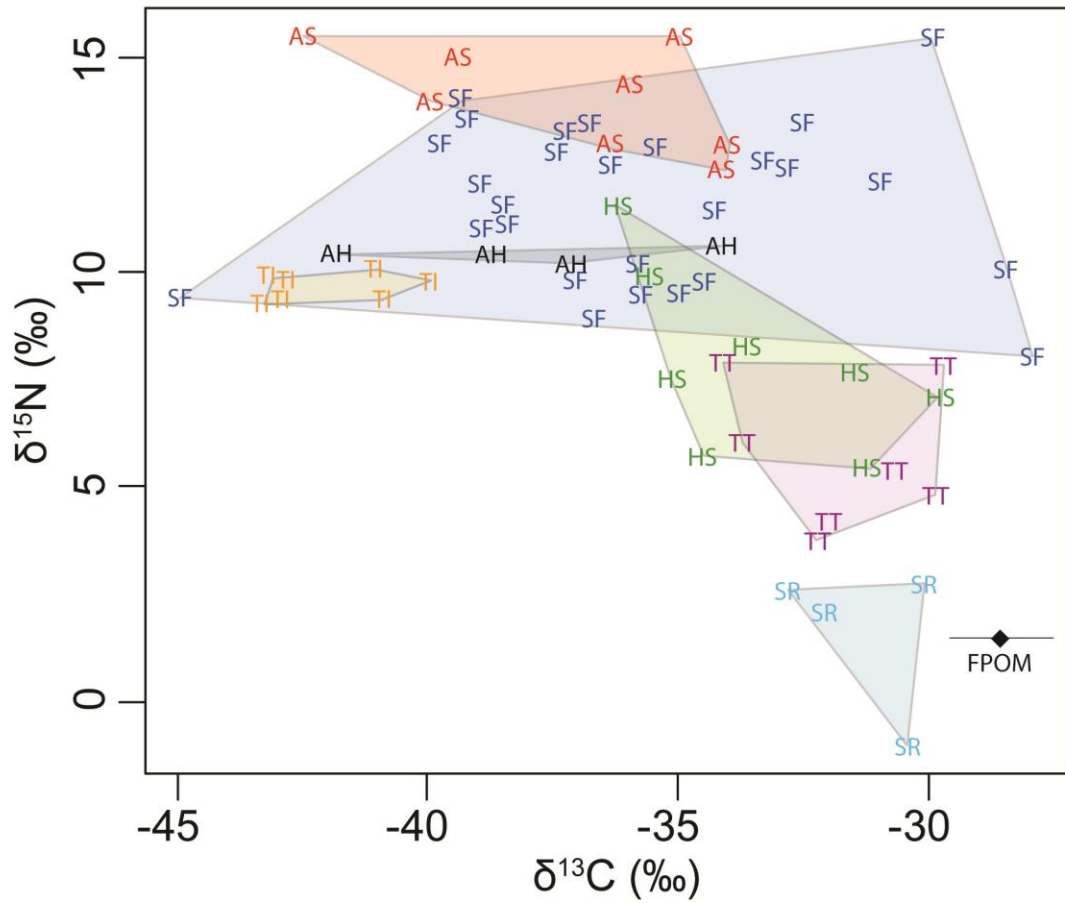


Figure 3.1: Isotope biplot of individual amphipods and fine particulate organic matter (FPOM) from the sampling site. Bar shows FPOM standard deviation (none for $\delta^{15}\text{N}$ because $N = 1$). AS = *Artesia subterranea*, SF = *Stygobromus flagellatus*, AH = *Allotexiweckelia hirsuta*, TI = *Texiweckeliopsis insolita*, HS = *Holsingerius samacos*, TT = *Texiweckelia texensis*, SR = *Stygobromus russelli*.

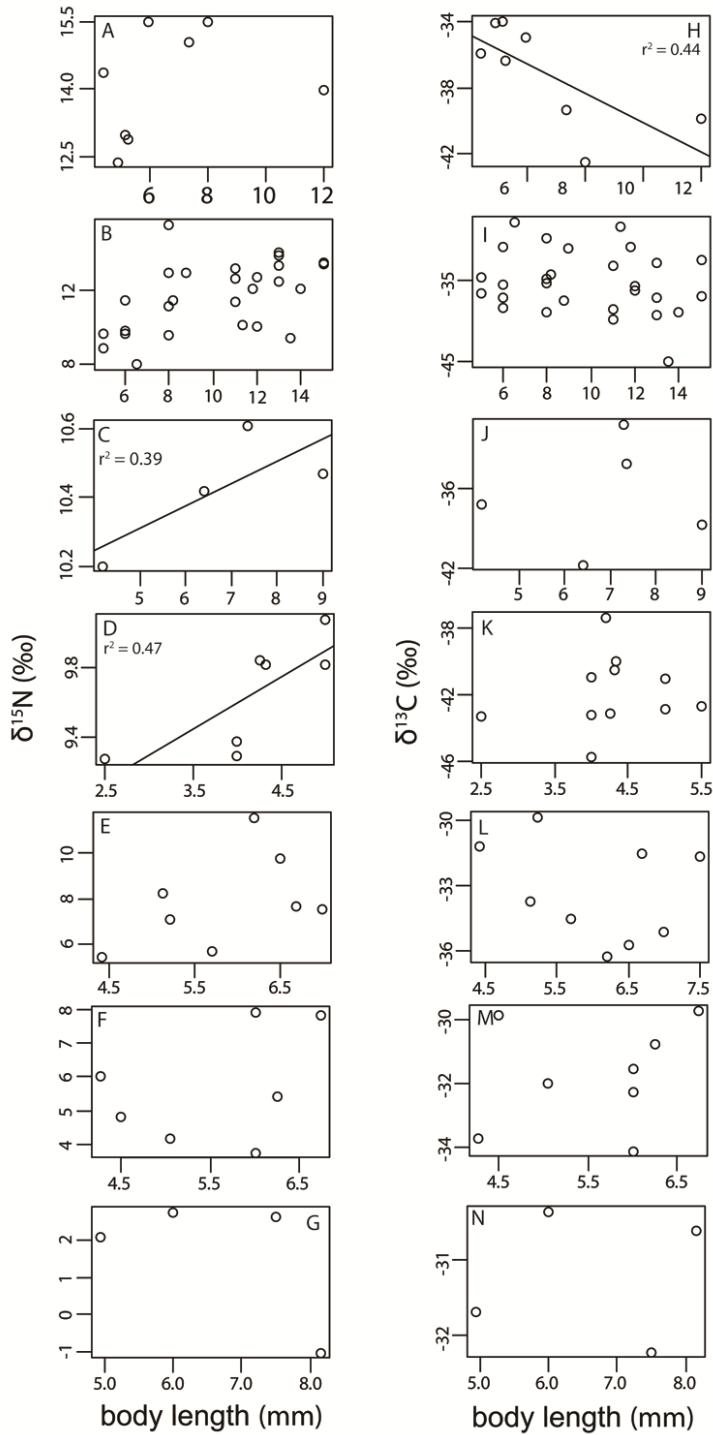


Figure 3.2: Species-specific $\delta^{15}\text{N}$ – body length and $\delta^{13}\text{C}$ – body length relationships. A, H = *Artesia subterranea*; B, I = *Stygobromus flagellatus*; C, J = *Allotexiweckelia hirsuta*; D, K = *Texiweckeliopsis insolita*; E, L = *Holsingerius samacos*; F, M = *Texiweckelia texensis*; G, N = *Stygobromus russelli*. Trendlines and R^2 values are shown for significant relationships.

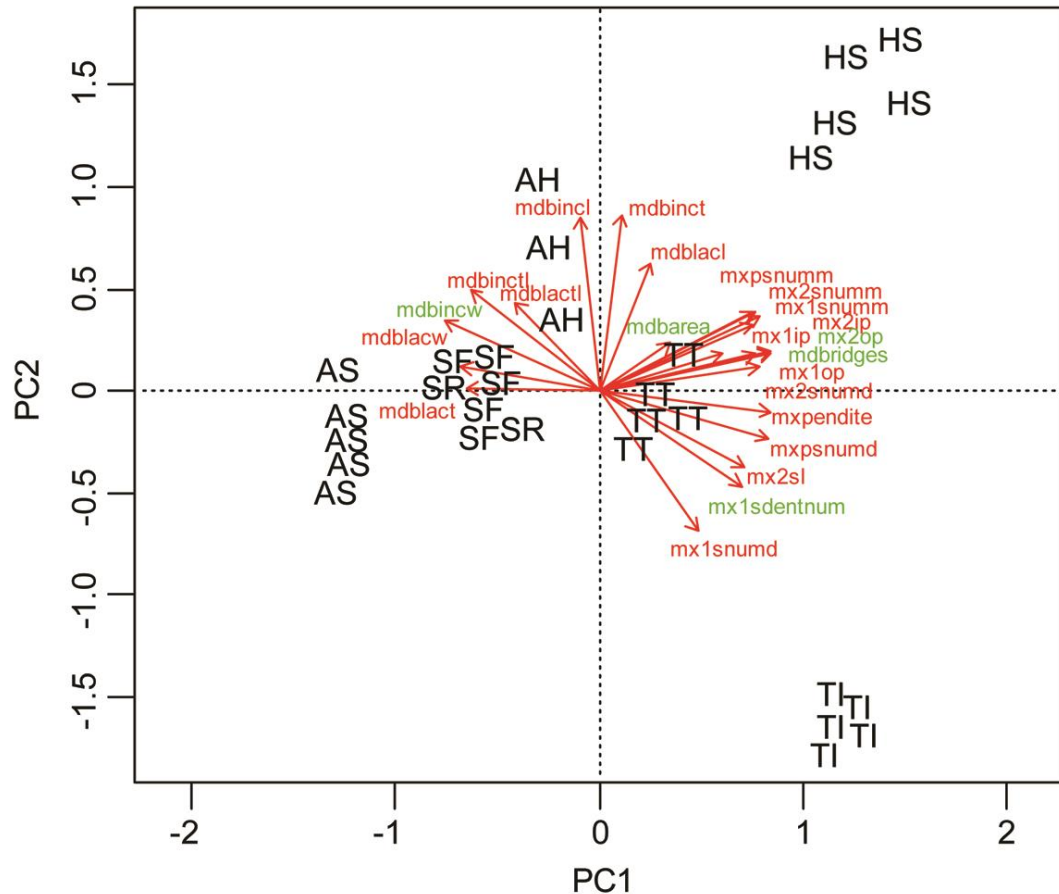


Figure 3.3: PCA biplot of amphipod positions in morphometric space. Proportion of variance explained = 54% and 21% for PC1 and PC2, respectively. AS = *Artesia subterranea*, SF = *S. flagellatus*, AH = *A. hirsuta*, TI = *T. insolita*, HS = *H. samacos*, TT = *T. texensis*, SR = *S. russelli*. mxpsnumd = number of setae on distal margin of inner plate of maxilliped; mxpsnumm = number of setae on medial margin of inner plate of maxilliped; mx1snumm = number of setae on medial margin of inner plate of 1st maxilla; mx1snumd = number of setae on distal margin of 1st maxilla; mx1sdentnum = average number of denticles on setae on distal margin of outer plate of 1st maxilla; mx2snumm = number of setae on medial margin of inner plate of 2nd maxilla; mx2snumd = number of setae on distal margin of outer plate of 2nd maxilla; mdbridges = number of molar ridges on left mandible; mdbinct = number of incisor teeth on left mandible; mdblact = number of lacinae mobilis teeth on left mandible; mxppalp = length of 4 distal segments of maxilliped palp (includes tooth); mxpendite = length of inner plate of maxilliped; mx1ip = length of inner plate of 1st maxilla; mx1op = length of outer plate of 1st maxilla; mx2ip = length of inner plate of 2nd maxilla; mx2op = length of outer plate of 2nd maxilla; mx2sl = maximum length of distal setae on outer plate of 2nd maxilla; mdbarea = planar area of molar of left mandible; mdbincl = length of incisor of left mandible; mdbincw = width of incisor of left mandible; mdbinctl = maximum tooth length of incisor of left mandible; mdblacl = length of lacinae mobilis of left mandible; mdblacw = width of lacinae mobilis of left mandible; mdblactl = maximum length of lacinae mobilis tooth of left mandible. Morphometrics used in linear regressions are shown in green.

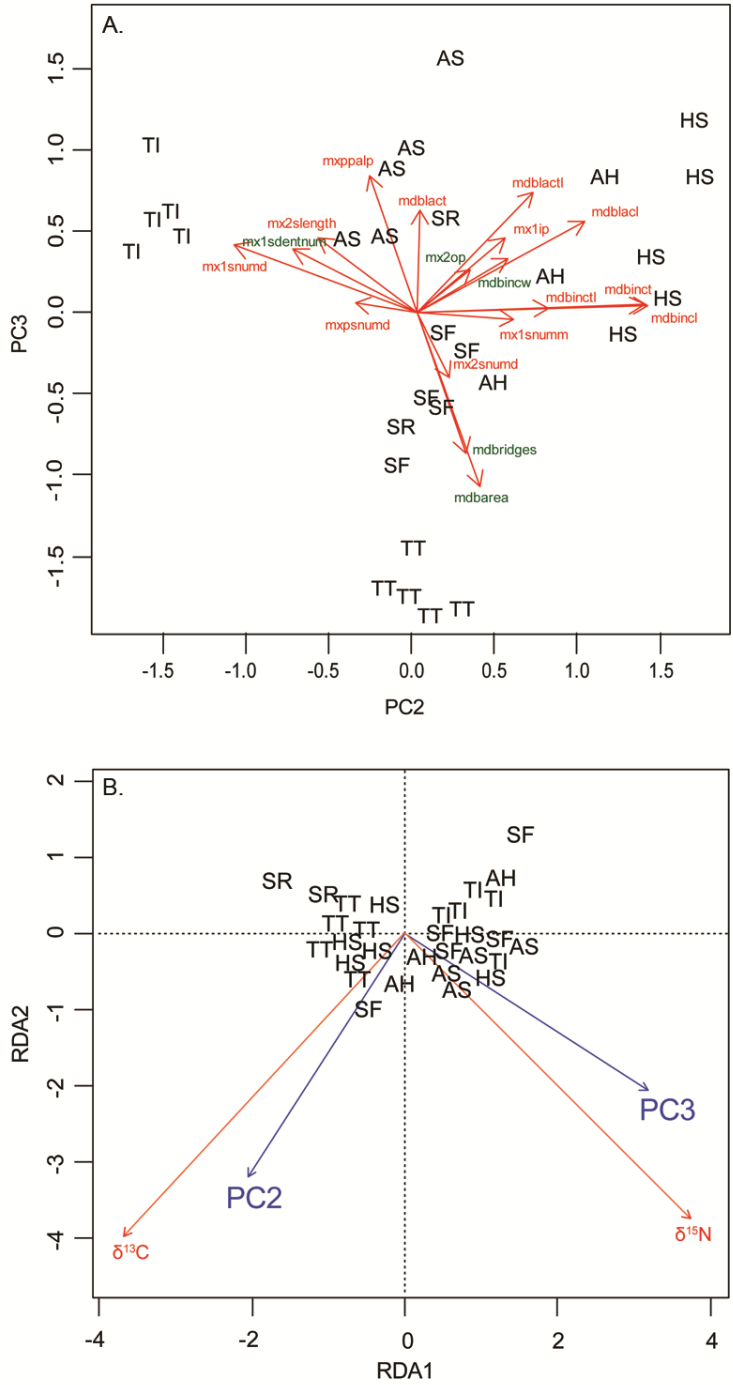


Figure 3.4: A: PCA biplot on PC 2 and PC 3. B: Biplot of result of reduncancy analysis (RDA) showing relation between significant principal components, shown in A, and stable isotope values for individuals. Only RDA axis 1 is significant, explaining 29% of variance in isotope values. RDA2 explains less than 1% of variance. Text is as in figure 3.3.

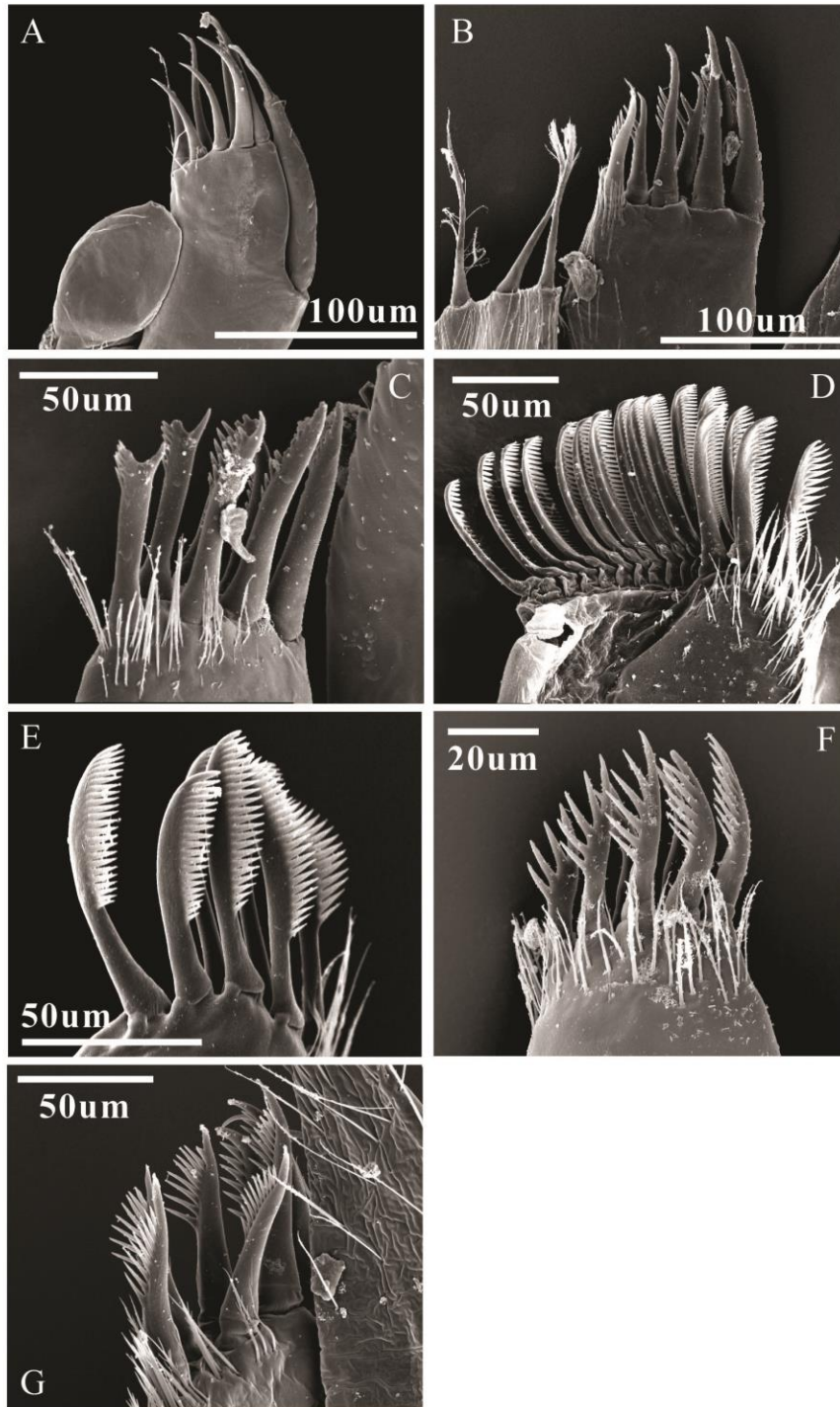


Figure 3.5: SEM images of setae on the distal margin of outer plate of 1st maxilla (mx1). A = *Artesia subterranea*, B = *Stygbromus flagellatus*, C = *Allotexiweckelia hirsuta*, D = *Texiweckeliopsis insolita*, E = *Holsingerius samacos*, F = *Texiweckelia texensis*, G = *Stygbromus russelli*.

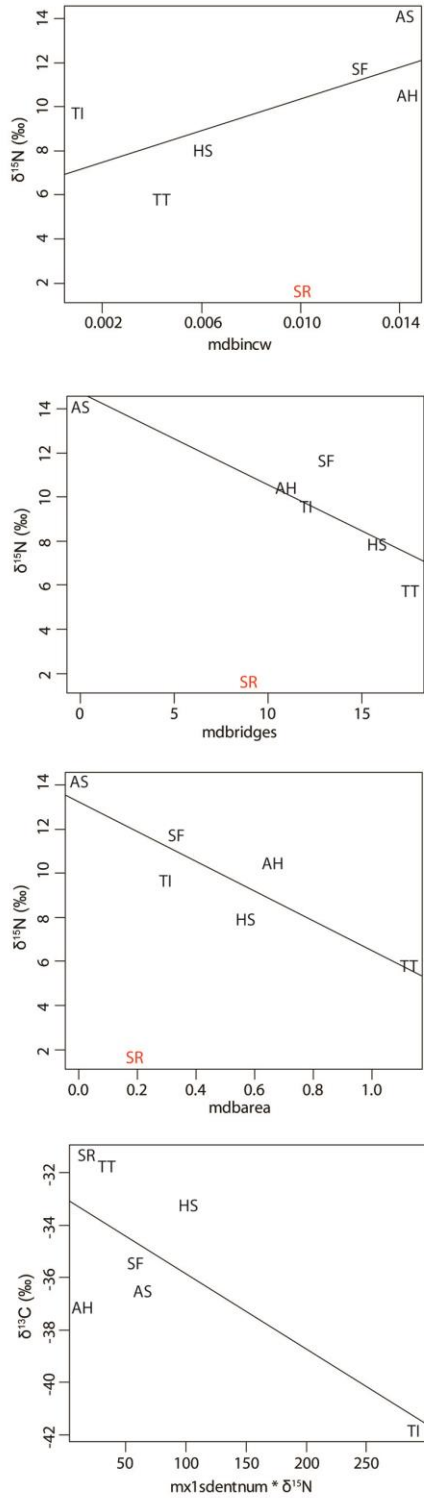


Figure 3.6: Linear regression of species average isotope values as a function of morphometric or morphometric · isotopic data. For regressions predicting $\delta^{15}\text{N}$ values, *S. russelli* is shown in red, but was excluded from regression analysis. AS = *A. subterranea*, SF = *S. flagellatus*, AH = *A. hirsuta*, TI = *T. insolita*, HS = *H. samacos*, TT = *T. texensis*, SR = *S. russelli*.

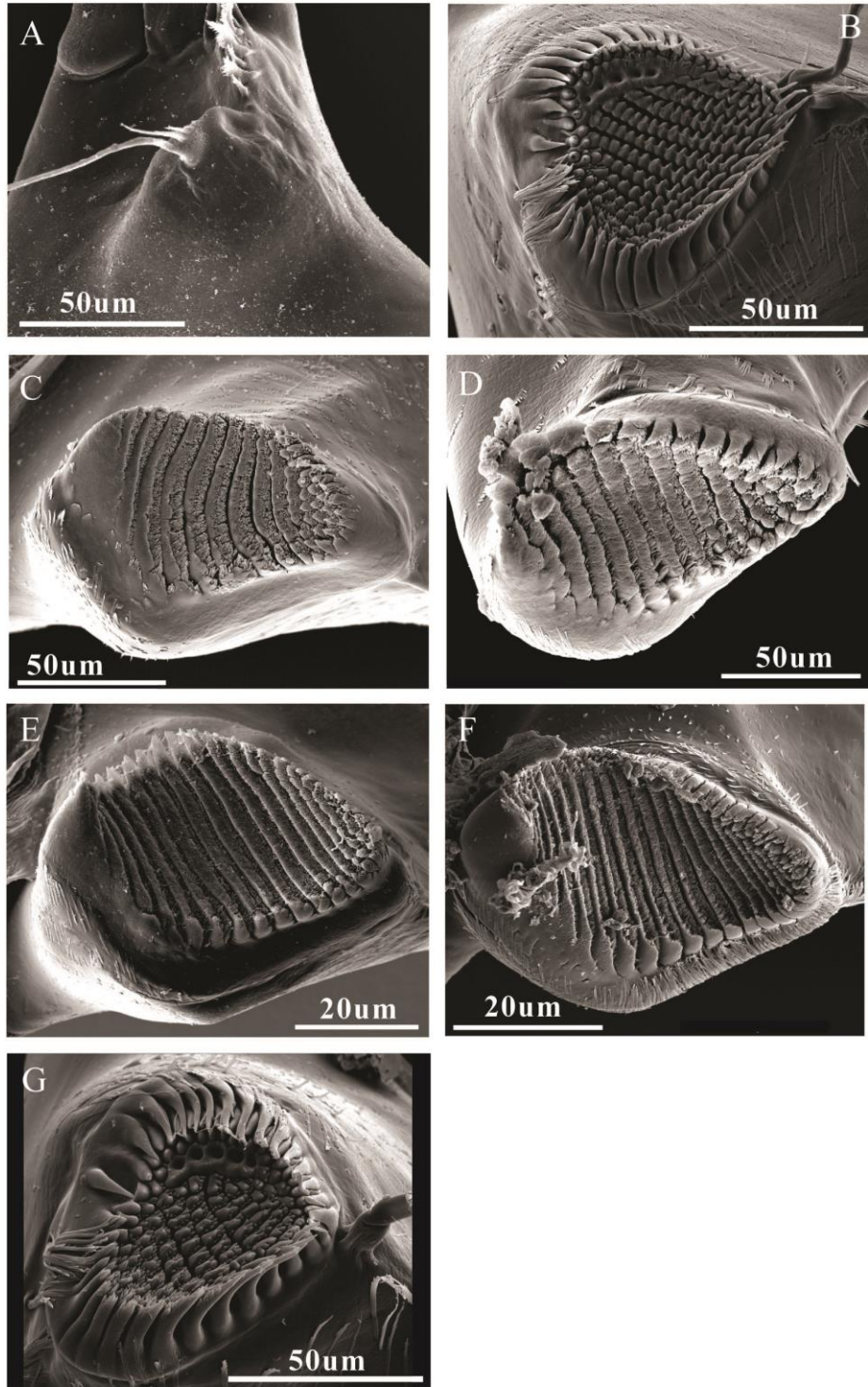


Figure 3.7: SEM images of the left molar (mdb). A = *Artesia subterranea*, B = *Stygbromus flagellatus*, C = *Allotexiweckelia hirsute*, D = *Texiweckeliopsis insolita*, E = *Holsingerius samacos*, F = *Texiweckelia texensis*, G = *Stygbromus russelli*.

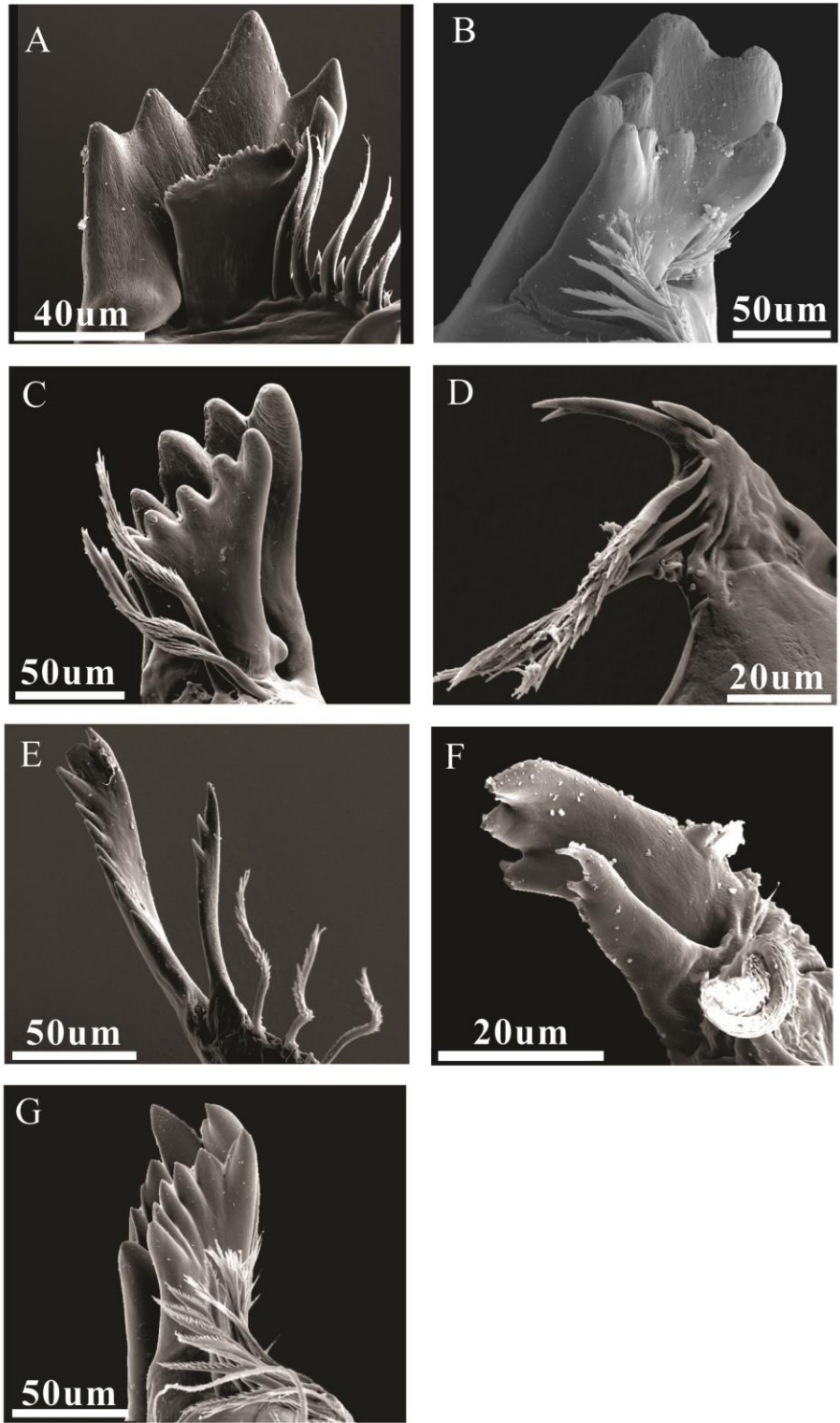


Figure 3.8: SEM images of the left incisor and lacinae mobilis (inc & lac). A = *Artesia subterranea*, B = *Stygbromus flagellatus*, C = *Allotexiweckelia hirsute*, D = *Texiweckeliopsis insolita*, E = *Holsingerius samacos*, F = *Texiweckelia texensis*, G = *Stygbromus russelli*.

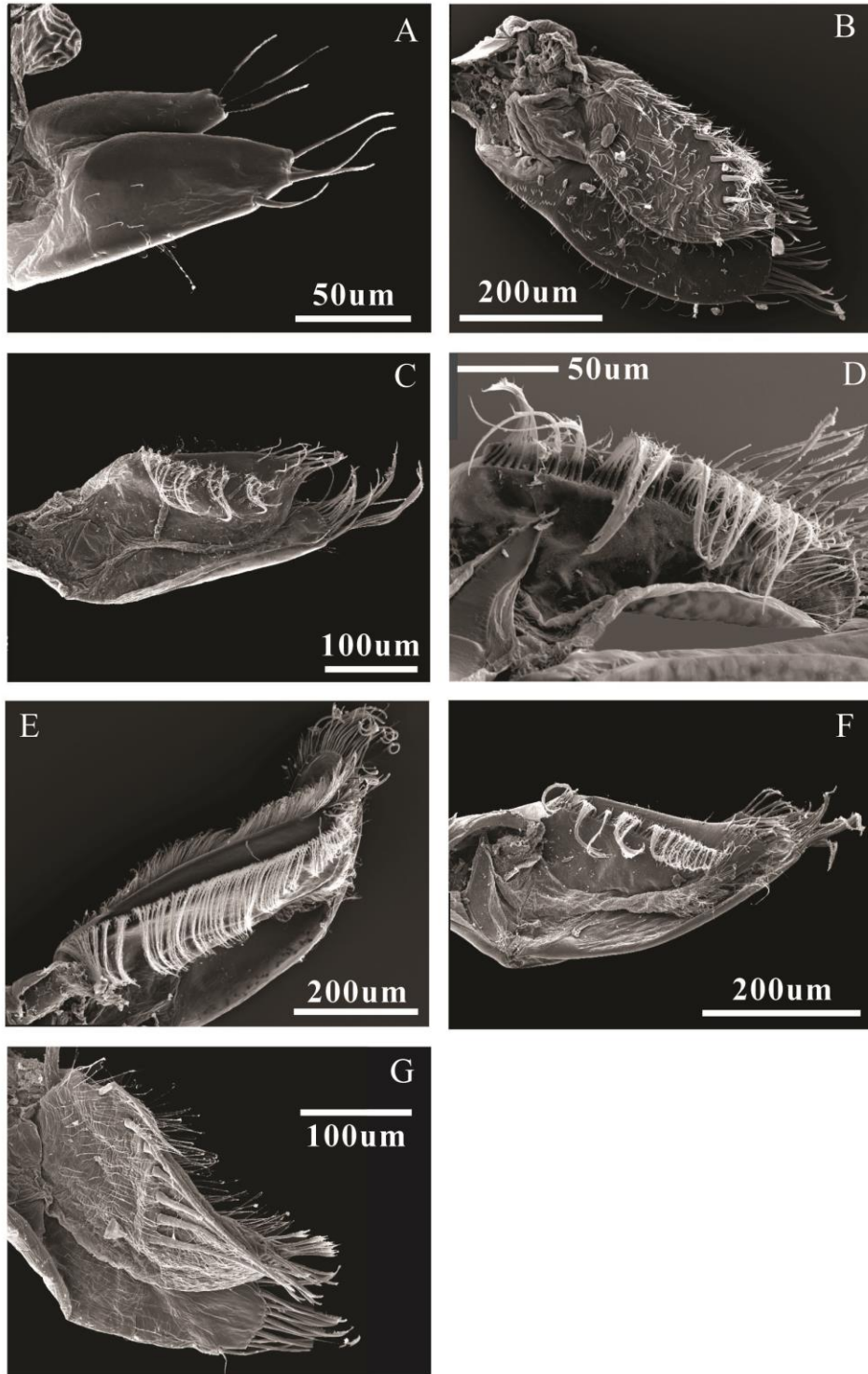


Figure 3.9: SEM images of 2nd maxilla (mx2). Only inner plate shown for *Texiweckeliopsis insolita*. A = *Artesia subterranea*, B = *Stygbromus flagellatus*, C = *Allotexiweckelia hirsute*, D = *Texiweckeliopsis insolita*, E = *Holsingerius samacos*, F = *Texiweckelia texensis*, G = *Stygbromus russelli*.

IV: TROPHIC COMPLEXITY IN A SUBTERRANEAN FOOD WEB WITH CHEMOLITHOAUTOTROPHIC AND PHOTOSYNTHETIC FOOD CHAINS

Abstract

In globally widespread habitats without sunlight chemolithoautotrophy can replace or subsidize allochthonous input of photosynthetically derived organic matter as a food source, which promotes niche specialization and evolution of higher trophic levels.

There is a prevailing paradigm that subterranean food webs are dominated by trophic generalists occupying one to two trophic levels. This paradigm is based on relatively few studies biased towards a particular habitat (i.e. air-filled caves). I argue that the current subterranean food web paradigm be re-evaluated, and re-focused on ecological and historical factors that influence observable variability in trophic complexity. In support of this, I present isotopic and geochemical evidence of a groundwater food chain in which primary consumers show morphologic specializations for scraper/benthic foraging and filter feeding. Specialization is an adaptation to the presence of two disparate food sources: primary chemolithoautotrophic production by epilithic biofilms, constituting up to 88% (95% ETCI = 82% - 94%) of species diets, and photosynthetically produced organic matter, constituting up to 93% (0% - 22%) of species diets. The relative prevalence of each food source varies as a function of hydrological proximity to geographically separated chemolithoautotrophic and photosynthetic organic matter inputs ($r^2 = 068$). Horizontal trophic diversity resulting from scraping chemolithoautotrophic and filtering photosynthetic food chains increases biomass available to support higher trophic levels, including secondary predators. Within the aquifer, species richness

decreases with increasing distance from chemolithoautotrophic sources, indicating that chemolithoautotrophy is fundamental for maintaining trophic complexity, especially during periods of decreased photosynthetic production and groundwater recharge during the mid-Holocene altithermal period. Although the Edwards Aquifer may not be representative of typical groundwater food chains, the conditions promoting trophic complexity in groundwater, that include chemolithoautotrophy, are probably not as exceptional as typically assumed.

Introduction

Generalist feeding strategies facilitate exploitation of a wide range of food resources when food resources are unpredictable whereas specialized feeding strategies optimize feeding efficiency when resource supply exceeds demand (MacArthur & Pianka 1966; chapter 3). When resource supply rate is sufficiently constant, niche partitioning, defined as foraging by potential competitors on partially non-overlapping food resources, can evolve as a mechanism for reducing interspecific variation (MacArthur 1958; Levinton 1972; Pianka 1974; Schoener 1974; Chapter 3). Despite these general predictions, specific hypotheses about community-scale trophic structure under various resource supply regimes can be difficult to test because of the large number of species in most food webs (Polis & Strong 1996), the potential for multiple food sources (Phillips & Gregg 2003), and variability due to non-trophic environmental conditions (Fridley *et al.* 2007). Subterranean habitats are often touted as ideal natural laboratories for community ecological studies because of the prevalence of communities comprised of few species that occupy a relatively stable habitat with a reduced number of food resources (Poulson

& White 1969; Culver *et al.* 1995; Juan *et al.* 2010). Nevertheless, the prevailing paradigm in speleobiological literature, that suggests subterranean food webs are generalist-dominated, short food chains resulting from severely limiting and/or heterogeneously distributed resources (Gibert & Deharveng 2002; Hüppop 2012; Poulson 2012) (Table 4.1), is based on surprisingly few observations (Simon *et al.* 2007) and contradicts recent evidence that “even the most extreme, energy-poor environments still maintain the potential for diversification via differentiation of niches” (Fišer *et al.* 2012).

Food web studies in subterranean systems have primarily been limited to terrestrial or vadose aquatic habitats (humanly accessible caves) dependent on allochthonous resources. These studies have revealed omnivory in taxa that are typically predacious in epigean habitats (Gibert & Deharveng 2002) and, in the case of aquatic systems, food webs with one to two trophic levels based on heterotrophic bacteria utilizing dissolved organic matter (DOM) or fine particulate organic matter (FPOM) from the surface (Graening & Brown 2003; Simon *et al.* 2003). However, a number of food web studies in phreatic groundwater habitats have employed stable isotope techniques to illustrate food webs based, at least in part, on chemolithoautotrophic production, reviewed in chapter 2. Measured rates of carbon fixation by phreatic chemolithoautotrophs in a biodiverse aquifer in Romania (281 g C/m²/yr, Porter *et al.* 2009) fall within ranges reported for a variety of epigean habitats, including boreal forests and semi-deserts (Roy *et al.* 2001), lakes (Sabo *et al.* 2009), and oceanic pelagic zones (Saba *et al.* 2011). These habitats can have complex food webs and trophic specialists are known to occur.

Although reviews of subterranean food web structure acknowledge the presence of chemolithoautotrophy in groundwater systems (Poulson & Lavoie 2000; Gibert & Deharveng 2002; Hüppop 2012; Poulson 2012), these studies repeatedly consider chemolithoautotrophic systems as exceptions to the general rule. But, phreatic aquifers are widespread if not the most common groundwater habitat, conditions favorable for chemolithoautotrophy (i.e. an inorganic carbon source and redox boundary) are, at a minimum, locally present within many phreatic aquifers, established high diversity in phreatic aquifers, and widespread acknowledgement that chemolithoautotrophic production is important in other aquatic habitats with redox gradients, including lakes (Casamayor *et al.* 2008), mid- and deep-water marine environments (Fry *et al.* 1991; Swan *et al.* 2011), and streams (Kohzu *et al.* 2004).

I propose that the general paradigm of short food chains and pervasive generalist feeding strategies in groundwater be reconsidered and refocused to address the historical and ecological factors that influence observed variability in trophic structure in subterranean habitats. In support of this argument, I use the Edwards Aquifer of Central Texas as an example system that does not conform to the prevailing paradigm. I use patterns in the isotopic and chromophoric properties of dissolved organic matter across a hydrogeochemical gradient within the Edwards Aquifer to illustrate that chemolithoautotrophic and photosynthetic organic matter (COM and POM) are variably present and utilized by stygobionts within the aquifer. I use Bayesian mixing models to elucidate the ecological consequences of disparate and, in the case of COM, constant resource supply in a groundwater. This research provides evidence that

chemolithoautotrophy maintains metazoan diversity in a phreatic aquifer whose community is comprised of both trophic specialists and secondary predators.

Evidence for chemolithoautotrophy in the Edwards Aquifer

For several decades, the karstic Edwards Aquifer of South-Central Texas, USA (Fig. 4.1), has been an acknowledged hotspot of aquatic subterranean (stygobiont) biodiversity (Longley 1981). Surface streams sink along the north-western margin of the aquifer, thereby recharging water and importing photosynthetically derived organic matter (POM) into the aquifer (Barker *et al.* 1994; chapter 1). To the south and east, the aquifer is confined below non-karst clays and marls that prevent recharge (Barker *et al.* 1994). Oxygenated, low total dissolved solids (TDS) waters from surface recharge are juxtaposed against dysoxic and anoxic, high TDS waters where electrical conductivity increases from 500 uS/cm to over 15,000 uS/cm (Fig. 4.1) and sulfide concentrations exceed 100 mg/L along a rapid transition zone called the freshwater-saline water interface (FWSWI).

Putative chemolithoautotrophic microbes along this steep redox gradient are described from 16S rRNA Sanger sequenced gene sequences and 454 tag pyrosequencing (Engel & Randall 2011; Gray & Engel 2013). Microbial mats and water samples in the saline zone and at the FWSWI are dominated by Proteobacteria, including *Gammaproteobacteria* (e.g. *Thiothrix* spp.), *Alphaproteobacteria*, and *Betaproteobacteria*, which include chemolithoautotrophic sulfur-oxidizing and methane-oxidizing taxa. This community composition mirrors that found in other sulfidic, chemolithoautotrophic groundwater

systems (Porter *et al.* 2009). The stable carbon isotopic composition of FPOM ($\delta^{13}\text{C}_{\text{FPOM}}$) along the FWSWI is significantly more negative than $\delta^{13}\text{C}_{\text{FPOM}}$ in surface streams recharging the aquifer ($\Delta = 8.76\text{‰}$; $t = 2.44_{28.58}$, $p = 0.021$) where organic matter (OM) is produced via photosynthesis, suggesting that FWSWI FPOM is not solely derived from surface inputs. Rather, a significant positive relationship between FWSWI $\delta^{13}\text{C}_{\text{FPOM}}$ and the stable carbon isotopic composition of dissolved inorganic carbon ($\delta^{13}\text{C}_{\text{DIC}}$) ($F = 10.42_{1,18}$, $r^2 = 0.33$, $p = 0.005$) (chapter 1) provides evidence that DIC is serving as a carbon substrate for *in-situ* carbon fixation by the FWSWI microbial assemblage. A central goal of this research was to assess the relative importance of COM and POM as food resources for metazoans.

A biogeochemical gradient between recharge dominated and freshwater – saline water interface dominated groundwater

COM and POM origins in the Edwards Aquifer are hydrogeologically isolated from one another, occurring along the south-east and north-west margins of the freshwater zone, respectively. Consequently, sites in the freshwater zone of the Edwards Aquifer capable of supporting metazoan taxa occur along a hydrologic gradient between sites where geochemistry and OM composition is dominantly influenced by the effects of recharging, surface water to sites influenced by processes occurring along the FWSWI (referred to here as the recharge-FWSWI gradient). Because of anisotropy and heterogeneity within the aquifer (Scanlon *et al.* 2003), linear distances from OM sources (the recharge zone and FWSWI) are not fully representative of hydrologic distances, but as indicators of biogeochemical processes resulting from surface water-groundwater exchange near

recharge features and redox reactions occurring near the FWSWI, concentrations of O_2 and NO_3^- help clarify the position of groundwater sites along this gradient.

In the Edwards Aquifer, dissolved O_2 and NO_3^- concentrations are highest near recharge features because inputs of both compounds are restricted to the recharge zone. Although ammonia is also locally present in the saline portion of the aquifer, nitrification of saline zone ammonia probably contributes little to the freshwater NO_3^- pool because of coupling between NO_3^- reduction and sulfide oxidation (Burgin & Hamilton 2008; Gray & Engel 2013) along the FWSWI. With increasing hydrologic proximity to the FWSWI, concentrations of both compounds decrease because of microbial decomposition of POM (Katz *et al.* 2004), microbial assimilation and denitrification (Arango *et al.* 2007; Burgin & Hamilton 2007), and reduction coupled with sulfide oxidation during chemolithoautotrophic carbon fixation (Engel *et al.* 2004; Burgin & Hamilton 2008) and the FWSWI.

Patterns in $\delta^{13}C_{DIC}$ and the composition of chromophoric dissolved organic matter (CDOM) provide additional support that hydrologic proximity to the FWSWI and corresponding changes in dissolved O_2 and NO_3^- concentrations reflect a recharge-FWSWI gradient. $\delta^{13}C_{DIC}$ values become progressively enriched with decreasing concentrations of dissolved O_2 and NO_3^- ($F = 62.8_{1,35}$, $R^2 = 0.63$, $p < 0.001$) (Fig. 4.2A). Although possible mechanisms responsible for this enrichment were untested, they include 1) degassing of isotopically light CO_2 (Deuser & Degens 1967) in the updip, unconfined portion of the aquifer, 2) atomic exchange with bedrock (Gonfiantini & Zuppi

2003), which increases with residence time in the confined and saline portions of the aquifer (Lindgren *et al.* 2004) and 3) a transition from carbonic acid dissolution near the recharge zone where the decomposition of soil OM contributes to elevated levels of CO₂ (thereby producing carbonic acid) to sulfuric acid dissolution near the FWSWI where chemolithoautotrophic microbes oxidize reduced sulfur compounds to sulfuric acid. The latter explanation is supported by a decrease in terrigenous, humified and humic-like CDOM and increase in unhumified biologically produced, small, proteinaceous-like CDOM with proximity to FWSWI influenced sites ($F = 16.27_{2,15}$, $R^2 = 0.64$, $p < 0.001$) (Fig. 4.2B). The change is consistent with a microbial, chemolithoautotrophic origin for OM near the FWSWI and a decrease in the prevalence of surface derived OM with increasing hydrologic distance from recharge features, and supports similar conclusions of Birdwell & Engel (2009) that OM near the FWSWI was likely produced *in-situ*.

Along the recharge-FWSWI gradient, mean $\delta^{13}\text{C}$ values in microbial mats and metazoan taxa decrease from values indicative of a POM trophic base at sites in hydrologic proximity to recharge features to values indicative of a chemolithoautotrophic trophic base at sites near the FWSWI ($r^2 = 0.68$, $F = 12.49_{2,9}$, $p = 0.003$) (Fig. 4.2C). To summarize, OM composition, concentration of oxidized compounds, and stable isotopes of inorganic and organic carbon indicate the presence of a gradient from sites dominated by surface water input to sites dominated by mixing with saline waters. With hydrologic proximity to recharge features, stygobiont food webs are supported by terrigenous POM. The recharge-FWSWI gradient corresponds to a gradient between OM of predominantly photosynthetic to predominantly chemolithoautotrophic origins. With increasing

influence from the FWSWI, the presence of terrigenous POM decreases, and stygobiont food webs are increasingly supported by chemolithoautotrophic microbes. The trophic consequences of the heterogeneous distribution and utilization of disparate OM resources by stygobionts is the focus of the remainder of this chapter.

Trophic structure along a photosynthesis – chemolithoautotrophy gradient

Changes in the relative contributions of COM and POM across the COM-POM gradient are apparent in the food web structure at three sites with diverse assemblages of abundant stygobionts (Fig. 4.3, Table 4.2). The total contribution of COM and POM C and N to top predators (identified by $\delta^{15}\text{N}$ values), which integrate disparate OM sources utilized by lower trophic level consumers, in particular, provides a metric with which to evaluate the relative importance of COM and POM to food webs along the COM-POM gradient. At a flowing artesian well near the FWSWI (SM well), the amphipod *Artesia subterranea* exhibited the highest $\delta^{15}\text{N}$ values, but this species was represented in collections by only a single individual at both Ezell's Cave and Comal Springs, where the flatworm *Sphalloplana mohri*, and the isopod *Cirolanides texensis*, respectively, exhibited the highest average $\delta^{15}\text{N}$ values. Whether these species are top predators or apparent trophic positions are an artifact of incomplete sampling is unknown, but *A. subterranea* exhibits mouthparts consistent with predation (Chapter 3) and *S. mohri* and *C. texensis* are documented scavengers (Mitchell 1974; Krejca 2009), so all three species likely incorporate biomass from a variety of sources, including other predaceous species.

Results from Bayesian mixing models incorporating $\delta^{13}\text{C}$ and $\delta^{15}\text{N}$ isotope data suggest that, at the SM well site, the posterior estimate for the contribution of COM to animal

diets (ppd-COM) is as great as 88% (95% Equal-tailed credible intervals = 82% - 94%) for some species, and as little as 35% (4% - 58%) for others. For the top predator (defined by $\delta^{15}\text{N}$ values), *A. subterranea*, ppd-COM is 69% (56% - 78%), assimilated entirely through predation on intermediate consumers. Spatial, physicochemical, and isotopic data from microbial mats suggest that COM constitutes a higher proportion of total OM at some other sites (e.g., Tschirhart well, Fig 1-2), but I was unable to collect animals at these sites. SM well, therefore, represents the most COM-dependent site for which I have food web data. At Ezell's Cave, an intermediate site on the COM-POM spectrum that receives some terrestrial input at the entrance and as bat guano, but also intersects phreatic groundwater near the FWSWI, ppd-COM is between 37% (23% - 50%) and 53% (31% - 69%) for individual species (Table 4.2). For *S. mohri*, ppd-COM is 47% (32% - 60%), and assimilation of COM is, as with *A. subterranea*, entirely through predation. Comal Springs, near the photosynthetic end of the COM-POM spectrum, is a near surface site overlain by highly fractured limestones that facilitate POM input as detritus and living roots. ppd-COM is between 7% (0% - 22%) and 31% (22% - 50%) for individual species at Comal Springs, and the ppd-COM to *C. texensis* is 25% (11% - 46%), derived from a combination of predation and direct consumption of COM. At a fourth site, Ruiz well (Fig. 4.1-4.2), *C. texensis* appears to assimilate similar proportions of COM, at 10% (1% - 27%), but sample size was small and no additional species were collected.

Disparate resources promote niche specialization

Based on significantly different $\delta^{13}\text{C}$ values, two distinct food chains are apparent in isotope biplots from SM well (Fig. 4.3A). Within the food chain with more negative $\delta^{13}\text{C}$ values, species are characterized by morphologic traits associated with scraping feeding habits whereas in the food chain with less negative $\delta^{13}\text{C}$ values, species are characterized by morphologic traits associated with filter-feeding. The difference in $\delta^{13}\text{C}$ values suggest that the filter-feeder food chain is based primarily on POM and the scraping/benthic foraging food chain is based primarily on COM. Observations from the Floridan Aquifer, USA in which extensive phreatic conduits are accessible via SCUBA, provide a framework in which to understand the functional feeding group - OM resource relationships in the Edwards Aquifer. In the Floridan Aquifer, sulfide-oxidizing microbes occur as epilithic biofilms in the redox gradient at the interface between oxygenated conduit water and anoxic matrix water, but despite dense microbial mats on bedrock surfaces, concentrations of organic matter entrained in the conduit water are low (Mills *et al.* in press). I propose that similar conditions are present in the Edwards Aquifer. Microbial mats have been identified in down-bore video logs (Engel *et al.* 2004, Engel & Randall 2011) and collected from agricultural wells for this study. However, even at groundwater sites with abundant metazoan taxa (e.g. discharge of the decapod crustacean *Palaemonetes antrorum* from SM well, for instance, averages 169 individuals per day, pers. obs.), suspended fine particulate OM concentrations in the water column are often low (less than 1mg/L), suggesting an alternative food source (i.e. epilithic microbial mats) not present in the water column.

As expected, filter-feeders exhibit $\delta^{13}\text{C}$ values similar to FPOM entrained in conduit water, which is a mixture of 35% COM (5% - 75%) and 65% POM (25% - 95%) which is effectively transported from recharge features by conduit flow. Scraping foragers have significantly more negative $\delta^{13}\text{C}$ values (Table 4.4), indicative of a chemolithoautotrophic food source, which probably occurs as epilithic microbial mats attached to conduit walls.

Morphologic evidence for distinct feeding habits is most apparent in the comparison of closely related species pairs with representatives in each food chain. Chapter 3 illustrated that the Hadziid amphipod *Texiweckeliopsis insolita* has $\delta^{13}\text{C}$ values that position it in the COM-dominated scraping forager food chain, with mouthpart morphology adapted for scraping (i.e. strong, dentate setae of the 2nd maxilla). Conversely, the Hadziid *Holsingerius samacos* has $\delta^{13}\text{C}$ values indicating consumption of FPOM entrained in the water column (i.e. predominantly POM) and extensive setation on the 1st and 2nd maxilla, which has been previously hypothesized as an adaptation to filter feeding (Holsinger & Longley 1980). The decapods *Palaemonetes antrorum* and *Calathaemon holthuisi* have similar patterns. *P. antrorum* has $\delta^{13}\text{C}$ values that position it in the COM-dominated food chain and mouthparts similar to other stygobitic Palaemonids that are documented benthic foragers (Bruce & Short 1994; Cooper & Cooper 2011). Conversely, although isotopic data were only collected for a single individual, *C. holthuisi* has enriched $\delta^{13}\text{C}$ values relative to *P. antrorum* ($p = 0.001$), placing it in the POM-dominated, filter-feeder food chain with mouthparts uniquely adapted for filter-feeding (Bruce & Short 1994).

Discussion

Scraping forager and filter-feeding food chains are integrated at higher trophic levels, where predaceous species exhibit higher $\delta^{15}\text{N}$ values, intermediate $\delta^{13}\text{C}$ values, and morphologic adaptations associated with predation (Chapter 3). Based on a literature review of stable isotope studies of groundwater food webs, Chapter 2 describes the Edwards Aquifer stygobiont community as the longest food chain yet reported from a groundwater habitat, and that it almost certainly contains secondary predators. Through utilization of both COM and POM by trophic specialists (i.e. scraper/ benthic foragers and filter feeders), increased horizontal trophic diversity increases efficiency in resource acquisition and biomass available to support these higher trophic levels (Duffy *et al.* 2007; Cardinale *et al.* 2009).

Even in productive systems, however, food chain length is a function of environmental stability (Sabo *et al.* 2010). The supply rate of allochthonous POM varies as a function of precipitation that influences both photosynthetic rate and groundwater recharge (Fay *et al.* 2003; LBG-Guyton & Assoc. & Aqua Terra Consultants 2005). In Central Texas, in particular, deposition of eolian sediments, faunal and archeological remains (Holliday 1989), and magnetic susceptibility measurements in cave sediments (Ellwood & Gose 2006) strongly suggest multiple episodes of pronounced aridity during the middle-Holocene altithermal period between 7000-700 years before present (Al-Rabab'Ah & Williams 2004; Ellwood & Gose 2006). These periods of increased aridity would have resulted in decreased recharge and POM input in the Edwards Aquifer recharge zone,

thereby reducing groundwater metazoan population sizes and potentially causing local extirpations.

Under these aquifer conditions, chemolithoautotrophic production, would have provided a long-term, consistent nutrient supply that would have been largely independent of changing surface conditions. Environmental stability, in this context meaning a stable resource supply, can 1) decrease extinction rates by effectively increasing metazoan populations sizes and ranges relative to 'islands' of favorable habitat centered around discrete POM inputs, as reviewed by Mittelbach *et al.* (2007), and 2) promote diversification through allopatric (Mittelbach *et al.* 2007) and sympatric speciation (Bolnick 2004). Both lower extinction rates and higher diversification rates result in higher diversity of local competitors (Cardinale *et al.* 2009). Stygobiont biodiversity decreases with increasing distance from the source of chemolithoautotrophic primary production at the FWSWI (Fig. 4.4), which provides support for lower extinction rates or higher diversification rates near the FWSWI relative to the recharge zone. Furthermore, the presence of marine-derived species (i.e. Hadziid and Sebid amphipods, Cirolanid isopods) that likely colonized during the Late Cretaceous (Holsinger & Longley 1980) provides direct evidence for long-term persistence of species despite long-term variability in POM availability.

Is the Edwards Aquifer unique?

The prevalence of primary production, secondary predators, and trophically specialized consumers in the Edwards Aquifer do not support the paradigm of generalist dominated,

truncated functional diversity in subterranean ecosystems. However, is the Edwards Aquifer merely an exception to the general rule of subterranean trophic structure (Gibert & Deharveng 2002)?

In a review of stable isotope studies in groundwater habitats (excluding hyporheic zones), Chapter 2 illustrated that five of the ten published studies reported chemolithoautotrophy as a contributor to the groundwater food web. Habitats ranged from small cave systems with drainage areas less than 10 km² (Sarbu *et al.* 2000) to economically important, regionally extensive aquifers, such as the Yucatán Peninsula (Pohlman *et al.* 1997) which underlies an area greater than 165,000 km² (Bauer-Gottwein *et al.* 2011).

Chemolithoautotrophy also supports or, at least, subsidizes metazoan food webs in non-karstic groundwater habitats, such as alluvial stream hyporheic zones (Kohzu *et al.* 2004). Consequently, although data are currently unavailable to quantify the global extent of phreatic habitats or prevalence of chemolithoautotrophy within those habitats, phreatic habitats are certainly a major, and likely the most common, stygobiont environment and the potential exists for chemolithoautotrophic production in many phreatic systems. These habitats, however, are underrepresented in speleobiological literature on metazoan communities because of their inaccessibility relative to more traditional habitats, such as caves and springs.

Food chain length and niche specialization of the Edwards Aquifer is not globally representative of stygobiont community structure. I acknowledge that a long-term history of colonization by marine and freshwater species, the presence of both COM and POM,

ecosystem size, ecosystem stability, and favorable predator prey mass ratios (Post 2002; Chapter 2), have acted synergistically to promote trophic complexity in the Edwards Aquifer. However, the data provided here give cause to re-evaluate current assumptions about trophic structure in groundwater habitats. Recognition that trophic specialization and trophic complexity are variable in groundwater food webs should encourage research into the historical and ecological mechanisms responsible for that variability, allowing groundwater habitats to be utilized as model systems. Particular avenues of research that I feel would be most fruitful are 1) more complete characterization of trophic structure in diverse groundwater communities in which chemolithoautotrophy has been previously identified, 2) quantification of nutrient supply rate at aquifer scales, and 3) determination of chemolithoautotrophic subsidies in hyporheic and vadose groundwater systems.

Increasing human impacts on groundwater ecosystems make research on groundwater food webs increasingly important. Withdrawal of water from phreatic aquifers exceeds recharge rate in many aquifers around the world (Gleeson *et al.* 2012), potentially impacting complex metazoan and microbial communities. Stygobionts are characterized by a suite of life history traits (eg. low reproductive potential), and ecological characteristics (e.g. small range sizes and poor competitive abilities as reviewed in Culver *et al.* (2000) and Culver & Pipan (2009), that result in increased sensitivity to habitat degradation. Furthermore, preservation efforts targeting groundwater habitats are still in their infancy (Michel *et al.* 2009), partially because the global stygobiont fauna is still poorly known relative to surface fauna (Gibert *et al.* 2009). Although stygobionts likely

provide important ecosystem services (Gibert *et al.* 2009), these services are almost completely unquantified (but see Mermillod-Blondin *et al.* 2002; Boulton *et al.* 2008).

Methods

Sample collection and analysis

Between May 2010 and May 2013, 300 animals belonging to 29 species were collected from ten groundwater sites, including springs, caves, and wells. Additionally, nine microbial biofilm samples were collected from four different wells. At these and 28 additional wells, water samples were collected for stable carbon isotope analysis of dissolved inorganic carbon (DIC), and a subset of samples were taken for analysis of chromophoric dissolved organic matter (CDOM). During all sampling events, dissolved oxygen (DO) was measured in the field with an In-Situ Inc. Troll[®] 9500 multi-parameter probe with optical DO sensor (accuracy = ± 0.1 mg/L at 0 - 8 mg/L DO and ± 0.2 mg/L at > 8 mg/L DO). Water samples were collected and filtered through 0.45 μ m Fisherbrand nylon syringe filters and stored in the dark at 4°C until NO₃⁻ concentration was measured in the lab using a Dionex ICS-1600 ion chromatograph (Bannockburn, IL).

For animal stable isotope analysis, species were kept alive in filtered spring water for approximately 3 hours to clear their digestive tracts. Animals were then dried at 50°C for 48 hours. Between 0.4 μ g and 1.2 μ g were analyzed for $\delta^{13}\text{C}$ and $\delta^{15}\text{N}$ at the University of California (UC) Davis Stable Isotope Facility using a PDZ Europa ANCA-GSL elemental analyzer interfaced to a PDZ Europa 20-20 isotope ratio mass spectrometer (Sercon Ltd., Cheshire, UK). For small species, between 2 and 42 individuals were

collated to acquire adequate mass. Snails were removed from their shells prior to analysis. *Eurycea rathbuni* tissue samples were taken from the base of the tail.

Microbial mats were divided into two subsamples, one that was fumigated in an HCL chamber for 24 hours to remove carbonates prior to carbon isotope composition analysis, and one that was untreated for nitrogen isotope composition analysis.

For $\delta^{13}\text{C}_{\text{DIC}}$ analysis, samples were filtered through 0.45 μm Fisherbrand nylon syringe filters, poisoned with 15 mM sodium azide, and stored in glass vials with butyl rubber septa (Doctor *et al.* 2008) at 4°C until analysis. Analysis was conducted at the UC Davis Stable Isotope Facility using a GasBench II system interfaced to a Delta V Plus IRMS (Thermo Scientific, Bremen, Germany).

For CDOM analysis, water samples were filtered through 0.2 μm Whatman PVDF filters and stored in the dark at 4°C until analysis, following methods of Birdwell & Engel (2009). Analysis was conducted at the University of Tennessee-Knoxville, Department of Earth and Planetary Sciences. Fluorescence spectra were collected using a Jobin Yvon Fluoromax-4 multi-wavelength fluorescence spectrophotometer (Horiba Scientific, Edison, NJ). Fluorescence EEM spectra were assembled from 63 emission scans (λ_{EM} 250–550-nm, 2.5-nm steps; λ_{EX} 240–550-nm, 5-nm steps). Instrument settings were: PMT voltage 800V, EX/EM slits 5-nm each, integration time 0.1 sec. All spectra were collected in ratio mode, where emission intensities are normalized to the intensity of the lamp at their corresponding excitation wavelength in order to account for differences in excitation intensity. Instrument correction factors provided by the manufacturer were not

employed. EEM corrections were done in the following sequence: 1) Spectral corrections for primary and secondary inner filter effects of all EEMs were made using absorbance spectra collected using a Thermo Scientific Evolution 200 series spectrophotometer in a 1-cm cuvette over the 200-700 nm wavelength range with deionized water as the reference. 2) Raman scattering was removed from EEMs by subtracting a blank spectrum collected on pyrogen-free deionized (>18.1 M Ω) water from each sample spectrum. Rayleigh scattering effects were also edited from each spectrum, following correction and blank subtraction. 3) Instrument corrections were done by dividing the EEMs by the area of an emission scan (λ_{EX} 350-nm and λ_{EM} 365–450-nm). BIX was determined from the ratio of fluorescence intensity at 380 nm to that at 430 nm, at the excitation wavelength of 310 nm from corrected EEM spectra (Huguet *et al.* 2009).

Geographic information systems

Spatial data for sampling sites were entered into a GIS using ArcMap 10.2. An open-source shapefile available from the Edwards Aquifer Authority was used to create a line feature representing the FWSWI. Distance between sampling sites and the FWSWI were calculated using the Proximity tool. Conductivity data for the Edwards Aquifer were acquired from the Edwards Aquifer Authority geochemical database (accessed October, 2009). The conductivity base layer in Figure 4.1 was created using the spline function with the fswi as a barrier and is for illustrative purposes only.

Food web structure

Relative contributions of food sources for stygobionts were estimated using Bayesian mixing models in the R package, SIAR v4.2 (Parnell & Jackson 2013). Photosynthetic, surface stream FPOM, chemolithoautotrophic FPOM, and other stygobionts were used as sources. The chemolithoautotrophic endmember was estimated using three separate methods: the stygobiont method, inorganics method, and microbial method.

Stygobiont method (N = 15): 2 species: *Texiweckeliopsis insolita* and *Lirceolus smithii*, from SM well were assumed to feed on 100% chemolithoautotrophic OM. This assumption was based on 1) on average, these species had the most negative $\delta^{13}\text{C}$ values recorded from the well, 2) these species had low $\delta^{15}\text{N}$ values and appeared to be primary consumers at the base of a food chain that was isotopically distinct from filter feeders, and 3) based on mouthpart morphology and foraging habits observed in closely related species, these species all have scraping/ benthic foraging habits (Culver *et al.* 1991; Cooper & Cooper 2001; Chapter 3) consistent with the hypothesis that chemolithoautotrophic production is occurring in epilithic biofilms on conduit walls at the interface between oxygenated conduit water and anoxic matrix water. A point estimation of average $\delta^{13}\text{C}$ and $\delta^{15}\text{N}$ of food items for each individual of each species was calculated as $\delta^{13}\text{C}$ and $\delta^{15}\text{N}$ of the individual -0.58‰ and -2.81‰ . This correction accounts for trophic fractionation by ammonitelic freshwater invertebrates (Vanderklift & Ponsard 2003; chapter 2). Mean values and standard deviation were used as the chemolithoautotrophic endmember in mixing models.

2: Inorganics method (N = 5 – 12): For each site, repeated measures of $\delta^{13}\text{C}_{\text{DIC}}$ and $\delta^{15}\text{N}_{\text{NO}_3^-}$ were used to calculate local chemolithoautotrophic production assuming DIC as the carbon source during C fixation and assuming assimilation of NO_3^- . $\delta^{13}\text{C}\text{-COM}$ was calculated as $\delta^{13}\text{C}\text{-DIC} - 28.44\text{‰}$ (chapter 1) and $\delta^{15}\text{N}\text{-COM}$ was calculated as $\delta^{15}\text{N}\text{-NO}_3^- - 0.725\text{‰}$ (Granger *et al.* 2010). Mean values and standard deviation were used as the chemolithoautotrophic endmember in mixing models.

3: Microbial biofilm method (N = 12): Microbial biofilms collected at 4 different sites in the Edwards Aquifer were used as chemolithoautotrophic endmembers. Mean values and standard deviation were used as the chemolithoautotrophic endmember in mixing models.

To simplify mixing models, a number of assumptions were made. 1) Because of consistently high $\delta^{15}\text{N}$ values and no ecological data suggesting omnivory, OM was not used as a source item for *Artesia subterranea*, *Eurycea rathbuni*, or *Sphalloplana mohri*.

2) No models incorporated source items with higher mean $\delta^{15}\text{N}$ values than the consumer. 4) Animals were not used as source items for consumers of the same species,

3) Animals which had extensive overlap of isotope values (convex hulls had approximately 50% or greater overlap) were combined into a single food source.

Models were run with a burn in of 50,000 steps and a thinning value of 15 and MCMC chains of between 2,050,010 and 8,050,040 iterations. Models incorporated uncertainty in consumer and source isotope values and trophic enrichment (Chapter 2). Model performance was assessed by visually assessing that models had converged on stable

variable estimates, checking for convergence between MCMC chains, and visually assessing that consumers fell within convex hulls implied by sources. For a small number of species, small sample size ($n \leq 3$) prohibited incorporating uncertainty in population isotope values. In these cases, the single data point approach (Inger *et al.* 2010) was employed. For two models, (FPOM at SM well and Comal Springs) nitrogen isotope data were not available, so only carbon isotopes were used to estimate the relative contribution of COM and POM.

The relative contribution of COM and POM to higher level consumers was calculated as

$$p(COM_{tot}) = p(COM_{direct}) + \sum_{n=1}^i p(i) * p(COM_i) \quad (\text{Eqtn 1})$$

where $p(COM_{tot})$ is the posterior estimate for the total contribution of COM, $p(COM_{direct})$ is the posterior estimate for the contribution of COM through direct consumption, $p(i)$ is the posterior estimate of the contribution of species i , and $p(COM_i)$ is the posterior estimate of for the total contribution of COM (direct and indirect) to species i . For *Artesia subterranea* from the artesian well, sources species included *Palaemonetes antrorum*, *Haedioporus texanus*, *Lirceolus smithii*, *Texiweceliopsis insolita*, *Texiweckelia texensis*, *Cirolanides texensis*, *Holsingerius samacos*, *Allotexiweckelia hirsuta*, and *Stygobromus flagellatus*. For *Sphalloplana mohri* from Ezell's Cave, sources species included *Texiweckelia texensis*, *Holsingerius samacos*, *Palaemonetes antrorum*, and *Cirolanides texensis*. For *C. texensis* from Comal Springs, source species included *Lirceolus spp.*, *Mexiweckelia hardeni*, *Stygobromus russelli*, and *Stygobromus pecki*. MCMC chains were run for 6050030 steps with a thinning rate of 15 and a burn-in of 50000.

A significant difference between the $\delta^{13}\text{C}$ value for the single individual *Calathaemon holthuisi* collected from SM well and $\delta^{13}\text{C}$ values for *P. antrorum* was evaluated using the `dnorm` function in R, which calculates the probability of drawing a value equal to or more extreme than $\delta^{13}\text{C}_{\text{C.holthuisi}}$ from a normal distribution derived from the *P. antrorum* data.

Statistical analyses

Linear regressions were used to evaluate the relationships between the stable carbon isotopic composition of animal tissues ($\delta^{13}\text{C}_{\text{spp}}$) and microbial mats and spatial and geochemical variables at groundwater sites. Predictor variables included the sum of the molar concentrations of O_2 and NO_3^- , the stable carbon isotopic composition of dissolved inorganic carbon ($\delta^{13}\text{C}_{\text{DIC}}$), log transformed distances from sampling sites to the FWSWI and recharge zone and interactions among variables. Variables were chosen because of their importance as electron acceptors (O_2 and NO_3^-), carbon source for chemolithoautotrophic production ($\delta^{13}\text{C}_{\text{DIC}}$), and as indicators of hydrologic distance from OM inputs (geographic distances). $\delta^{13}\text{C}_{\text{spp}}$ values were calculated as the mean of species mean $\delta^{13}\text{C}$ values. Akaike Information Criterion was used to select from competing models (Table 4.3). Analyses were conducted in R v3.0.1.

The best model predicting $\delta^{13}\text{C}_{\text{spp}}$ was then assessed as a predictor of the biologic freshness index of CDOM (Huguet *et al.* 2009): a measure of the relative intensity of two fluorescence peaks attributed to autochthonous DOM production and terrestrial humics,

respectively. The model was also assessed as a predictor of $\delta^{13}\text{C}_{\text{DIC}}$. For $\delta^{13}\text{C}_{\text{DIC}}$, the model containing both distance to the FWSWI and concentration of O_2 and NO_3^- was significant, distance to the FWSWI was not a significant variable. Consequently, FWSWI was removed and a simple linear regression of $\delta^{13}\text{C}_{\text{DIC}}$ as a function of O_2 and NO_3^- was reported.

To assess whether species occupy the same position in trophic space (as defined by $\delta^{13}\text{C}$ and $\delta^{15}\text{N}$ values), multivariate analysis of variance (MANOVA) was performed to assess global differences in isotope values among species. Afterwards, post-hot tests (Fisher's LSD) of separate analyses of variance (ANOVAS) on $\delta^{13}\text{C}$ and $\delta^{15}\text{N}$ values were used to define putative trophic groups (groups of species with significantly different $\delta^{13}\text{C}$ or $\delta^{15}\text{N}$ values suggesting utilization of at least partially non-overlapping food sources (Supplement)). Analysis was performed in R v3.0.1 using the agricolae package (de Mendiburu 2013) to conduct the Fishers LSD tests.

To test whether species richness varied with proximity to the FWSWI, occurrence records and site locations for stygobionts in the Edwards and Edwards-Trinity aquifers were compiled from primary literature, the Texas Speleological Database (accessed spring, 2010), and personal communications with experts (Randy Gibson, U.S. Fish and Wildlife Service; Jean Krejca, Zara Environmental, LLC; James Reddell). Proximity to the FWSWI was calculated in ArcMAP v10.2 as discussed above. Quantile regression on log transformed species richness values was performed in R v3.0.1 using the quantreg

package v5.02 (Koenker *et al.* 2013). Significance of slopes was assessed using the “nid” method.

Supplement

Supplement 1: Defining scraping forager and filter feeding trophic groups for mixing models

MANOVA indicated significant differences among species $\delta^{13}\text{C}$ and $\delta^{15}\text{N}$ values (Pillai trace = 1.392, approx $F = 23.084_{24, 242}$, $p < 0.001$), which were confirmed by isotope specific ANOVAs ($\delta^{13}\text{C}$: $F = 14.1_{12,121}$, $p < 0.001$; $\delta^{15}\text{N}$: $F = 39.41_{12,121}$, $p < 0.001$). Results of Fisher’s LSD post hoc tests (Table 4.4) are the basis for classification of scraping/ benthic foraging and filter feeding trophic groups. Scraper/ benthic foragers belong to carbon post-hoc group d and no other carbon groups (Table 4.4). Filter feeders were less clear, but consist of species from nitrogen post-hoc groups f and g (Table 4.4). Other species in nitrogen post-hoc groups f and g were excluded from the grazer group because of significantly different $\delta^{13}\text{C}$ values (Table 4.4). One species, *T. texensis*, while belonging to a different nitrogen post-hoc group (Table 4.4) was included as a filter-feeder because it belonged to the same carbon post-hoc group and its $\delta^{13}\text{C} - \delta^{15}\text{N}$ convex hull showed substantial overlap with the other two filter-feed group species (Fig. 4.3).

Supplement 2: Comparison of Bayesian mixing models using different estimates of chemolithoautotrophic endmember

Alternative methods of estimating the COM endmember had insignificant effects on estimates of the relative contributions of COM and POM to food webs (Table 4.5-4.7),

evidenced by overlap between posterior 95% equal-tail credible intervals. Differences among the 3 different models were primarily changes in the size of 95% ETCIs that resulted from differences in sample sizes and standard deviations of the datasets used for estimating the prior distributions of the COM endmembers (animal tissues, inorganic constituents, microbial biofilms). The COM endmember estimated from microbial biofilms also had a lower mean $\delta^{15}\text{N}$ (2.59‰) than endmembers estimated from animal tissue and inorganic constituents (6.64‰ and 5.87‰, respectively). This affected estimates of the relative contributions of COM and COM consuming prey items as sources for stygobionts near the base of the scraping/ benthic forager food chain, but had little effect on species in the filter feeding food chain or on species at higher trophic levels.

References

- Al-Rabab'Ah, M. A., & C. G. Williams. 2004. An ancient bottleneck in the Lost Pines of central Texas. *Molecular Ecology* 13: 1075-1084. Doi: 10.1111/j.1365-294X.2004.02142.x
- Arango, C. P., J. L. Tank, J. L. Schaller, T. V. Royer, M. J. Bernot, & M. B. David. 2007. Benthic organic carbon influences denitrification in streams with high nitrate concentration. *Freshwater Biology* 52: 1210-1222. DOI: 10.1111/j.1365-2427.2007.01758.x
- Barker, R. A., P. W. Bush, E. T. Baker, Jr. 1994. Geologic history and hydrogeologic setting the Edwards-Trinity Aquifer System, West-Central Texas. U.S. Geological Survey Water-Resources Investigations Report 94-4039. Austin, Texas.
- Bauer-Gottwein, P., B. R. N. Gondwe, G. Charvet, L. E. Marín, M. Rebolledo-Vieyra, G. Merediz-Alonso. 2011. Review: The Yucatán Peninsula karst aquifer, Mexico. *Hydrogeology Journal* 19: 507-524. DOI 10.1007/s10040-010-0699-5.
- Bruce, A. J., & J. W. Short. 1994. *Leptopalaemon gagadjui* gen. nov., sp. nov., a new freshwater palaemonid shrimp from Arnhem land, and a re-evaluation of *Palaemonetes holthuisi* Strenth, with the designation of a new genus, *Calathaemon*. *Hydrobiologia* 257: 73-94. DOI 10.1007/BF00005948
- Burgin, A. J., & S. K. Hamilton. 2007. Have we overemphasized the role of denitrification in aquatic ecosystems? A review of nitrate removal pathways. *Frontiers in Ecology and the Environment* 5: 89-96. DOI: 10.1890/1540-9295(2007)5[89:HWOTRO]2.0.CO;2
- Burgin, A. J., & S. K. Hamilton. 2008. NO₃⁻-driven SO₄²⁻ production in freshwater ecosystems: Implications for N and S cycling. *Ecosystems* 11: 908-922. DOI: 10.1007/s10021-008-9169-5
- Cardinale, B. J., D. M. Bennett, C. E. Nelson, & K. Gross. 2009. Does productivity drive diversity or vice versa? A test of the multivariate productivity-diversity hypothesis in streams. *Ecology* 90: 1227-1241. DOI: 10.1890/08-1038.1
- Casamayor, E. O., J. García-Cantizano, & C. Pedrós-Alió. 2008. Carbon dioxide fixation in the dark by photosynthetic bacteria in sulfide-rich stratified lakes with oxic-anoxic interfaces. *Limnology and Oceanography* 53: 1193-1203. DOI: 10.4319/lo.2008.53.4.1193.
- Cooper, J. E. & M. R. Cooper. 2011. Observations on the biology of the endangered stygobiotic shrimp *Palaemonias alabamae*, with notes on *P. ganteri* (Decapoda: Atyidae). *Subterranean Biology* 8: 9-20. DOI: 10.3897/subtbiol.8.1226.

- Correa, S. B., & K. Winemiller. 2013. Niche partitioning among frugivorous fishes in response to fluctuating resources in the Amazonian floodplain forest. Ecology, in press.
- Culver, D. C., D. W. Fong, R. W. Jernigan. 1991. Species interactions in cave stream communities: experimental results and microdistribution effects. American Midland Naturalist 126: 364-379.
- Culver, D. C., T. C. Kane, & D. W. Fong. 1995. Adaptation and natural selection in caves: The evolution of *Gammarus minus*. Harvard University Press. Cambridge, Massachusetts. 223 pps.
- Culver, D. C., L. L. Master, M. C. Christman, H. H. Hobbs III. 2000. Obligate cave fauna of the 48 contiguous United States. Conservation Biology 14: 386-401. DOI: 10.1046/j.1523-1739.2000.99026.x.
- Culver, D. C., & T. Pipan. 2009. The biology of caves and other subterranean habitats. Oxford University Press Oxford. 254 pps.
- de Mendiburu, F. 2013. agricolae: Statistical procedures for agricultural research v1.1-4. <http://cran.r-project.org/web/packages/agricolae/index.html>.
- Deuser, W. G., & E. T. Degens. 1967. Carbon isotope fractionation in the system CO₂(gas)-CO₂(aqueous)-HCO₃⁻(aqueous). Nature 215: 1033-1035.
- Doctor, D. H., C. Kendall, S. D. Sebestyen, J. B. Shanley, N. Ohte, & E. W. Boyer. 2008. Carbon isotope fractionation of dissolved inorganic carbon (DIC) due to outgassing of carbon dioxide from a headwater streams. Hydrological Processes 22: 2410-2423. DOI: 10.1002/hyp.6833.
- Duffy, J. E., B. J. Cardinale, K. E. France, P. B. McIntyre, E. Thébault & M. Loreau. 2007. The functional role of biodiversity in ecosystems: incorporating trophic complexity. Ecology Letters 10:522-538. DOI: 10.1111/j.1461-0248.2007.01037.x
- Ellwood, B. B., & W. A. Gose. 2006. Heinrich H1 and 8200 yr B.P. climate events recorded in Hall's Cave, Texas. Geology 34: 753-756. DOI: 10.1130/G22549.1.
- Engel, A. S. & K. W. Randall. 2011. Experimental evidence for microbially mediated carbonate dissolution from the saline water zone of the Edwards Aquifer, Central Texas. Geomicrobiology Journal 28:313-327. DOI: 10.1080/01490451.2010.500197.

- Engel, A. S., L. A. Stern, & P. C. Bennett. 2004. Microbial contributions to cave formation: new insights into sulfuric acid speleogenesis. *Geology* 32: 369-372. DOI: 10.1130/G20288.1.
- Fay, P. A., J. D. Carlisle, A. K. Knapp, J. M. Blair, & S. L. Collins. 2003. Productivity responses to altered rainfall patterns in a C₄-dominated grassland. *Oecologia* 137: 245-251. DOI: 10.1007/s00442-003-1331-3.
- Fišer, C., A. Blejcek, & P. Trontelj. 2012. Niche-based mechanisms operating within extreme habitats: a case study of subterranean amphipod communities. *Biology Letters* 8: 578-581. DOI: 10.1098/rsbl.2012.0125.
- Fridley, J. D., D. B. Vandermast, D. M. Kuppinger, M. Manthey, & R. K. Peet. 2007. Co-occurrence based assessment of habitat generalists and specialists: a new approach for the measurement of niche width. *Journal of Ecology* 95: 707-722. DOI: 10.1111/j.1365-2745.2007.01236.x.
- Fry, B., H. W. Jannasch, S. J. Molyneaux, C. O. Wirsen, J. A. Muramoto, & S. King. 1991. Stable isotope studies of the carbon, nitrogen, and sulfur cycles in the Black Sea and the Cariaco Trench. *Deep-Sea Research* 38, Suppl. 2: S1003-S1019. DOI: 10.1016/S0198-0149(10)80021.4.
- Gibert, J., & L. Deharveng. 2002. Subterranean ecosystems: a truncated functional biodiversity. *BioScience* 52: 473 – 481. DOI: 10.1641/0006-3568(2002).
- Gibert, J., D. C. Culver, M-J Dole-Olivier, F. Malard, M. C. Christman, L. Deharveng. 2009. Assessing and conserving groundwater biodiversity: synthesis and perspectives. *Freshwater Biology* 54: 930-941. DOI: 10.1111/j.1365-2427.2009.02201.x.
- Gleeson, T., Y. Wada, M. F. P. Bierkens, & L. P. H. van Beek. 2012. Water balance of global aquifers revealed by groundwater footprint. *Nature* 488: 197-200. DOI: 10.1038/nature11295.
- Gonfiantini, R., & G. M. Zuppi. 2003. Carbon isotope exchange rate of DIC in karst groundwater. *Chemical Geology* 197: 319-336.
- Graening, G. O., & A. V. Brown. 2003. Ecosystem dynamics and pollution effects in an Ozark cave stream. *Journal of the American Water Resources Association*. 39: 1497-1507. DOI: 10.1111/j.1752-1688.2003.tb04434.x.
- Granger, J., D. M. Sigman, M. M. Rohde, M. T. Maldonado, P. D. Tortell. 2010. N and O isotope effects during nitrate assimilation by unicellular prokaryotic and eukaryotic plankton cultures. *Geochimica et Cosmochimica Acta* 74: 1030-1040. DOI: 10.1016/j.gca.2009.10.044.

- Gray, C. J., & A. S. Engel. 2013. Microbial diversity and impact on carbonate geochemistry across a changing geochemical gradient in a karst aquifer. *The ISME Journal* 7: 325-337. DOI: 10.1038/ismej.2012.105.
- Holliday, V. T. 1989. Middle Holocene drought on the Southern High Plains. *Quaternary Research* 31: 74-82. DOI: 10.1016/0033-5894(89)90086-0.
- Holsinger J. R. & G. Longley. 1980. The subterranean amphipod crustacean fauna of an artesian well in Texas. *Smithsonian Contributions to Zoology* 308: 72pps.
- Huguet, A., L. Vacher, S. Relexans, S. Saubusse, J. M. Froidefond, & E. Parlanti. 2009. Properties of fluorescent dissolved organic matter in the Gironde Estuary. *Organic Geochemistry* 40: 706-719. DOI: 10.1016/j.orggeochem.2009.03.002.
- Hüppop, K. 2012. Adaptation to low food. In: White, W. B., & D. C. Culver (Eds.). *Encyclopedia of Caves*, 2nd Edition. Elsevier, Amsterdam. pps. 1-8.
- Inger, R., A. Jackson, A. Parnell, & S. Bearhop. 2010. SIAR V4 (Stable Isotope Analysis in R): An Ecologist's Guide.
- Juan, C., M. T. Guzik, D. Jaume, & S. J. Cooper. 2010. Evolution in caves: Darwin's 'wrecks of ancient life' in the molecular era. *Molecular Ecology* 19: 3865-3880. DOI: 10.1111/j.1365-294X.2010.04759.x.
- Katz, B. G., A. R. Chelette, & T. R. Pratt. 2004. Use of chemical and isotopic tracers to assess nitrate contamination and ground-water age, Woodville Karst Plain, USA. *Journal of Hydrology* 289: 36-61. DOI: 10.1016/j.jhydrol.2003.11.001.
- Kohzu, A., C. Kato, T. Iwata, D. Kishi, M. Murakami, S. Nakano, & E. Wada. 2004. Stream food web fueled by methane-derived carbon. *Aquatic Microbial Ecology* 36: 189-194. DOI: 10.3354/ame036189.
- Koenker, R., S. Portnoy, P. Tian Ng, A. Zeileis, P. Grosjean, B. D. Ripley. 2013. *quantreg: Quantile Regression v5.05*. <http://cran.r-project.org/web/packages/quantreg/index.html>
- Krejca, J. K. 2009. New records for *Cirolanides texensis* Benedict, 1896 (Isopoda: Cirolanidae), including possible extirpations at impacted Texas caves. *Cave and Karst Science* 35: 41-46.
- LBG-Guyton & Associates & Aqua Terra Consultants. 2005. HSPF recharge models for the San Antonio segment of the Balcones Fault Zone Edwards Aquifer. Edwards Aquifer Authority Contract 02-87-AS.
- Levinton, J. 1972. Stability and trophic structure in deposit-feeding and suspension-feeding communities. *The American Naturalist* 166: 472-486.

- Lindgren, R. J., A. R. Dutton, S. D. Hovorka, S. R. H. Worthington, S. Painter. 2004. Conceptualization and simulation of the Edwards Aquifer, San Antonio Region, Texas. U.S. Geological Survey Scientific Investigations Report 2004-5277. Reston, VA. 143pps.
- Longley, G. 1981. The Edwards Aquifer: Earth's most diverse groundwater ecosystem? *International Journal of Speleology* 11: 123-128.
- MacArthur, R. H. 1958. Population ecology of some warblers of northeastern coniferous forests. *Ecology* 39: DOI: 10.2307/1931600.
- MacArthur, R. H., & E. R. Pianka. 1966. On optimal use of a patchy environment. *The American Naturalist* 100: 603-609.
- Michel, G., F. Malard, L. Deharveng, T. Di Lorenzo, B. Set, C. De Broyer. 2009. Reserve selection for conserving groundwater biodiversity. *Freshwater Biology* 54: 861-876. DOI: 10.1111/j.136-2427.2009.02192.x.
- Mills, A. L., T. N. Tysall, & J. S. Herman. *In Press*. An approach for collection of nearfield groundwater samples in submerged limestone caverns. *Acta Carsologica*.
- Mitchell, R. W. 1974. The cave-adapted flatworms of Texas; systematics, natural history, and responses to light and temperature. In: Riser, N. W., & M. P. Morse (Eds.) *Biology of the Turbellaria* McGraw-Hill Inc., New York. Pps 402-430.
- Mittelbach, G. G., D. W. Schemse, H. V. Cornell, A. P. Allen, J. M. Brown, M. B. Bush, S. P. Harrison, A. H. Hurlbert, N. Knowlton, H. A. Lessios, C. M. McCain, A. R. McCune, L. A. McDade, M. A. McPeck, T. J. Near, T. D. Price, R. E. Ricklefs, K. Roy, D. F. Sax, D. Schluter, J. M. Sobel, M. Turelli. 2007. Evolution and the latitudinal diversity gradient: speciation, extinction and biogeography 10: 315-331. DOI: 10.1111/j.1461-0248.2007.01020.x.
- Parnell, A., & A. Jackson. 2013. siar: Stable Isotope Analysis in R v4.2. <http://cran.r-project.org/web/packages/siar/index.html>
- Phillips, D. L., & J. W. Gregg. 2003. Source partitioning using stable isotopes: coping with too many sources. *Oecologia* 136: 261-269. DOI: 10.1007/s00442-003-1218-3.
- Pianka, E. R. 1974. Niche overlap and diffuse competition. *Proceedings of the National Academy of Sciences of the United States of America* 71: 2141-2145.

- Pohlman, J. W., T. M. Iliffe, L. A. Cifuentes. 1997. A stable isotope study of organic cycling and the ecology of an anchialine cave ecosystem. *Marine Ecology Progress Series* 155: 17-27. DOI: 10.3354/meps155017.
- Polis, G. A., & D. R. Strong. 1996. Food web complexity and community dynamics. *The American Naturalist* 147: 813-846.
- Porter, M. L., A. S. Engel, T. C. Kane, & B. K. Kinkle. 2009. Productivity-diversity relationships from chemolithoautotrophically based sulfidic arst systems. *International Journal of Speleology* 38: 27-40.
- Post, D. M. 2002. The long and short of food-chain length. *Trends in Ecology and Evolution* 17: 269-277. DOI: 10.1016/S0169-5347(02)02455-2.
- Poulson, T. L., & K. H. Lavoie. 2000. The trophic basis of subsurface ecosystems. In: Wilkens, H., D. C. Culver, & W. F. Humphreys (Eds.). *Subterranean ecosystems*. Elsevier Academic Press. Amsterdam. Pps. 231-250.
- Poulson, T. L., & W. B. White. 1969. The cave environment. *Science* 165: 971-981. DOI: 10.1126/science.165.3897.971.
- Poulson, T. L. 2012. Food Sources. In: White, W. B., and D. C. Culver (Eds.). *Encyclopedia of Caves*, 2nd Ed. Elsevier, Amsterdam. Pps. 323-333.
- Roy, J., B. Saugier, & H. A. Mooney (Eds.). 2001. *Terrestrial global productivity*. Academic Press, San Diego, CA. 573 pps.
- Saba, V. S., M. A. M. Friedrichs, D. Antoine, R. A. Armstrong, I. Asanuma, M. J. Behrenfeld, A. M. Ciotti, M. Dowell, N Hoepffner, K. J. W. Hyde, J. Ishizaka, T. Kameda, J. Marra, F. Mélin, A. Morel, J. O'Reilly, M. Scardi, W. O. Smith Jr., T. J. Smyth, S. Tang, J. Uitz, K. Waters, & T. K. Westberry. 2011. An evaluation of ocean color model estimates of marine primary productivity in coastal and pelagic regions across the globa. *Biogeosciences* 8: 489-503. DOI: 10.5194/bg-8-489-2011.
- Sabo, J. L., J. C. Finlay, D. M. Post. 2009. Food chains in freshwaters. *Annals of the New York Academy of Sciences* 1162: 187-220. DOI: 10.1111/j.1749-6632.2009.04445.x.
- Sabo, J. L., J. C. Finlay, T. Kennedy, & D. M. Post. 2010. The role of discharge variation in scaling of drainage area and food chain length in rivers. *Science* 330: 965-967.

- Scanlon, B. R., R. E. Mace, M. E. Barrett, B. Smith. 2003. Can we simulate regional groundwater flow in a karst system using equivalent porous media models? Case study, Barton Springs Edwards aquifer, USA. *Journal of Hydrology* 276: 137-158.
- Schoener, T. W. 1974. Resource partitioning in ecological communities. *Science* 185: 27-39. DOI: 10.1126/science.185.4145.27.
- Simon, K. S., E. F. Benfield, S. A. Macko. 2003. Food web structure and the role of epilithic biofilms in cave streams. *Ecology* 84: 2395-2406. DOI: 10.1890/02-334.
- Simon, K. S., T. Pipan, & D. C. Culver. 2007. A conceptual model of the flow and distribution of organic carbon in caves. *Journal of Cave and Karst Studies* 69: 279-284.
- Swan, B. K., M. Martinez-Garcia, C. M. Preston, A. Sczyrba, T. Woyke, D. Lamy, T. Reinthaler, N. J. Poulton, E. D. P. Masland, M. L. Gomez, M. E. Sieraci, E. F. DeLong, G. J. Herndl, R. Stepanauskas. 2011. Potential for chemolithoautotrophy among ubiquitous bacteria lineages in the dark ocean. *Science* 333: 1296-1300. DOI: 10.1126/science.1203690.
- Vanderklift, M. A., & S. Ponsard. 2003. Sources of variation in consumer-diet $\delta^{15}\text{N}$ enrichment: a meta-analysis. *Oecologia* 136: 169-182. DOI: 10.1007/s00442-003-1270-z.

Table 4.1: Quotes from speleobiological literature that summarize the prevailing paradigm of trophic structure of subterranean communities.

“The prevalence of allochthonously based subterranean communities remains the rule...” Gibert & Deharveng (2002)

“No second- or third-order predators live exclusively in caves...”
Poulson (2012)

“...all communities associated with the cave environment...are simple and composed of only a few trophic levels...” Gnaspini (2012)

[Feeding generalism is an adaptation to general food scarcity] Hüppop (2012) [Fig. 1. component paraphrase]

“As a rule, trophic linkages within subterranean food webs indicate extensive omnivory.” Gibert & Deharveng (2002)

“This trend toward opportunistic and generalist strategies is likely to be imposed by the scarcity and irregularity of food. Evolution of subterranean species life traits is directed towards...broadening the range of food resources, rather than specializing the diet to a particular food supply.” Gibert & Deharveng (2002)

Table 4.2: Posterior estimates of the contribution of food sources to consumers (95% equal tail confidence intervals). COM: chemolithoautotrophic organic matter; POM: photosynthetic organic matter; Ezell's Cave *Texiweckelia texensis* group: *T. texensis*, *Holsingerius samacos*, and *Artesia subterranea*; SM well *Stygobromus flagellatus* group: *S. flagellatus*, *Eurycea rathbuni*, and *Artesia subterranea*; SM well scraper/ benthic forager group: *Texiweckeliopsis insolita*, *Haedioporus texanus*, *Palaemonetes antrorum*, and *Lirceolus smithii*; SM well filter feeder group: *Holsingerius samacos*, *Moorbdella* sp. and *T. texensis*.

Consumer	Sources	Posterior estimate
Ruiz well		
<i>Cirolanides texensis</i>	COM	0.08 (0.00 - 0.25)
	POM	0.92 (0.75 - 1.00)
Comal Springs		
<i>Cirolanides texensis</i>	<i>Lirceolus sp. & Mexiweckelia hardeni</i>	0.21 (0.01 - 0.45)
	<i>Stygobromus pecki</i>	0.26 (0.03 - 0.54)
	<i>Stygobromus russelli</i>	0.23 (0.02 - 0.47)
	COM	0.11 (0.01 - 0.31)
	POM	0.18 (0.01 - 0.40)
<i>Stygobromus pecki</i>	<i>Lirceolus sp. & Mexiweckelia hardeni</i>	0.14 (0.02 - 0.30)
	<i>Stygobromus russelli</i>	0.57 (0.43 - 0.69)
	COM	0.21 (0.18 - 0.25)
<i>Stygobromus russelli</i>	POM	0.06 (0.00 - 0.20)
	<i>Lirceolus sp. & Mexiweckelia hardeni</i>	0.45 (0.08 - 0.86)
	COM	0.11 (0.01 - 0.45)
<i>Lirceolus sp.</i>	POM	0.40 (0.05 - 0.75)
	COM	0.07 (0.00 - 0.22)
FPOM	POM	0.93 (0.78 - 1.00)
	COM	0.34 (0.05 - 0.67)
	POM	0.66 (0.33 - 0.95)
Ezell's Cave		
<i>Sphalloplana mohri</i>	<i>Texiweckelia texensis</i> group	0.50 (0.21 - 0.77)
	<i>Palaemonetes antrorum</i>	0.21 (0.02 - 0.48)
	<i>Cirolanides texensis</i>	0.27 (0.03 - 0.55)
<i>Cirolanides texensis</i>	<i>Texiweckelia texensis</i> group	0.29 (0.05 - 0.49)
	<i>Palaemonetes antrorum</i>	0.31 (0.05 - 0.57)
	COM	0.08 (0.00 - 0.24)
	POM	0.32 (0.18 - 0.46)
<i>Texiweckelia texensis</i>	COM	0.53 (0.31 - 0.69)
	POM	0.47 (0.31 - 0.69)
<i>Palaemonetes antrorum</i>	COM	0.46 (0.11 - 0.72)
	POM	0.54 (0.28 - 0.89)
FPOM	COM	0.31 (0.04 - 0.52)
	POM	0.69 (0.48 - 0.96)

Table 4.2: cont.

Consumer	Sources	Posterior estimate
	SM well	
<i>Artesia subterranea</i>	<i>Stygobromus flagellatus</i> group	0.44 (0.13 - 0.71)
	<i>Cirolanides texensis</i>	0.16 (0.01 - 0.44)
	<i>Texiweckeliopsis insolita</i> group	0.27 (0.03 - 0.49)
	<i>Holsingerius samacos</i> group	0.07 (0.00 - 0.29)
	<i>Stygobromus russelli</i>	0.03 (0.00 - 0.14)
<i>Eurycea rathbuni</i>	<i>Stygobromus flagellatus</i> group	0.29 (0.02 - 0.57)
	<i>Cirolanides texensis</i>	0.18 (0.01 - 0.48)
	scraper/ benthic forager group	0.34 (0.05 - 0.65)
	filter feeder group	0.09 (0.00 - 0.33)
	<i>Stygobromus russelli</i>	0.05 (0.00 - 0.21)
<i>Stygobromus flagellatus</i>	<i>Cirolanides texensis</i>	0.45 (0.13 - 0.77)
	scraper/ benthic forager group	0.25 (0.03 - 0.49)
	filter feeder group	0.12 (0.01 - 0.37)
	<i>Stygobromus russelli</i>	0.02 (0.00 - 0.09)
	COM	0.06 (0.00 - 0.24)
	POM	0.04 (0.00 - 0.15)
<i>Cirolanides texensis</i>	scraper/ benthic forager group	0.25 (0.06 - 0.42)
	filter feeder group	0.17 (0.01 - 0.35)
	<i>Stygobromus russelli</i>	0.17 (0.04 - 0.30)
	COM	0.27 (0.09 - 0.45)
	POM	0.15 (0.01 - 0.29)
<i>Texiweckeliopsis insolita</i>	scraper/ benthic forager group	0.35 (0.08 - 0.59)
	filter feeder group	0.06 (0.00 - 0.28)
	<i>Stygobromus russelli</i>	0.05 (0.00 - 0.18)
	COM	0.47 (0.19 - 0.77)
	POM	0.03 (0.00 - 0.18)
<i>Holsingerius samacos</i>	<i>Texiweckelia texensis</i>	0.26 (0.03 - 0.55)
	<i>Stygobromus russelli</i>	0.21 (0.02 - 0.43)
	COM	0.32 (0.17 - 0.46)
	POM	0.21 (0.02 - 0.40)
<i>Palaemonetes antrorum</i>	COM	0.88 (0.82 - 0.94)
	POM	0.12 (0.05 - 0.18)
<i>Texiweckelia texensis</i>	COM	0.43 (0.19 - 0.57)
	POM	0.57 (0.43 - 0.81)
<i>Phreatodrobia spp.</i>	COM	0.54 (0.10 - 0.89)
	POM	0.46 (0.11 - 0.90)
<i>Calathaemon holthuisi</i>	COM	0.35 (0.04 - 0.58)
	POM	0.65 (0.42 - 0.96)
FPOM	COM	0.30 (0.04 - 0.49)
	POM	0.70 (0.51 - 0.96)

Table 4.3: AIC model selection for hydrological and geochemical controls on animal stable carbon isotope content ($\delta^{13}\text{C}_{\text{spp}}$). FWSWI: log-transformed distance from freshwater-saline water interface (m); Recharge: log-transformed distance from recharge zone (m). $\delta^{13}\text{C}_{\text{DIC}}$: stable carbon isotope composition of dissolved inorganic carbon; Acceptors: sum of molar concentration of O_2 and NO_3^- . Chosen model is highlighted.

Model	AIC	Δ AIC	AIC weight
$\delta^{13}\text{C}_{\text{spp}} \sim \text{FWSWI}$	79.277	6.682	0.016
$\delta^{13}\text{C}_{\text{spp}} \sim \text{FWSWI} + \text{Recharge}$	83.983	11.387	0.002
$\delta^{13}\text{C}_{\text{spp}} \sim \text{FWSWI} + \delta^{13}\text{C}_{\text{DIC}}$	82.117	9.522	0.004
$\delta^{13}\text{C}_{\text{spp}} \sim \text{FWSWI} + \text{Acceptors}$	72.595	0	0.446
$\delta^{13}\text{C}_{\text{spp}} \sim \text{FWSWI} * \delta^{13}\text{C}_{\text{DIC}}$	82.351	9.756	0.003
$\delta^{13}\text{C}_{\text{spp}} \sim \text{FWSWI} * \text{Acceptors}$	73.518	0.923	0.281
$\delta^{13}\text{C}_{\text{spp}} \sim \text{FWSWI} * \delta^{13}\text{C}_{\text{DIC}} + \text{Acceptors}$	80.789	8.193	0.007
$\delta^{13}\text{C}_{\text{spp}} \sim \text{FWSWI} + \delta^{13}\text{C}_{\text{DIC}} * \text{Acceptors}$	75.411	2.816	0.109
$\delta^{13}\text{C}_{\text{spp}} \sim \text{FWSWI} * \text{Acceptors} + \text{Recharge}$	75.451	2.856	0.107
$\delta^{13}\text{C}_{\text{spp}} \sim \text{FWSWI} * \delta^{13}\text{C}_{\text{DIC}} * \text{Acceptors}$	80.789	8.193	0.007
$\delta^{13}\text{C}_{\text{spp}} \sim \text{FWSWI} * \delta^{13}\text{C}_{\text{DIC}} + \text{Acceptors} * \text{Recharge}$	80.408	7.813	0.009

Table 4.4: Fisher's LSD groupings for species from SM well. Species highlighted in purple were assigned to the scraper/ benthic forager group. Species highlighted in grey were assigned to the filter feeder group.

Species	$\delta^{13}\text{C}$		$\delta^{15}\text{N}$	
	Mean value (‰)	Post-hoc group	Mean value (‰)	Post-hoc group
<i>Artesia subterranea</i>	-37.13	c	14.07	a
<i>Eurycea rathbuni</i>	-33.58	abc	12.56	ab
<i>Stygobromus flagellatus</i>	-35.49	bc	11.65	bc
<i>Allotexiweckelia hirsuta</i>	-36.61	c	10.43	cd
<i>Texiweckeliopsis insolita</i>	-42.00	d	9.63	de
<i>Lirceolus smithii</i>	-42.51	d	9.08	def
<i>Cirolanides texnesis</i>	-35.74	c	8.85	ef
<i>Palaemonetes antrorum</i>	-40.44	d	8.54	f
<i>Holsingerius samacos</i>	-33.27	ab	7.87	fg
<i>Moorbdella sp.</i>	-32.21	ab	7.77	fg
<i>Haideoporus texanus</i>	-41.05	d	7.49	g
<i>Texiweckelia texensis</i>	-31.74	a	5.70	h
<i>Stygobromus russelli</i>	-31.34	a	1.61	i

Table 4.5: Comparison of mean posterior estimates of proportional contributions of source items to consumers at Comal Springs (95% equal-tail credible intervals) using different methods of estimating chemolithoautotrophic organic matter (COM) endmember. First row: animal isotope method; second row: Inorganics method; third row: microbial biofilm method. FPOM = fine particulate organic matter; POM = photosynthetic organic matter. Dashes indicate that source items weren't entered in the model.

Source Items	Consumers				
	<i>Cirolanides texensis</i>	<i>Stygobromus pecki</i>	<i>Stygobromus russelli</i>	<i>Lirceolus spp.</i>	FPOM
<i>Lirceolus spp.</i>	0.21 (0.01 - 0.45)	0.14 (0.02 - 0.30)	0.45 (0.08 - 0.86)		
<i>Mexiweckelia hardeni</i>	0.20 (0.01 - 0.43)	0.08 (0.01 - 0.22)	0.43 (0.06 - 0.83)	-	-
	0.21 (0.01 - 0.44)	0.08 (0.01 - 0.25)	0.43 (0.08 - 0.82)		
	0.26 (0.03 - 0.54)				
<i>Stygobromus pecki</i>	0.25 (0.02 - 0.53)	-	-	-	-
	0.26 (0.03 - 0.54)				
COM	0.11 (0.01 - 0.31)	0.21 (0.18 - 0.25)	0.11 (0.01 - 0.45)	0.07 (0.00 - 0.22)	0.34 (0.05 - 0.67)
	0.14 (0.01 - 0.34)	0.30 (0.25 - 0.35)	0.16 (0.01 - 0.50)	0.11 (0.01 - 0.31)	0.44 (0.08 - 0.82)
	0.12 (0.01 - 0.33)	0.21 (0.15 - 0.26)	0.18 (0.01 - 0.49)	0.22 (0.02 - 0.49)	0.45 (0.07 - 0.84)
POM	0.18 (0.01 - 0.40)	0.06 (0.00 - 0.20)	0.40 (0.05 - 0.75)	0.93 (0.78 - 1.00)	0.66 (0.33 - 0.95)
	0.17 (0.01 - 0.39)	0.05 (0.00 - 0.17)	0.38 (0.04 - 0.72)	0.89 (0.69 - 0.99)	0.56 (0.18 - 0.92)
	0.17 (0.01 - 0.40)	0.06 (0.00 - 0.18)	0.37 (0.04 - 0.71)	0.78 (0.51 - 0.98)	0.55 (0.16 - 0.93)
<i>Stygobromus russelli</i>	0.23 (0.02 - 0.47)	0.57 (0.43 - 0.69)			
	0.22 (0.02 - 0.46)	0.56 (0.43 - 0.66)	-	-	-
	0.22 (0.02 - 0.46)	0.64 (0.48 - 0.75)			

Table 4.6: Comparison of mean posterior estimates of proportional contributions of source items to consumers at Ezell’s Cave (95% ETCl) using different methods of estimating COM endmember. Explanations are as in table 4.1 and supplement table 4.3. Alternative models were not run for consumers that were not expected to directly utilize COM or POM.

Source Items	Consumer				
	<i>Sphalloplana mohri</i>	<i>Cirolanides texensis</i>	<i>Texiweckelia texensis</i>	<i>Palaemonetes antrorum</i>	FPOM
<i>Texiweckelia texensis</i> group	0.50 (0.21 - 0.77)	0.29 (0.05 - 0.49)			
		0.27 (0.04 - 0.47)	-	-	-
		0.32 (0.10 - 0.52)			
<i>Palaemonetes antrorum</i>	0.21 (0.02 - 0.48)	0.31 (0.05 - 0.57)			
		0.27 (0.03 - 0.54)	-	-	-
		0.32 (0.07 - 0.59)			
<i>Cirolanides texensis</i>	0.27 (0.03 - 0.55)				
		-	-	-	-
COM		0.08 (0.00 - 0.24)	0.53 (0.31 - 0.69)	0.46 (0.11 - 0.72)	0.31 (0.04 - 0.52)
	-	0.15 (0.01 - 0.36)	0.75 (0.47 - 0.92)	0.57 (0.17 - 0.88)	0.38 (0.04 - 0.64)
		0.07 (0.00 - 0.22)	0.49 (0.15 - 0.80)	0.46 (0.09 - 0.83)	0.40 (0.06 - 0.78)
POM		0.32 (0.18 - 0.46)	0.47 (0.31 - 0.69)	0.54 (0.28 - 0.89)	0.69 (0.48 - 0.96)
	-	0.30 (0.17 - 0.43)	0.25 (0.08 - 0.53)	0.43 (0.12 - 0.83)	0.60 (0.22 - 0.94)
		0.28 (0.14 - 0.42)	0.51 (0.20 - 0.85)	0.54 (0.17 - 0.91)	0.60 (0.22 - 0.94)

Table 4.7: Comparison of mean posterior estimates of proportional contributions of source items to consumers at SM well (95% ETCD) using different methods of estimating COM endmember. Explanations are as in table 1 & supplement table 3. Alternative models were not run for consumers that were not expected to utilize COM or POM directly.

Source Items	Consumers										
	<i>Artesia subterranea</i>	<i>Eurycea rathbuni</i>	<i>Stygobromus flagellatus</i>	<i>Cirulanides texensis</i>	<i>Texiweckelopsis insolita</i>	<i>Palaemonetes antrorum</i>	<i>Holsingerius samacos</i>	<i>Texiweckelia texensis</i>	<i>Phreatodrobia spp.</i>	<i>Calappaemon holthuisi</i>	FPOM
<i>Stygobromus flagellatus</i> group	0.44 (0.13 - 0.71)	0.29 (0.02 - 0.57)	-	-	-	-	-	-	-	-	-
<i>Stygobromus flagellatus</i> only	-	0.05 (0.00 - 0.21)	-	-	-	-	-	-	-	-	-
<i>Cirulanides texensis</i>	0.16 (0.01 - 0.44)	0.18 (0.01 - 0.48)	0.45 (0.13 - 0.77) 0.45 (0.13 - 0.77) 0.49 (0.14 - 0.79)	-	-	-	-	-	-	-	-
scraper/ benthic forager group	0.27 (0.03 - 0.49)	0.34 (0.05 - 0.65)	0.25 (0.03 - 0.49)	0.25 (0.06 - 0.42)	0.35 (0.08 - 0.59)	-	-	-	-	-	-
filter feeder group	0.07 (0.00 - 0.29)	0.09 (0.00 - 0.33)	0.12 (0.01 - 0.37)	0.17 (0.01 - 0.35)	0.06 (0.00 - 0.28)	-	-	-	-	-	-
<i>Texiweckelia texensis</i> only	-	-	0.11 (0.01 - 0.36)	0.14 (0.01 - 0.32)	0.14 (0.01 - 0.37)	-	0.26 (0.03 - 0.55) 0.27 (0.02 - 0.55) 0.39 (0.12 - 0.70)	-	-	-	-
<i>Stygobromus russelli</i>	0.03 (0.00 - 0.14)	-	0.10 (0.01 - 0.35)	0.19 (0.02 - 0.37)	0.15 (0.01 - 0.42)	-	0.21 (0.02 - 0.43) 0.18 (0.01 - 0.42) 0.18 (0.01 - 0.43)	-	-	-	-
COM	-	-	0.02 (0.00 - 0.09)	0.17 (0.04 - 0.30)	0.05 (0.00 - 0.18)	0.88 (0.82 - 0.94)	0.32 (0.17 - 0.46)	0.43 (0.19 - 0.57)	0.54 (0.10 - 0.89)	0.35 (0.04 - 0.58)	0.30 (0.04 - 0.49)
POM	-	-	0.05 (0.00 - 0.23)	0.29 (0.06 - 0.52)	0.29 (0.04 - 0.53)	0.99 (0.92 - 1.00)	0.41 (0.20 - 0.63)	0.56 (0.33 - 0.71)	0.68 (0.11 - 0.98)	0.42 (0.06 - 0.65)	0.39 (0.07 - 0.58)
	-	-	0.02 (0.00 - 0.11)	0.12 (0.01 - 0.24)	0.11 (0.01 - 0.32)	0.74 (0.43 - 0.92)	0.28 (0.08 - 0.44)	0.45 (0.21 - 0.67)	0.53 (0.10 - 0.94)	0.42 (0.04 - 0.87)	0.40 (0.06 - 0.79)
	-	-	0.04 (0.00 - 0.15)	0.15 (0.01 - 0.29)	0.03 (0.00 - 0.18)	0.12 (0.05 - 0.18)	0.21 (0.02 - 0.40)	0.57 (0.43 - 0.81)	0.46 (0.11 - 0.90)	0.65 (0.42 - 0.96)	0.70 (0.51 - 0.96)
	-	-	0.04 (0.00 - 0.14)	0.08 (0.01 - 0.23)	0.06 (0.00 - 0.25)	0.01 (0.00 - 0.25)	0.12 (0.01 - 0.35)	0.44 (0.29 - 0.67)	0.32 (0.02 - 0.89)	0.58 (0.35 - 0.94)	0.61 (0.42 - 0.93)
	-	-	0.04 (0.00 - 0.14)	0.09 (0.01 - 0.23)	0.06 (0.00 - 0.27)	0.26 (0.08 - 0.57)	0.18 (0.01 - 0.43)	0.55 (0.33 - 0.79)	0.47 (0.06 - 0.90)	0.58 (0.13 - 0.96)	0.60 (0.21 - 0.94)

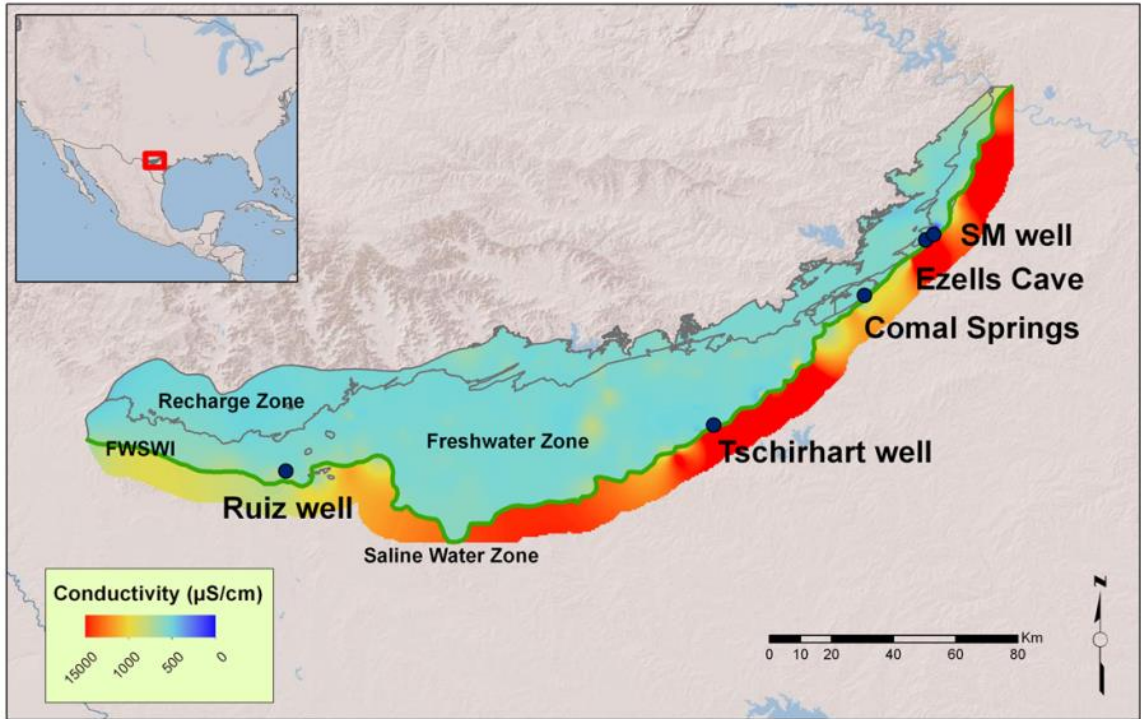


Figure 4.1: Conductivity and major hydrological divisions of the Edwards Aquifer, Texas, USA. Sampling locations discussed in the text are labeled.

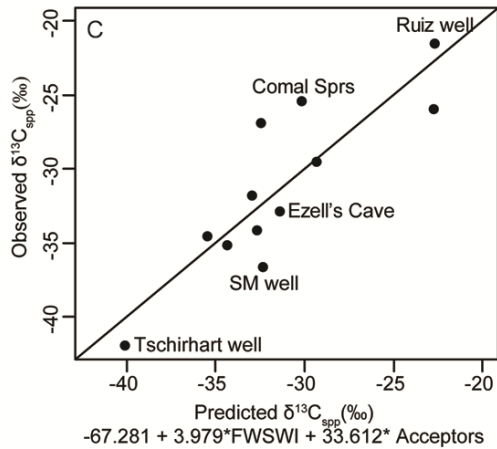
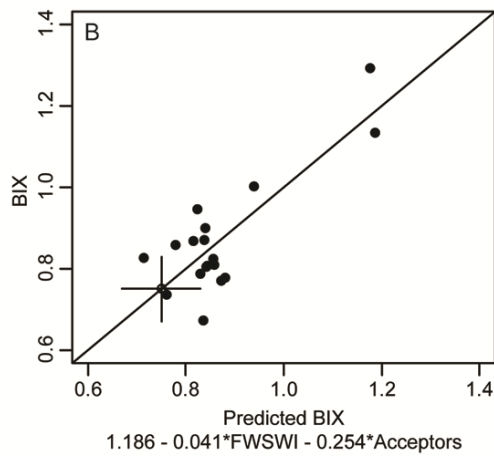
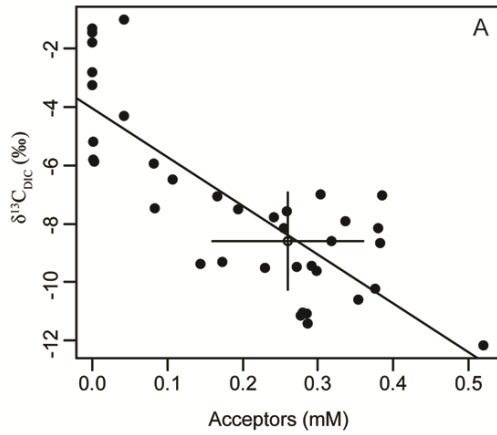


Figure 4.2: Simple and multiple linear regression results of $\delta^{13}\text{C}_{\text{DIC}}$ (A), chromophoric dissolved organic matter biologic index (BIX) (B), and species' mean $\delta^{13}\text{C}$ (C) as a function of log transformed distance to freshwater saline water interface (m) (FWSWI) and sum of molar concentration of the major electron acceptors O_2 and NO_3^- (Acceptors). A: results of simple linear regression, B-C: observed versus predicted values from multiple linear regression. Data points with error bars illustrate mean values and standard deviations for surface streams, which were not used in the regression.

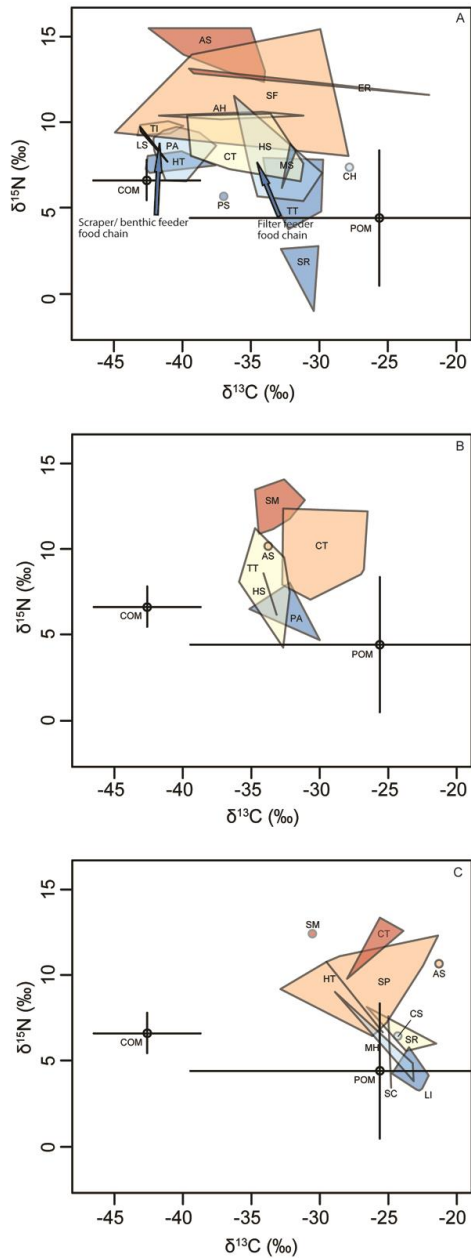


Figure 4.3: Isotope biplots for stygobionts from A: SM well, B: Comal Springs, and C: Ezell's Cave. Polygons are convex hulls encompassing all data points for species. N = 1 for species shown by small circles. AH = *Allotexiweckelia hirsuta*; AS = *Artesia subterranea*; CH = *Calathaemon holthuisi*, CS = *Comaldessus stygius*, CT = *Cirolanides texensis*, ER = *Eurycea rathbuni*, HS = *Holsingerius samacos*, HT = *Haedioporus texanus*, LS = *Lirceolus smithii*, LI = *Lirceolus* spp., MH = *Mexiweckelia hardeni*, MS = *Moorbdella* sp., PA = *Palaemonetes antrorum*, PS = *Phreatodrobia* spp., SC = *Stygoparnus comalensis*, SF = *Stygobromus flagellatus*, SM = *Sphalloplana mohri*, SP = *Stygobromus pecki*, SR = *Stygobromus russelli*, TI = *Texiweckeliopsis insolita*, TT = *Texiweckelia texensis*, COM = chemolithoautotrophic organic matter, POM = photosynthetic organic matter.

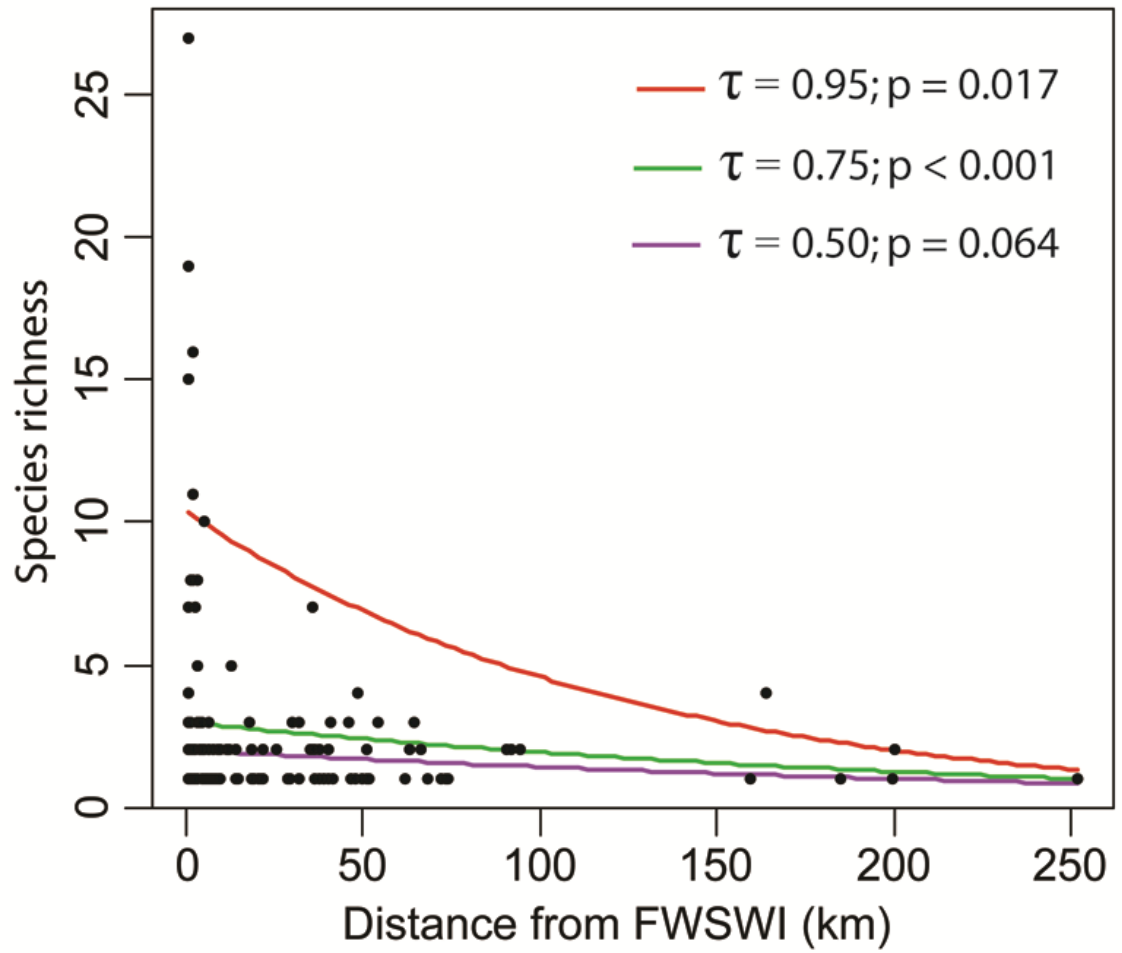


Figure 4.4: Quantile regression of species richness as a function of distance from the freshwater saline water interface (FWSWI). Trendlines are shown for significant quantiles (τ).